

BU ID No: - D71446/87

LOUGHBOROUGH  
UNIVERSITY OF TECHNOLOGY  
LIBRARY

AUTHOR/FILING TITLE

GURUNLU, C

ACCESSION/COPY NO.

283390/01

VOL. NO.

CLASS MARK

LOAN COPY

- 4 DEC 1994

028 3390 01

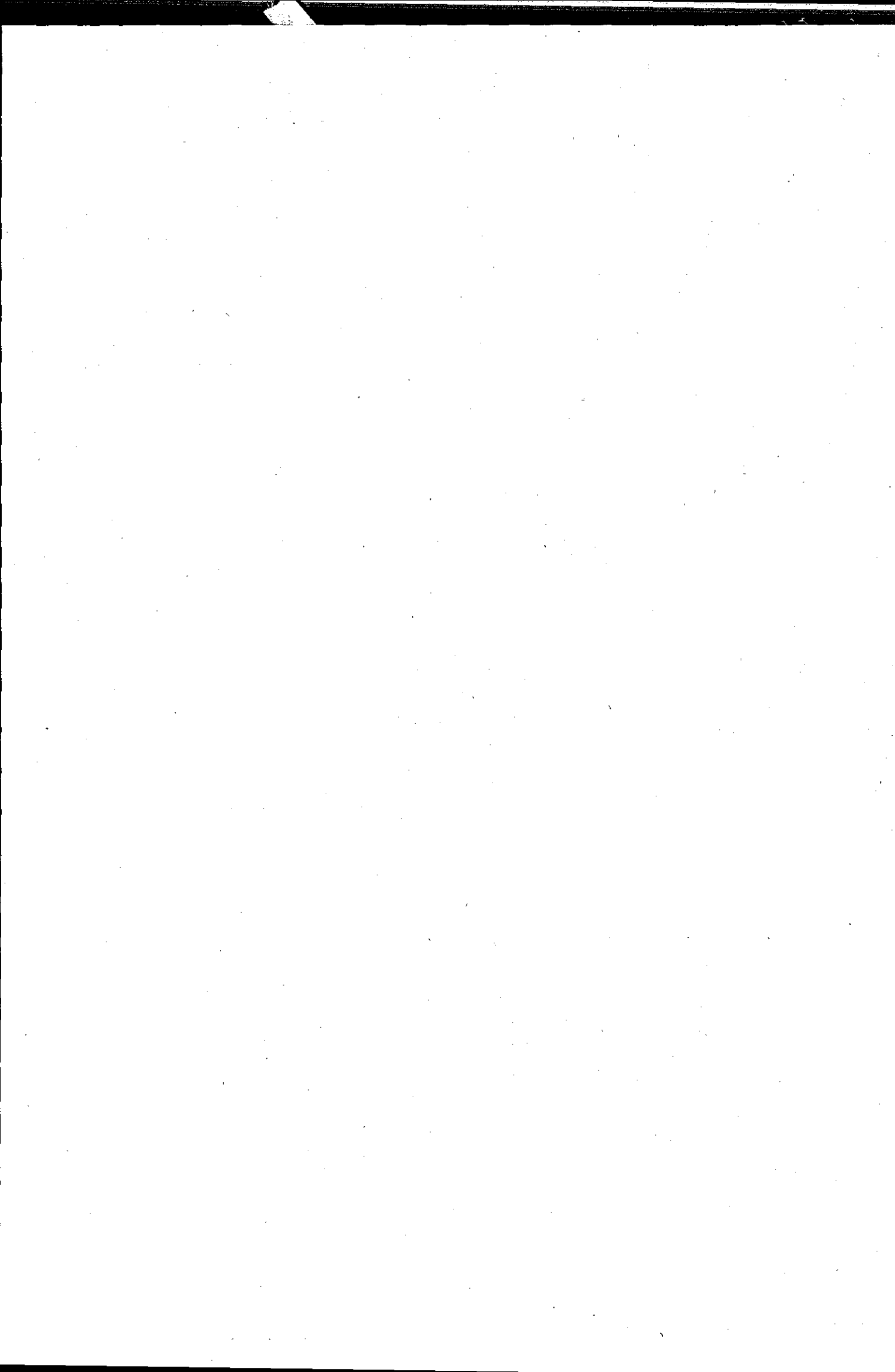


This book was bound by

**Badminton Press**

18 Half Croft, Syston, Leicester, LE7 8LD

Telephone: Leicester (0533) 602918.



SINGLE-PHASE OPERATIONS OF 3-PHASE GENERATORS

by

CEMIL GÜRÜNLÜ, BSc

A Doctoral Thesis

Submitted in partial fulfilment of the  
requirements for the award of the Degree of  
Doctor of Philosophy  
of  
Loughborough University of Technology

Supervisor: Professor I R Smith, BSc, PhD, DSc, CEng, FIEE

Head of Department of Electronic and Electrical Engineering  
Dean of Engineering Faculty

Loughborough University  
of Science and Technology  
Nov 1986  
2A3390 | 91

*This thesis is dedicated to my friends.*

ACKNOWLEDGEMENTS

The author wishes to express his sincere gratitude to Professor I R Smith, who supervised the project, for the help he provided by every possible means.

I wish to thank Mr J G Kettleborough for many stimulating and valuable discussions during the course of research.

Finally, I would like to thank Mrs Janet Smith for the trouble and care taken when she was typing this thesis.

## SYNOPSIS

The ever increasing demand for power, and the correspondingly greater complexity of power systems, is leading to more severe problems of system reliability. Modern society is so dependent on the usage of electrical power that even a short interruption of service can cause serious problems. A public utility cannot be expected to provide a perfect power supply, since many of the possible causes of a power disturbance are beyond its control.

The windings of small diesel-driven 3-phase generator sets are often capable of being connected in either a zig-zag or an Edison-delta arrangement, to provide a single-phase supply for standby or emergency purposes. Although many of these generators are genuinely on standby (i.e. they are brought into operation only as a result of a system failure), many others operate continuously in situations where no mains supply is available.

The thesis aims to investigate both the steady-state and the dynamic performance of a 3-phase salient-pole generator, when reconnected in either a zig-zag or an Edison-delta configuration, and to provide a performance comparison with the more familiar modes of single-phase operation involving line-to-line and line-to-neutral loading.

Symmetrical components are used to investigate the steady-state performance and a phase model is used to determine both the steady-state and transient performance. Analytical expressions are obtained for the short-circuit currents for various generator connections by utilising the modified Clarke transformation. The theoretical results from various models are compared with experimental results on a test machine. Losses, efficiency and voltage waveforms for various generator connections are experimentally obtained for the test machine. Results are discussed and suggestions for future research are included.

LIST OF PRINCIPAL SYMBOLS

[C]	=	Connection matrix
E	=	Excitation voltage (RMS)
$e_{ao}, e_{bo}, e_{co}$	=	Instantaneous a, b and c open-circuit phase voltages
$e_{\alpha}, e_{\beta}, e_{\gamma}$	=	Instantaneous $\alpha$ , $\beta$ and $\gamma$ components of phase voltages
$f_d, f_q, f_o$	=	D-axis, q-axis and zero sequence components of voltage/current/flux
$f_{\alpha}, f_{\beta}, f_{\gamma}$	=	$\alpha$ , $\beta$ and $\gamma$ components of voltage/current/flux
[G]	=	Rate-of-change of inductance matrix
[I]	=	Current vector
$i_a, i_b, i_c$	=	Instantaneous a, b and c armature phase currents
$i_f$	=	Instantaneous field current
$i_{kd}, i_{kq}$	=	Instantaneous d-axis and q-axis damper windings currents
$I_a, I_b, I_c$	=	a, b and c phase armature currents (RMS)
$I_{a1}, I_{a2}, I_{a0}$	=	Positive, negative and zero-sequence components of the a armature phase current
$I_{b1}, I_{b2}, I_{b0}$	=	Positive, negative and zero-sequence components of the b armature phase current
$I_{c1}, I_{c2}, I_{c0}$	=	Positive, negative and zero-sequence components of the c armature phase current
$ I_{a2}/I_{a1} $	=	Unbalance factor for the armature phase current
[L]	=	Inductance matrix
$L_d, L_q, L_o$	=	D-axis, q-axis and zero-sequence components of inductance
$L_{A0}$	=	Constant part of the armature phase self inductance
$L_f$	=	Field winding self inductance
$L_{kd}$	=	D-axis damper winding self inductance
$L_{kq}$	=	Q-axis damper winding self inductance
$L_2$	=	Second harmonic coefficient of armature phase self inductance

$L_m$	=	Second harmonic coefficient of armature phase self inductance of the ideal generator
$M_d$	=	Phase-to-d-axis damper winding mutual inductance coefficient
$M_f$	=	Phase-to-field winding mutual inductance coefficient
$M_{fkd}$	=	Field-to-d-axis damper winding mutual inductance
$M_q$	=	Phase-to-q-axis mutual inductance coefficient
$M_o$	=	Constant part of the armature phase-to-phase mutual inductance
$M_2$	=	Second harmonic coefficient of the armature phase-to-phase mutual inductance
$\psi_a, \psi_b, \psi_c$	=	a, b and c armature phase flux linkages
$\psi_f$	=	Field winding flux linkages
$\psi_{a0}, \psi_{b0}, \psi_{c0}$	=	a, b and c armature phase flux linkages for the unloaded generator
$\psi_d, \psi_q, \psi_o$	=	D-axis, q-axis and zero sequence flux linkages
$P_1$	=	Friction, windage and iron losses of the DC drive motor
$P_2$	=	Friction, windage losses of generator
$P_c$	=	Generator core losses
$P_{out}$	=	Generator output
[R]	=	Resistance matrix
R	=	Armature phase resistance
$R_f$	=	Field winding resistance
$R_{kd}$	=	D-axis damper winding resistance
$R_{kq}$	=	Q-axis damper winding resistance
$T'_{do}$	=	D-axis open-circuit transient time constant
$T'_d$	=	D-axis transient time constant
$T''_d$	=	D-axis subtransient time constant
$T'_q$	=	Q-axis transient time constant
$T''_q$	=	Q-axis subtransient time constant
[V]	=	Voltage vector
$v_a, v_b, v_c$	=	Instantaneous a, b and c armature phase voltages

$V_a, V_b, V_c$	=	a, b and c armature phase voltages (RMS)
$V_{a1}, V_{a2}, V_{a0}$	=	Positive, negative and zero sequence components of the a armature phase voltage
$V_{b1}, V_{b2}, V_{b0}$	=	Positive, negative and zero sequence components of the b armature phase voltage
$V_{c1}, V_{c2}, V_{c0}$	=	Positive, negative and zero sequence components of the c armature phase voltage
$ V_{a2}/V_{a1} $	=	Unbalance factor for the armature voltage
$X_a$	=	Armature leakage reactance
$X_{ad}$	=	D-axis magnetising reactance
$X_{aq}$	=	Q-axis magnetising reactance
$X_d$	=	D-axis synchronous reactance
$X'_d$	=	D-axis transient reactance
$X''_d$	=	D-axis subtransient reactance
$X_q$	=	Q-axis synchronous reactance
$X'_q$	=	Q-axis transient reactance
$X''_q$	=	Q-axis subtransient reactance
$X_0$	=	Zero-sequence reactance
$X_2$	=	Negative-sequence reactance
$[Z]$	=	Impedance matrix
$Z_1, Z_2, Z_0$	=	Positive, negative and zero sequence impedances
$\theta$	=	Rotor angle with respect to a-phase ( $^\circ e$ )
$\omega$	=	Angular frequency

### Subscripts

a, b, c	Armature windings
d	Direct-axis quantities
f	Field winding
kd	Direct-axis damper winding
kq	Quadrature-axis damper winding
q	Quadrature-axis quantities

CONTENTS

	<u>Page No</u>
ACKNOWLEDGEMENTS ... ..	i
SYNOPSIS ... ..	ii
LIST OF PRINCIPAL SYMBOLS ... ..	iii
CONTENTS ... ..	iv
CHAPTER 1: INTRODUCTION ... ..	1
CHAPTER 2: VARIOUS SINGLE-PHASE CONNECTIONS ...	5
CHAPTER 3: SYMMETRICAL COMPONENT MODEL FOR VARIOUS GENERATOR CONNECTIONS ... ..	9
3.1 Short-Circuit Faults ... ..	11
3.1.1 Line(1)-to-centre point fault for zig- zag connection ... ..	11
3.1.2 Line(2)-to-centre point fault for zig- zag connection ... ..	16
3.1.3 Double line-to-centre point fault for zig-zag connection ... ..	19
3.1.4 Line-to-line fault for Edison-delta connected generators ... ..	22
3.2 Analysis of Load Conditions ... ..	25
3.2.1 Zig-zag connection ... ..	25
3.2.2 Edison-delta connection ... ..	30
3.2.3 Line-to-line loaded generator ... ..	34
3.2.4 Line-to-neutral loaded generator ... ..	38
3.3 Conclusions ... ..	41
CHAPTER 4: PHASE MODEL FOR VARIOUS CONNECTIONS ...	42
4.1 State Equations for a 3-Phase Synchronous Generator ... ..	45
4.2 Inductance and Time-Rate-of-Change of Induc- tance Coefficients ... ..	46
4.2.1 Inductance coefficients ... ..	46
4.2.1.1 Stator self-inductances ... ..	46
4.2.1.2 Rotor self-inductances ... ..	47
4.2.1.3 Stator mutual inductances ... ..	47
4.2.1.4 Rotor mutual inductances ... ..	47

	<u>Page No.</u>
4.2.1.5 Stator-to-rotor mutual inductances ... ..	48
4.2.2 Time-Rate-of-Change of Inductance Coefficients ... ..	49
4.2.2.1 Time-rate-of-change of stator self-inductance ...	49
4.2.2.2 Time-rate-of-change of rotor self-inductance ...	49
4.2.2.3 Time-rate-of-change of stator mutual inductance ..	49
4.2.2.4 Time-rate-of-change of rotor mutual inductance ...	50
4.2.2.5 Time-rate-of-change of stator-to-rotor mutual inductances ... ..	50
4.3 State Equations for Various Connections ...	51
4.4 Transient Fault Tests ... ..	64
 CHAPTER 5: $\alpha, \beta, \gamma$ COMPONENT MODEL FOR VARIOUS GENERATOR CONNECTIONS ... ..	 70
5.1 Machine Equations in Terms of $\alpha, \beta, \gamma$ Components ... ..	74
5.2 Synchronous Generator on No-Load ...	78
5.3 Simulation of Disturbances ... ..	80
5.4 Terminal(1)-to-Centre Point Fault for Zig-Zag Connection ... ..	81
5.5 Terminal(2)-to-Centre Point Fault for Zig-Zag Connection ... ..	88
5.6 Double Line-to-Centre Point Fault for Zig-Zag Connection ... ..	96
5.7 Line-to-Line Fault for an Edison-Delta Connection ... ..	102
5.8 Summary and Comments ... ..	110
 CHAPTER 6: EXPERIMENTAL PROCEDURE USED WITH THE VARIOUS GENERATOR CONNECTIONS AND RESULTS ...	 112
6.1 Available Power Output ... ..	112
6.2 Voltage Waveforms ... ..	114
6.3 Losses ... ..	121
6.4 Efficiency ... ..	123

	<u>Page No</u>
CHAPTER 7: CONCLUSIONS AND SUGGESTIONS ... ..	127
7.1 Conclusions ... ..	127
7.2 Suggestions for Further Investigations ...	130
APPENDICES:	
Appendix I: MEASUREMENT OF D-Q PARAMETERS ... ..	133
1. The Experimental Machine ... ..	133
2. Resistance Measurement ... ..	133
3. Reactance Measurement ... ..	134
3.1 Direct-axis synchronous reactance ( $X_d$ )	134
3.2 Quadrature-axis synchronous reactance ( $X_q$ ) ... ..	134
3.3 Armature leakage reactance ( $X_a$ ) ...	134
3.4 Direct-axis magnetising reactance ( $X_{md}$ )	138
3.5 Quadrature-axis magnetising reactance ( $X_{mq}$ ) ... ..	138
3.6 Direct-axis transient reactance ( $X'_d$ )	138
3.7 Direct-axis subtransient reactance ( $X''_d$ ) ... ..	140
3.8 Quadrature-axis subtransient reactance ( $X''_q$ ) ... ..	140
3.9 Negative-sequence reactance ( $X_2$ ) ...	140
3.10 Zero-sequence reactance ( $X_0$ ) ...	141
4. Time Constants ( $T'_{do}$ , $T'_d$ , $T''_d$ ) ... ..	141
5. Summary of Experimental Machine Parameters	142
Appendix II: CALCULATION OF PHASE PARAMETERS FROM D-Q PARAMETERS ... ..	143
1. Parameter Relationships ... ..	144
2. Conversion Equations ... ..	146
2.1 D-axis armature/field turns ratio ...	146
2.2 Phase parameters (accessible windings)	147
2.3 D-axis damper winding parameters ...	148
2.4 Q-axis damper winding parameters ...	149
3. Phase Parameters for the Experimental Machine ... ..	150

	<u>Page No.</u>
Appendix III: DETERMINATION OF LOSSES ... ..	151
1. Losses of the Driving Motor ... ..	151
2. Windage, Bearing, Friction and Brush-Fric- tion Losses ... ..	152
3. Open Circuit Core-Loss ... ..	152
4. Total Losses of the Generator ... ..	153
Appendix IV: NUMERICAL INTEGRATION METHODS ... ..	154
1. Round-off Error ... ..	154
2. Truncation Error... ..	154
3. Instability ... ..	155
4. Choice of Integration Method ... ..	156
4.1 Explicit one-step numerical integration method ... ..	158
4.2 Implicit one-step integration method	158
Appendix V: SOME MATHEMATICAL MANIPULATIONS ... ..	162
Appendix VI: SERIES EXPANSION OF SOME MATHEMATICAL EXPRES- SIONS ... ..	164
Appendix VII: TRANSFORMATIONS ... ..	167
Appendix VIII: CALCULATION OF DECREMENT FACTORS FOR TERMINAL (1)-TO-CENTRE POINT FAULT ... ..	169
Appendix IX: CALCULATION OF DECREMENT FACTORS FOR TERMINAL (2)-TO-CENTRE POINT FAULT ... ..	178
Appendix X: CALCULATION OF DECREMENT FACTORS FOR DOUBLE- LINE-TO-CENTRE POINT ... ..	187
Appendix XI: CALCULATION OF DECREMENT FACTORS FOR LINE-TO- LINE FAULT OF EDISON-DELTA CONNECTION ... ..	196
REFERENCES ... ..	205

## CHAPTER 1

### INTRODUCTION

While all users of electrical power desire constant frequency, voltage stability, and reliability at all times, these features clearly cannot necessarily be realised in practice. Within any complex system the requirements are continually changing and becoming more demanding and interrelated.

An electric utility cannot be expected to provide an ideal power supply, since many of the possible causes of power disturbance are beyond the control of its operators. For example, vehicles hit line support poles, lightning strikes overhead lines, high winds blow trees, branches and other debris onto the power lines. Lightning, wind and rain all cause power disturbances in the form of power interruptions or other transients. Tornadoes take their toll on the power system, as do the more frequently encountered snow storms, ice and floods. Although there is obviously less chance of a supply interruption on an underground system, any interruption which does occur may last much longer, because of the longer time required to locate and repair the failure. Even the malfunction of protective devices can cause a power supply disturbance.

Modern society is so dependent on its usage of electrical power that even a short interruption of service can cause serious problems. Hospitals must have a highly reliable emergency power supply for life-support systems, to ensure that sick and disabled people are protected. A machine operator may be a high injury-risk during the first few seconds after a lightning strike has plunged his workshop into darkness. Power interruption may cause severe problems for lifts. Emergency or standby power for perimeter and security lighting is often deemed necessary to reduce the risk of injury, theft, or property damage.

The windings of small diesel-driven 3-phase generator sets are often capable of being connected in either a zig-zag or an Edison-delta arrangement, to provide a single-phase supply for standby or emergency purposes. Although many of these generators are genuinely on standby (i.e. they are brought into operation only as a result of a failure), many others operate continuously in situations where no mains supply is available. It appears to be Griffen<sup>1</sup> who first examined the possibilities of such re-connections and also discussed the voltage waveforms, power outputs and distribution factors of the re-connected generators.

The problems associated with the performance prediction of unbalanced load and unsymmetrical fault conditions of conventional star-connected 3-phase salient-pole synchronous machine have attracted the attention of many authors since the beginning of this century. In 1918, Fortescue<sup>2</sup> developed the concept of symmetrical components analysis, which has subsequently been applied to many practical problems<sup>3,4,5,6</sup>. However, a symmetrical component model assumes that both balanced and unbalanced current and voltage waveforms are sinusoidal, and such a model clearly will give large discrepancies when compared with practical results from a system in which the currents and voltages contain a considerable harmonic content.

Blondel<sup>7</sup> analysed the salient-pole synchronous machine by resolving the fundamental space component of mmf along the two axes of symmetry, the direct or pole axis and the quadrature or interpole axis. His basic theory has been extended considerably by Doherty and Nickle<sup>8,9,10,11,12</sup> and by Park<sup>13,14,15</sup> who gave the now familiar definition of an ideal synchronous machine. This d-q model has subsequently been used to investigate many practical problems associated with synchronous machines, with many of the research results being presented by Adkins and Harley<sup>16</sup>. The advantage of the d-q model is that its basic differential equations are expressed with time-invariant coefficients, leading to analytical solutions for balanced load or symmetrical fault conditions. The disadvantage of the model arises from certain oversimplifications in the development

of its equations, while it also requires further transformations for the solution of unbalanced load conditions or unsymmetrical faults.

In 1954, Ching and Adkins<sup>17</sup> investigated the transient theory of 3-phase salient-pole synchronous generators under unsymmetrical fault conditions. Laplace transformations applied to the basic differential equations of an ideal synchronous generator led to solutions for the various currents and voltages in the form of infinite series. The method of solution is fully explained for a line-to-line short-circuit fault, although only the equations and the results were quoted for line-to-neutral and double-line-to-ground short-circuit faults. However, throughout the analysis approximations were made on the basis of the relative magnitudes of the machine parameters. Experimental verification was provided by results from a rather special machine, with a uniform air-gap, and no damper windings.

In 1971, Subramaniam and Malik<sup>18</sup> solved the complete phase differential equations of an ideal synchronous generator under unbalanced load and unsymmetrical fault conditions using a digital computer. Smith and Snider<sup>19</sup> included both saturation and space harmonics in a digital computer based investigation of unbalanced load and unsymmetrical fault conditions, and also verified experimentally their theoretical results.

The objective of the present study is to investigate the performance of a 3-phase salient-pole synchronous generator when re-connected in either a zig-zag or an Edison-delta configuration, and to provide a performance comparison with the more familiar modes of single-phase operations involving line-to-line or line-to-neutral loading. Symmetrical components are used to investigate the steady-state performance, with in both cases a phase-model being used as the basis for the various generator re-connections. D-q model parameters for the experimental machine are measured, and the required phase-model parameters are determined from those using familiar relationships. Analytical expressions are obtained for the short-circuit currents of

various generator re-connections, by utilising the modified Clarke's transformations and a successive approximation technique. Losses, efficiency, available power output and voltage waveforms are experimentally obtained for the test machine. Results are discussed and a comparison between the various generator re-connections is made. Suggestions for future research work are also included.

CHAPTER 2VARIOUS SINGLE PHASE CONNECTIONS

The users of 3-phase generators need sometimes to re-arrange the connections to the armature windings of their machines so as to provide a single-phase output when an existing single-phase generator has broken down, or simply when such a machine is unavailable. A single-phase supply may be obtained from a 3-phase armature by any one of the four following possibilities:

- a) Line-to-neutral loading
- b) Line-to-line loading
- c) Zig-zag connection
- d) Edison-delta connection

The positive direction of current and voltages relating to a 3-phase generator are defined in Figure 2.1 and these will be used throughout the thesis.

The connection of a line-to-neutral load to the armature of a generator is illustrated by Figure 2.2 with the maximum power output available clearly being only 33% of the 3-phase rating. Figure 2.3 illustrates the situation when the load is taken from between two output lines of the generator. Since the output voltage is now  $\sqrt{3}$  times that in the line-to-neutral connection, the maximum power output available becomes 57% of the 3-phase rating. The armature arrangement in a zig-zag connected generator is shown in Figure 2.4, where the two armature phases b and c are now series connected. Since the armature voltages of a 3-phase generator are equal and displaced in both space and time phase by  $120^\circ$ , the sum of the voltages of b and c has the same magnitude as, and is in antiphase with, the a phase voltage. The voltage output  $V_2$  is defined as  $V_2 = -V_b - V_c$  in Figure 2.4. The maximum power output available from a zig-zag connected generator is clearly 67% of the 3-phase rating.

Figure 2.5 shows the Edison-delta connection, in which a single-phase supply is taken from two corners of a 3-phase delta-connected armature, with one of the phases being centre-tapped. Within the armature the load current divides in the ratio 1:2, so that the maximum available power output obtainable is 50% of the 3-phase rating.

In both the zig-zag and Edison-delta connections, the impedance of the two loads should not be allowed to differ by more than 15%<sup>1</sup>, otherwise the magnitude of the reverse rotating field in the air-gap may cause intolerable eddy current losses and excessive heating of the rotor body.

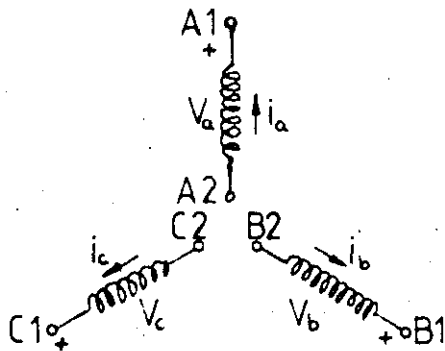


FIGURE 2.1: Positive direction of current and voltages

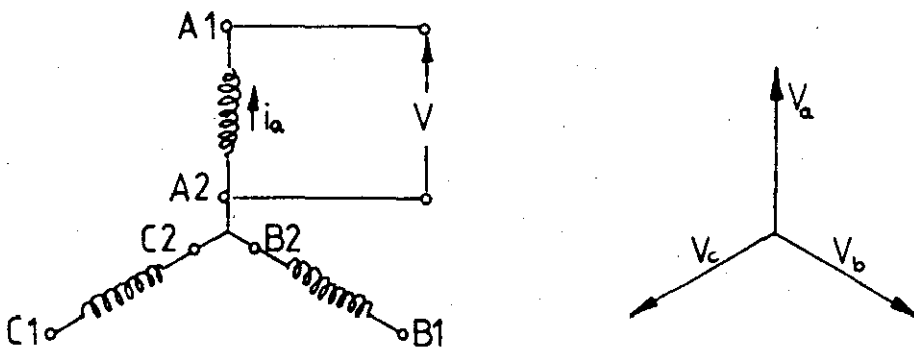


FIGURE 2.2: Line-to-neutral loading

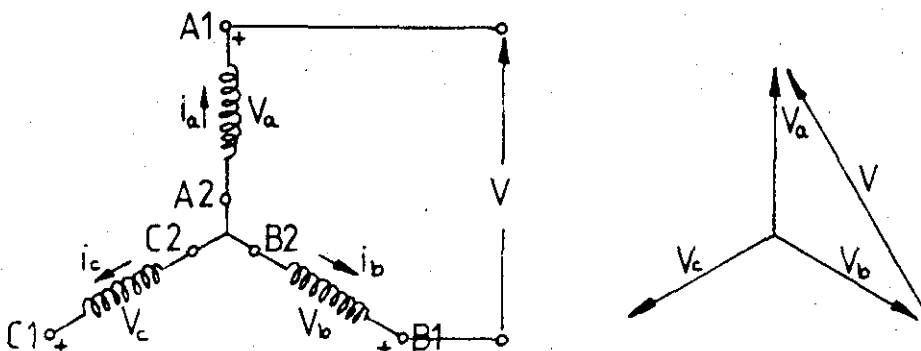


FIGURE 2.3: Line-to-line loading

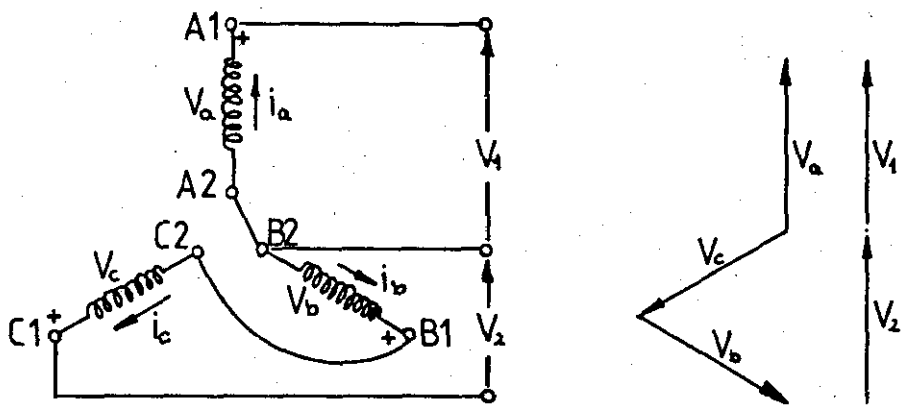


FIGURE 2.4: Zig-Zag Connection

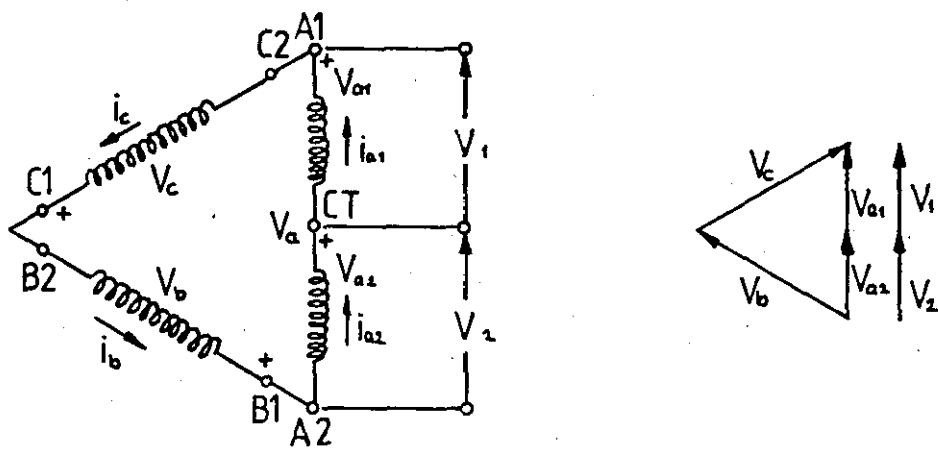


FIGURE 2.5: Edison-delta Connection

### CHAPTER 3

#### SYMMETRICAL COMPONENT MODEL FOR VARIOUS GENERATOR CONNECTIONS

In 1912, Fortescue<sup>2</sup> showed that the three phasors which represent any unbalanced 3-phase system can be resolved into three balanced systems of phasors:

- a) The positive-sequence components, consisting of three phasors equal in magnitude, displaced mutually by  $120^\circ$  and with the same phase sequence as the original unbalanced phasors.
- b) The negative-sequence components, consisting of three phasors equal in magnitude, displaced mutually by  $120^\circ$  and with a phase sequence opposite to that of the original phasors.
- c) The zero-sequence components, consisting of three phasors equal in magnitude and with zero phase displacement.

The three sets of balanced phasors which form the symmetrical components of the unbalanced phasors are shown in Figure 3.1. Since each original unbalanced phasor is the sum of its three components, the original phasors can be expressed in terms of their components as:

$$\begin{aligned} V_a &= V_{a1} + V_{a2} + V_{a0} \\ V_b &= V_{b1} + V_{b2} + V_{b0} \\ V_c &= V_{c1} + V_{c2} + V_{c0} \end{aligned} \tag{3.1}$$

Reference to Figure 3.1 verifies the following relations, in which  $a = e^{j120^\circ}$ ,

$$\begin{aligned}
 V_{b1} &= a^2 V_{a1} & V_{c1} &= a V_{a1} \\
 V_{b2} &= a V_{a2} & V_{c2} &= a^2 V_{a2}
 \end{aligned}
 \tag{3.2}$$

and

$$V_{b0} = V_{a0} \quad V_{c0} = V_{a0}$$

so that

$$\begin{aligned}
 V_a &= V_{a1} + V_{a2} + V_{a0} \\
 V_b &= a^2 V_{a1} + a V_{a2} + V_{a0}
 \end{aligned}
 \tag{3.3}$$

and

$$V_c = a V_{a1} + a^2 V_{a2} + V_{a0}$$

Conversely, it can be shown that the three unsymmetrical phasors are resolved into their symmetrical components by

$$\begin{aligned}
 V_{a1} &= \frac{1}{3} (V_a + a V_b + a^2 V_c) \\
 V_{a2} &= \frac{1}{3} (V_a + a^2 V_b + a V_c)
 \end{aligned}
 \tag{3.4}$$

and

$$V_{a0} = \frac{1}{3} (V_a + V_b + V_c)$$

Clearly, a similar discussion is valid for the corresponding set of currents, so that

$$\begin{aligned}
 I_a &= I_{a1} + I_{a2} + I_{a0} & I_{a1} &= \frac{1}{3} (I_a + a I_b + a^2 I_c) \\
 I_b &= a^2 I_{a1} + a I_{a2} + I_{a0} & I_{a2} &= \frac{1}{3} (I_a + a^2 I_b + a I_c)
 \end{aligned}
 \tag{3.5}$$

and

$$I_c = aI_{a1} + a^2I_{a2} + I_{a0} \quad I_{a0} = \frac{1}{3} (I_a + I_b + I_c)$$

Assuming that a synchronous generator produces only positive-sequence components of voltage, the sequence networks for a 3-phase machine<sup>20,21,22</sup> are given in Figure 3.2, with the corresponding voltage drop equations being

$$\begin{aligned} V_{a1} &= E - Z_1 I_{a1} \\ V_{a2} &= - Z_2 I_{a2} \end{aligned} \quad (3.6)$$

and

$$V_{a0} = - Z_0 I_{a0}$$

### 3.1 SHORT-CIRCUIT FAULTS

#### 3.1.1 Line(1)-to-Centre Point Fault for Zig-Zag Connection

The circuit diagram for a zig-zag connected 3-phase synchronous generator with a line(1)-to-centre point fault is shown in Figure 3.3. It is clear that, under this condition, the following constraints exist:

$$I_b = 0 \quad I_c = 0 \quad V_a = 0 \quad (3.7)$$

Applying these to the expressions for the symmetrical components of the currents yields

$$\begin{aligned} I_{a1} &= \frac{1}{3} (I_a + aI_b + a^2I_c) = \frac{1}{3} I_a \\ I_{a2} &= \frac{1}{3} (I_a + a^2I_b + aI_c) = \frac{1}{3} I_a \end{aligned} \quad (3.8)$$

and

$$I_{a0} = \frac{1}{3} (I_a + I_b + I_c) = \frac{1}{3} I_a$$

so that

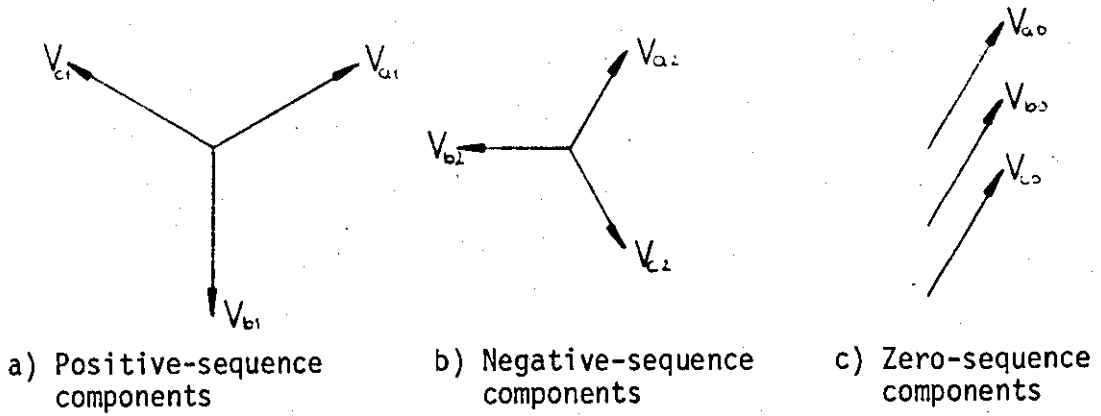


FIGURE 3.1: Symmetrical components of an unbalanced 3-phase system

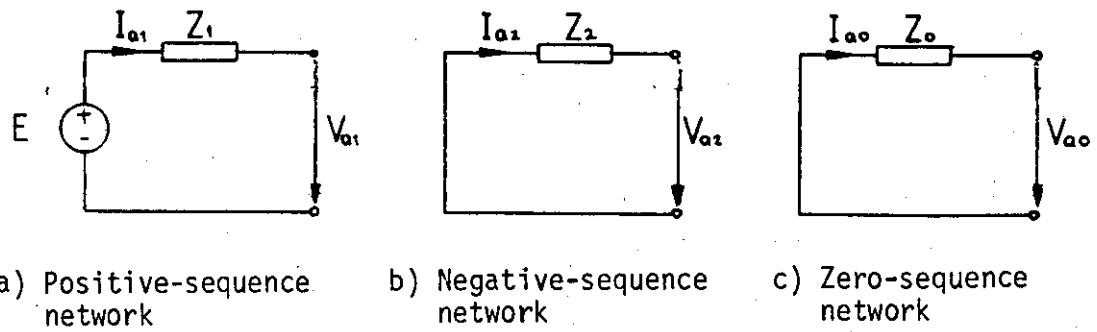


FIGURE 3.2: Sequence networks of a 3-phase synchronous generator

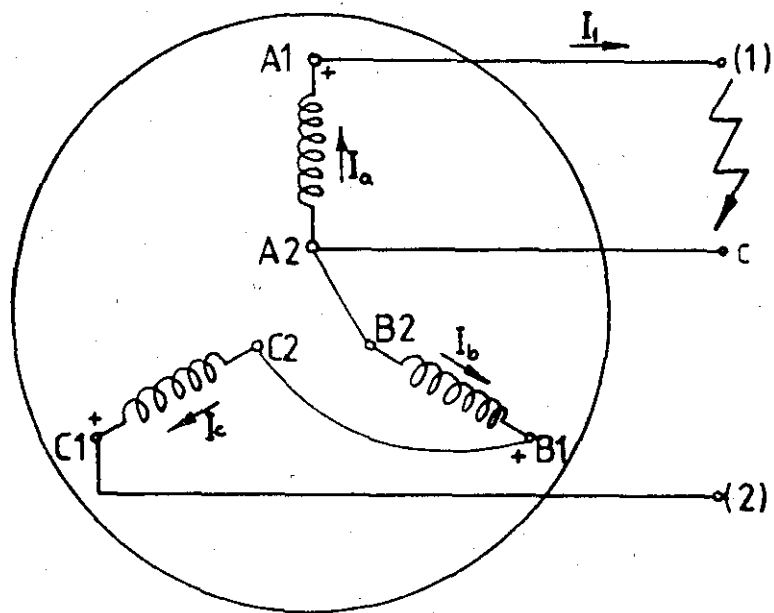


FIGURE 3.3: Line (1)-to-centre point fault for zig-zag connection

$$I_{a0} = I_{a1} = I_{a2} = \frac{1}{3} I_a \quad (3.9)$$

Applying Kirchhoff's second law to the phase sequence voltage drop equations gives

$$\begin{aligned} V_{a1} &= E - Z_1 I_{a1} = E - \frac{1}{3} Z_1 I_a \\ V_{a2} &= -Z_2 I_{a2} = -\frac{1}{3} Z_2 I_a \end{aligned} \quad (3.10)$$

and

$$V_{a0} = -Z_0 I_{a0} = -\frac{1}{3} Z_0 I_a$$

Since phase a is short-circuited  $V_a = 0$ , and it follows that

$$V_{a0} + V_{a1} + V_{a2} = 0$$

and that

$$-\frac{1}{3} Z_0 I_a + E - \frac{1}{3} Z_1 I_a - \frac{1}{3} Z_2 I_a = 0$$

or

$$I_a = \frac{3E}{Z_0 + Z_1 + Z_2} \quad (3.11)$$

Hence

$$I_{a0} = I_{a1} = I_{a2} = \frac{E}{Z_0 + Z_1 + Z_2} \quad (3.12)$$

The symmetrical components of the phase a voltage are therefore

$$\begin{aligned} V_{a1} &= E - \frac{Z_1 E}{Z_0 + Z_1 + Z_2} = \frac{Z_0 + Z_2}{Z_0 + Z_1 + Z_2} E \\ V_{a2} &= -\frac{Z_2 E}{Z_0 + Z_1 + Z_2} \end{aligned} \quad (3.13)$$

and

$$V_{a0} = - \frac{Z_0 E}{Z_0 + Z_1 + Z_2}$$

respectively. Correspondingly, the voltage of the open-circuit phases are

$$V_b = V_{a0} + a^2 V_{a1} + a V_{a2} = \frac{(a^2 - 1)Z_0 + (a^2 - a)Z_2}{Z_0 + Z_1 + Z_2} E$$

and

$$V_c = V_{a0} + a V_{a1} + a^2 V_{a2} = \frac{(a - 1)Z_0 + (a - a^2)Z_2}{Z_0 + Z_1 + Z_2} E \quad (3.14)$$

respectively.

Using the parameters of the experimental 3 kVA generator given in Appendix I of  $Z_1 = 21.2 \Omega/\text{phase}$ ,  $Z_2 = 7.20 \Omega/\text{phase}$  and  $Z_0 = 1.46 \Omega/\text{phase}$ , the short-circuit current for an open-circuit voltage of 127 V/phase was calculated as 12.8A compared with a measured value of 13.0A. The predicted b and c voltages are  $V_b = V_c = 59.2\text{V}$  compared with measured values of  $V_b = 70.5\text{V}$  and  $V_c = 68.0\text{V}$ .

### 3.1.2 Line(2)-to-Centre Point Fault for Zig-Zag Connection

The circuit diagram of Figure 3.4 shows a zig-zag connected generator with a line(2)-to-centre point short circuit. The constraints which now exist are

$$I_a = 0 \quad I_b = -I_2 \quad I_c = -I_2 \quad V_b + V_c = 0 \quad (3.15)$$

and when these are applied to the expressions for the symmetrical components of the currents, it follows that

$$I_{a1} = \frac{1}{3} (I_a + a I_b + a^2 I_c) = \frac{1}{3} I_2$$

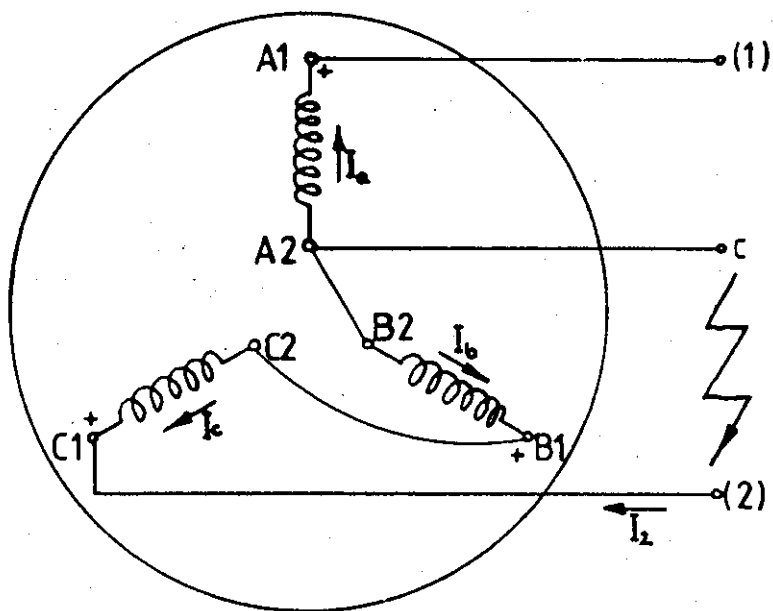


FIGURE 3.4: Line (2)-to-centre point fault for a zig-zag connection

$$I_{a2} = \frac{1}{3} (I_a + a^2 I_b + a I_c) = \frac{1}{3} I_2 \quad (3.16)$$

and

$$I_{a0} = \frac{1}{3} (I_a + I_b + I_c) = -\frac{2}{3} I_2$$

Hence the sequence components of voltage are

$$V_{a1} = E - Z_1 I_{a1} = E - \frac{1}{3} Z_1 I_2$$

$$V_{a2} = -Z_2 I_{a2} = -\frac{1}{3} Z_2 I_2 \quad (3.17)$$

and

$$V_{a0} = -Z_0 I_{a0} = \frac{2}{3} Z_0 I_2$$

respectively. From the conditions of the fault it follows that

$$V_b + V_c = 0$$

and therefore that

$$V_b = V_{a0} + a^2 V_{a1} + a V_{a2}$$

$$V_c = V_{a0} + a V_{a1} + a^2 V_{a2}$$

Hence

$$V_b + V_c = 2V_{a0} - V_{a1} - V_{a2}$$

or

$$2\frac{2}{3} Z_0 I_2 - E + \frac{1}{3} Z_1 I_2 + \frac{1}{3} Z_2 I_2 = 0$$

giving

$$I_2 = \frac{3E}{4Z_0 + Z_1 + Z_2} \quad (3.18)$$

The symmetrical components of the short-circuit current are

$$\begin{aligned} I_{a1} &= \frac{1}{3} I_2 = \frac{E}{4Z_0 + Z_1 + Z_2} \\ I_{a2} &= \frac{1}{3} I_2 = \frac{E}{4Z_0 + Z_1 + Z_2} \end{aligned} \quad (3.19)$$

and

$$I_{a0} = -\frac{2}{3} I_2 = -\frac{2E}{4Z_0 + Z_1 + Z_2}$$

respectively, and the corresponding components of the sequence voltages are

$$\begin{aligned} V_{a1} &= E - Z_1 I_{a1} = \frac{4Z_0 + Z_2}{4Z_0 + Z_1 + Z_2} E \\ V_{a2} &= -Z_2 I_{a2} = -\frac{Z_2}{4Z_0 + Z_1 + Z_2} E \end{aligned} \quad (3.20)$$

and

$$V_{a0} = -Z_0 I_{a0} = -\frac{2Z_0}{4Z_0 + Z_1 + Z_2} E$$

The voltage of the open-circuit phase is

$$V_a = V_{a0} + V_{a1} + V_{a2} = \frac{6Z_0 E}{4Z_0 + Z_1 + Z_2} \quad (3.21)$$

With the voltage of phase b being

$$V_b = V_{a0} + a^2 V_{a1} + a V_{a2} = -j\sqrt{3} \frac{Z_2 + 2Z_0}{4Z_0 + Z_1 + Z_2} E \quad (3.22)$$

and that of phase c

$$V_c = V_{a0} + a V_{a1} + a^2 V_{a2} = j\sqrt{3} \frac{Z_2 + 2Z_0}{4Z_0 + Z_1 + Z_2} E \quad (3.23)$$

The predicted short-circuit current is  $I_2 = 11.4A$  compared with a measured value of  $I_2 = 10.5A$ . The predicted a, b and c voltages are  $V_a = 32.5V$ ,  $V_b = 65.2V$  and  $V_c = 65.2V$  compared with measured values

of  $V_a = 53.0V$ ,  $V_b = 92.0V$  and  $V_c = 92.0V$ .

### 3.1.3 Double Line-to-Centre Point Fault for Zig-Zag Connection

When a double line-to-centre point fault is applied, the circuit diagram of Figure 3.5 shows that the terminal conditions at the fault are

$$I_c = I_b \quad V_a = 0 \quad V_b + V_c = 0 \quad (3.24)$$

Applying these constraints to the expression for the symmetrical components of currents gives

$$\begin{aligned} I_{a1} &= \frac{1}{3} (I_a + aI_b + a^2I_c) = \frac{1}{3} (I_a - I_b) \\ I_{a2} &= \frac{1}{3} (I_a + a^2I_b + aI_c) = \frac{1}{3} (I_a - I_b) \end{aligned} \quad (3.25)$$

and

$$I_{a0} = \frac{1}{3} (I_a + I_b + I_c) = \frac{1}{3} (I_a + 2I_b)$$

Applying Kirchoff's second law to the phase sequence voltage drops gives

$$\begin{aligned} V_{a1} &= E - Z_1 I_{a1} = E - \frac{1}{3} Z_1 (I_a - I_b) \\ V_{a2} &= -Z_2 I_{a2} = -\frac{1}{3} Z_2 (I_a - I_b) \end{aligned} \quad (3.26)$$

and

$$V_{a0} = -Z_0 I_{a0} = -\frac{1}{3} Z_0 (I_a + 2I_b)$$

Since

$$V_a = V_{a0} + V_{a1} + V_{a2} = 0$$

then

$$(Z_0 + Z_1 + Z_2)I_a - (-2Z_0 + Z_1 + Z_2)I_b = 3E \quad (3.27)$$

And since

$$V_b + V_c = 2V_{a0} - V_{a1} - V_{a2} = 0$$

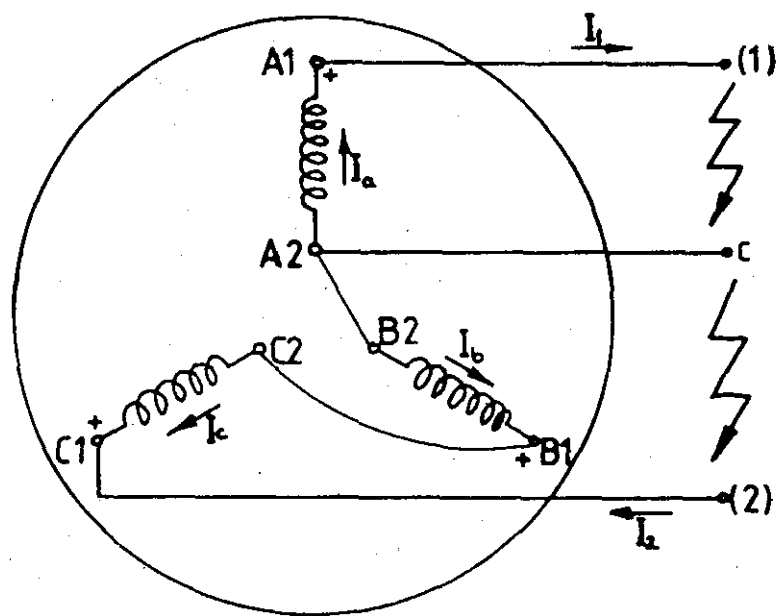


FIGURE 3.5: Double line-to-centre point fault for a zig-zag connected 3-phase synchronous generator

then

$$(-2Z_0 + Z_1 + Z_2)I_a - (4Z_0 + Z_1 + Z_2)I_b = 3E \quad (3.28)$$

Solving equations (3.27) and (3.28) simultaneously yields

$$I_a = \frac{2E}{Z_1 + Z_2} \quad I_b = -\frac{E}{Z_1 + Z_2} \quad (3.29)$$

so that the symmetrical components of the currents are

$$I_{a1} = \frac{1}{3}(I_a - I_b) = \frac{E}{Z_1 + Z_2}$$

$$I_{a2} = \frac{1}{3}(I_a - I_b) = \frac{E}{Z_1 + Z_2} \quad (3.30)$$

and

$$I_{a0} = \frac{1}{3}(I_a + 2I_b) = 0$$

and those of the voltages are

$$V_{a1} = E - Z_1 I_{a1} = \frac{Z_2}{Z_1 + Z_2} E$$

$$V_{a2} = -Z_2 I_{a2} = -\frac{Z_2}{Z_1 + Z_2} E \quad (3.31)$$

and

$$V_{a0} = -Z_0 I_{a0} = 0$$

The corresponding phase voltages are

$$V_a = V_{a0} + V_{a1} + V_{a2} = 0$$

$$V_b = V_{a0} + a^2 V_{a1} + a V_{a2} = -j \frac{\sqrt{3} Z_2}{Z_1 + Z_2} E \quad (3.32)$$

$$V_c = V_{a0} + a V_{a1} + a^2 V_{a2} = j \frac{\sqrt{3} Z_2}{Z_1 + Z_2} E$$

The short-circuit currents calculated using the above equations are  $I_a = 8.9A$  and  $I_b = 4.5A$ , compared with measured values of  $12.8A$  and  $2.6A$  respectively. Similarly the calculated b and c phase voltages of  $V_b = V_c = 54.6V$  compared with the measured values  $V_b = V_c = 73.0V$ .

### 3.1.4 Line-to-Line Fault for Edison Delta Connected Generators

The circuit diagram for the Edison-delta connected synchronous generator subject to a line-to-line fault is shown in Figure 3.6, by giving the terminal conditions at the fault of

$$I = I_a - I_b, \quad I_c = I_b, \quad V_a = 0, \quad V_b + V_c = 0 \quad (3.33)$$

The symmetrical components of the currents are

$$I_{a1} = \frac{1}{3} (I_a + aI_b + a^2I_c) = \frac{1}{3} (I_a - I_b)$$

$$I_{a2} = \frac{1}{3} (I_a + a^2I_b + aI_c) = \frac{1}{3} (I_a - I_b) \quad (3.34)$$

and

$$I_{a0} = \frac{1}{3} (I_a + I_b + I_c) = \frac{1}{3} (I_a + 2I_b)$$

respectively. The phase-sequence voltage drops are

$$V_{a1} = E - Z_1 I_{a1} = E - \frac{1}{3} Z_1 (I_a - I_b)$$

$$V_{a2} = -Z_2 I_{a2} = -\frac{1}{3} Z_2 (I_a - I_b) \quad (3.35)$$

and

$$V_{a0} = -Z_0 I_{a0} = -\frac{1}{3} Z_0 (I_a + 2I_b)$$

Since

$$V_a = V_{a0} + V_{a1} + V_{a2} = 0$$

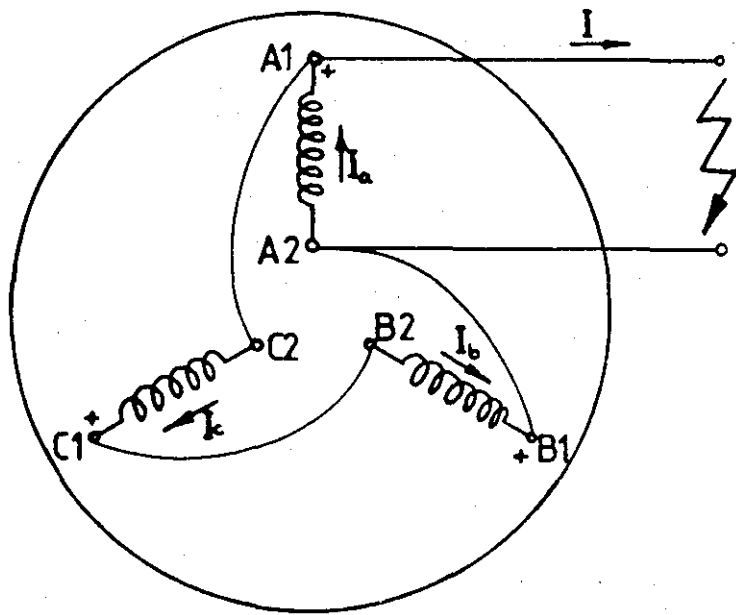


FIGURE 3.6: Line-to-line fault for Edison-delta connected generator

then  $(Z_0 + Z_1 + Z_2)I_a + (2Z_0 - Z_1 - Z_2)I_b = 3E$  (3.36)

and since  $V_b + V_c = 2V_{a0} - V_{a1} - V_{a2} = 0$

then

$$(-2Z_0 + Z_1 + Z_2)I_a - (4Z_0 + Z_1 + Z_2)I_b = 3E \quad (3.37)$$

Solving equations (3.36) and (3.37) simultaneously yields

$$I_a = \frac{2E}{Z_1 + Z_2} \quad I_b = -\frac{E}{Z_1 + Z_2} \quad (3.38)$$

The symmetrical components of the short-circuit currents are therefore

$$\begin{aligned} I_{a1} &= \frac{1}{3} (I_a - I_b) = \frac{E}{Z_1 + Z_2} \\ I_{a2} &= \frac{1}{3} (I_a - I_b) = \frac{E}{Z_1 + Z_2} \end{aligned} \quad (3.39)$$

and  $I_{a0} = \frac{1}{3} (I_a + 2I_b) = 0$

and the symmetrical components of the voltages are

$$\begin{aligned} V_{a1} &= E - Z_1 I_{a1} = \frac{Z_2 E}{Z_1 + Z_2} \\ V_{a2} &= -Z_2 I_{a2} = -\frac{Z_2 E}{Z_1 + Z_2} \end{aligned} \quad (3.40)$$

and  $V_{a0} = -Z_0 I_{a0} = 0$

The phase voltages are

$$V_b = V_{a0} + a^2 V_{a1} + a V_{a2} = -j \frac{\sqrt{3} Z_2 E}{Z_1 + Z_2}$$

and

(3.41)

$$V_c = V_{a0} + aV_{a1} + a^2V_{a2} = j \frac{\sqrt{3} Z_2 E}{Z_1 + Z_2}$$

The short-circuit current is

$$I = I_a - I_b = \frac{3E}{Z_1 + Z_2} \quad (3.42)$$

The predicted currents are  $I_a = 8.9A$ ,  $I_b = 4.5A$ ,  $I_c = 4.5A$  and  $I = 13.4A$  compared with measured values of  $I_a = 12.6A$ ,  $I_b = 2.4A$ ,  $I_c = 2.4A$  and  $I = 15.2A$ . The predicted b and c voltages are  $V_b = V_c = 55.2A$  compared with measured values of  $V_b = V_c = 72.0A$ .

## 3.2 ANALYSIS OF LOAD CONDITIONS

### 3.2.1 Zig-Zag Connection

Figure 3.7 shows the circuit diagram of a zig-zag connected 3-phase synchronous generator supplying unbalanced loads  $Z_a$  and  $Z_b$ . From the figure it is evident that

$$I_c = I_b \quad V_a = Z_a I_a \quad V_b + V_c = Z_b I_b \quad (3.43)$$

Applying these conditions to the familiar expressions for the symmetrical components of the generator currents gives

$$\begin{aligned} I_{a1} &= \frac{1}{3} (I_a + aI_b + a^2I_c) = \frac{1}{3} (I_a - I_b) \\ I_{a2} &= \frac{1}{3} (I_a + a^2I_b + aI_c) = \frac{1}{3} (I_a - I_b) \\ I_{a0} &= \frac{1}{3} (I_a + I_b + I_c) = \frac{1}{3} (I_a + 2I_b) \end{aligned} \quad (3.44)$$

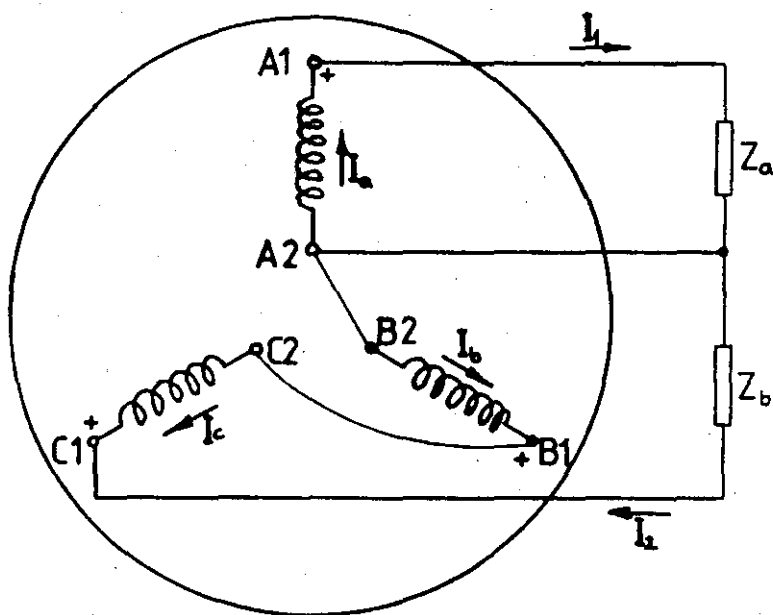


FIGURE 3.7: A zig-zag connected 3-phase synchronous generator on load

i.e.  $I_{a1} = I_{a2}$

Hence

$$\begin{aligned} V_{a1} &= E - Z_1 I_{a1} = E - \frac{1}{3} Z_1 (I_a - I_b) \\ V_{a2} &= -Z_2 I_{a2} = -\frac{1}{3} Z_2 (I_a - I_b) \end{aligned} \quad (3.45)$$

and  $V_{a0} = -Z_0 I_{a0} = -\frac{1}{3} Z_0 (I_a - I_b)$

Since  $V_a = Z_a I_a$

or  $V_{a0} + V_{a1} + V_{a2} = Z_a I_a$

then

$$(Z_0 + Z_1 + Z_2 + 3Z_a)I_a - (-2Z_0 + Z_1 + Z_2)I_b = 3E \quad (3.46)$$

and since  $V_b + V_c = Z_b I_b$

or  $2V_{a0} - V_{a1} - V_{a2} = Z_b I_b$

then  $(-2Z_0 + Z_1 + Z_2)I_a - (4Z_0 + Z_1 + Z_2 + 3Z_b)I_b = 3E \quad (3.47)$

Solving simultaneously equations (3.46) and (3.47) yields

$$I_a = \frac{9E(2Z_0 + Z_b)}{(Z_0 + Z_1 + Z_2 + 3Z_a)(4Z_0 + Z_1 + Z_2 + 3Z_b) - (-2Z_0 + Z_1 + Z_2)^2} \quad (3.48)$$

and

$$I_b = \frac{9E(Z_0+Z_a)}{(Z_0+Z_1+Z_2+3Z_a)(4Z_0+Z_1+Z_2+3Z_b)-(-2Z_0+Z_1+Z_2)^2}$$

The symmetrical components of the generator currents follow as:

$$I_{a1} = \frac{1}{3} (I_a - I_b) = \frac{3E(3Z_0+Z_a+Z_b)}{(Z_0+Z_1+Z_2+3Z_a)(4Z_0+Z_1+Z_2+3Z_b)-(-2Z_0+Z_1+Z_2)^2}$$

$$I_{a2} = \frac{1}{3} (I_a - I_b) = \frac{3E(3Z_0+Z_a+Z_b)}{(Z_0+Z_1+Z_2+3Z_a)(4Z_0+Z_1+Z_2+3Z_b)-(-2Z_0+Z_1+Z_2)^2} \quad (3.49)$$

and

$$I_{a0} = \frac{1}{3} (I_a + 2I_b) = \frac{3E(Z_b-2Z_a)}{(Z_0+Z_1+Z_2+3Z_a)(4Z_0+Z_1+Z_2+3Z_b)-(-2Z_0+Z_1+Z_2)^2}$$

and the symmetrical components of the voltage as

$$V_{a1} = E - Z_1 I_{a1} = E - \frac{3E Z_1 (3Z_0+Z_a+Z_b)}{(Z_0+Z_1+Z_2+3Z_a)(4Z_0+Z_1+Z_2+3Z_b)-(-2Z_0+Z_1+Z_2)^2}$$

$$V_{a2} = -Z_2 I_{a2} = \frac{3E Z_2 (3Z_0+Z_a+Z_b)}{(Z_0+Z_1+Z_2+3Z_a)(4Z_0+Z_1+Z_2+3Z_b)-(-2Z_0+Z_1+Z_2)^2} \quad (3.50)$$

and

$$V_{a0} = -Z_0 I_{a0} = \frac{3E Z_0 (2Z_a-Z_b)}{(Z_0+Z_1+Z_2+3Z_a)(4Z_0+Z_1+Z_2+3Z_b)-(-2Z_0+Z_1+Z_2)^2}$$

respectively.

The phase voltages are therefore

$$V_a = V_{a0} + V_{a1} + V_{a2}$$

$$= E - \frac{3E[Z_0(Z_b-2Z_a) + Z_1(3Z_0+Z_a+Z_b) + Z_2(3Z_0+Z_a+Z_b)]}{(Z_0+Z_1+Z_2+3Z_a)(4Z_0+Z_1+Z_2+3Z_b)-(-2Z_0+Z_1+Z_2)^2}$$

$$V_b = V_{a0} + a^2 V_{a1} + a V_{a2}$$

$$= a^2 E - \frac{3E[Z_0(Z_b-2Z_a) + a^2 Z_1(3Z_0+Z_a+Z_b) + a Z_2(3Z_0+Z_a+Z_b)]}{(Z_0+Z_1+Z_2+3Z_a)(4Z_0+Z_1+Z_2+3Z_b)-(-2Z_0+Z_1+Z_2)^2} \quad (3.51)$$

and

$$\begin{aligned} V_c &= V_{a0} + aV_{a1} + a^2V_{a2} \\ &= aE - \frac{3E[Z_0(Z_b - 2Z_a) + aZ_1(3Z_0 + Z_a + Z_b) + a^2(3Z_0 + Z_a + Z_b)]}{(Z_0 + Z_1 + Z_2 + 3Z_a)(4Z_0 + Z_1 + Z_2 + 3Z_b) - (-2Z_0 + Z_1 + Z_2)^2} \end{aligned}$$

respectively.

If an unbalance factor for the generator currents is defined as  $|I_{a2}/I_{a1}|$  then

$$\left| \frac{I_{a2}}{I_{a1}} \right| = 1$$

while a corresponding unbalance factor for the voltage is

$$\left| \frac{V_{a2}}{V_{a1}} \right| = \left| \frac{-3Z_2(3Z_0 + Z_a + Z_b)}{[(Z_0 + Z_1 + Z_2 + 3Z_a)(4Z_0 + Z_1 + Z_2 + 3Z_b) - (-2Z_0 + Z_1 + Z_2)^2] - 3Z_1(3Z_0 + Z_a + Z_b)} \right|$$

When the impedances of the two loads are identical

$$Z_a = Z_b = Z$$

the load currents become

$$I_1 = \frac{3E(2Z_0 + Z)}{(Z_0 + Z_1 + Z_2 + 3Z)(4Z_0 + Z_1 + Z_2 + 3Z) - (-2Z_0 + Z_1 + Z_2)^2}$$

and

$$I_2 = \frac{9E(Z_0 + Z)}{(Z_0 + Z_1 + Z_2 + 3Z)(4Z_0 + Z_1 + Z_2 + 3Z) - (-2Z_0 + Z_1 + Z_2)^2} \quad (3.52)$$

and the generator phase voltages are

$$V_a = E - \frac{3E[-Z_0Z + Z_1(3Z_0 + 2Z) + Z_2(3Z_0 + Z)]}{(Z_0 + Z_1 + Z_2 + 3Z)(4Z_0 + Z_1 + Z_2 + 3Z) - (-2Z_0 + Z_1 + Z_2)^2}$$

$$V_b = a^2 E - \frac{3E[-Z_0 Z + a Z_1(3Z_0 + 2Z) + a Z_2(3Z_0 + 2Z)]}{(Z_0 + Z_1 + Z_2 + 3Z)(4Z_0 + Z_1 + Z_2 + 3Z) - (-2Z_0 + Z_1 + Z_2)^2} \quad (3.53)$$

and

$$V_c = a E - \frac{3E[(-Z_0 Z + a Z_1(3Z_0 + 2Z) + A Z_2(3Z_0 + 2Z_0))]}{(Z_0 + Z_1 + Z_2 + 3Z)(4Z_0 + Z_1 + Z_2 + 3Z) - (-2Z_0 + Z_1 + Z_2)^2}$$

Under balanced conditions, the unbalance factor for the voltage is

$$\left| \frac{V_{a2}}{V_{a1}} \right| = \left| \frac{-3Z_2(3Z_0 + 2Z)}{[(Z_0 + Z_1 + Z_2 + 3Z)(4Z_0 + Z_1 + Z_2 + 3Z) - (-2Z_0 + Z_1 + Z_2)^2] - 3Z_1(3Z_0 + 2Z)} \right|$$

### 3.2.2 Edison-Delta Connection

From the circuit diagram for an Edison-delta connected synchronous generator supplying a 2-wire load shown in Figure 3.8, the terminal conditions follow as:

$$I_a = I_c, \quad I = I_a - I_b, \quad V_a = ZI, \quad V_a + V_b + V_c = 0 \quad (3.54)$$

Hence

$$I_{a1} = \frac{1}{3} (I_a + aI_b + a^2I_c) = \frac{1}{3} (I_a - I_b)$$

$$I_{a2} = \frac{1}{3} (I_a + a^2I_b + aI_c) = \frac{1}{3} (I_a - I_b)$$

and

$$I_{a0} = \frac{1}{3} (I_a + I_b + I_c) = \frac{1}{3} (I_a + 2I_b) \quad (3.55)$$

i.e.

$$I_{a1} = I_{a2}$$

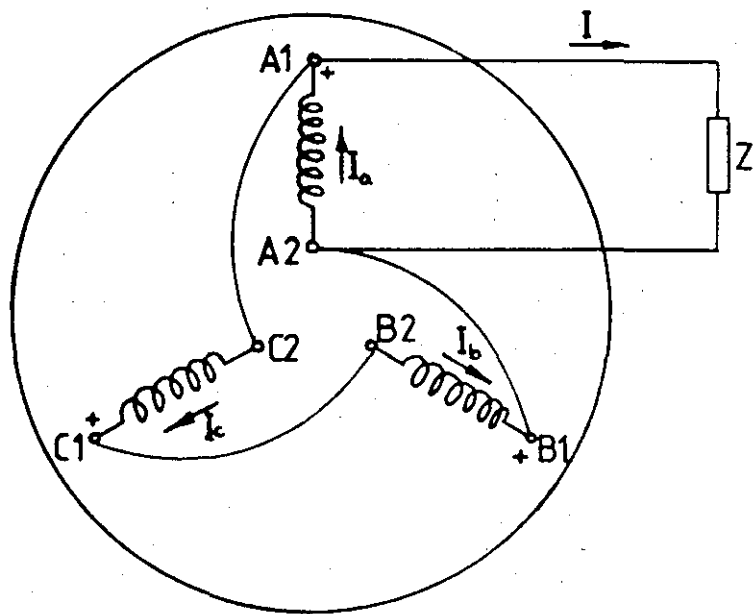


FIGURE 3.8: An Edison-delta connected synchronous generator

The equations for the phase sequence voltage drop are now

$$\begin{aligned} V_{a1} &= E - Z_1 I_{a1} = E - \frac{1}{3} Z_1 (I_a - I_b) \\ V_{a2} &= -Z_2 I_{a2} = -\frac{1}{3} Z_2 (I_a - I_b) \end{aligned} \quad (3.56)$$

and

$$V_{a0} = -I_{a0} Z_0 = -\frac{1}{3} Z_0 (I_a + 2I_b)$$

Since

$$V_a = V_{a0} + V_{a1} + V_{a2} = ZI$$

then

$$(Z_0 + Z_1 + Z_2 + 3Z)I_a + (2Z_0 - Z_1 - Z_2 - 3Z)I_b = 3E \quad (3.57)$$

and since

$$V_b + V_c = -V_{a1} - V_{a2} + 2V_{a0} = -ZI$$

or

$$-V_{a1} - V_{a2} + 2V_{a0} = -Z(I_a - I_b)$$

then

$$(-2Z_0 + Z_1 + Z_2 + 3Z)I_a - (4Z_0 + Z_1 + Z_2 + 3Z)I_b = 3E \quad (3.58)$$

Solving simultaneously equations (3.57) and (3.58)

$$I_a = \frac{2E}{Z_1 + Z_2 + 3Z} \quad I_b = -\frac{E}{Z_1 + Z_2 + 3Z} \quad (3.59)$$

and the load current is

$$I = I_a - I_b = \frac{3E}{Z_1 + Z_2 + 3Z} \quad (3.60)$$

The symmetrical components of the generator currents are

$$\begin{aligned}
 I_{a1} &= \frac{1}{3} (I_a - I_b) = \frac{E}{Z_1 + Z_2 + 3Z} \\
 I_{a2} &= \frac{1}{3} (I_a - I_b) = \frac{E}{Z_1 + Z_2 + 3Z} \\
 I_{a0} &= \frac{1}{3} (I_a + 2I_b) = 0
 \end{aligned}
 \tag{3.61}$$

and those of the voltages

$$\begin{aligned}
 V_{a1} &= E - Z_1 I_{a1} = \frac{(Z_2 + 3Z)E}{Z_1 + Z_2 + 3Z} \\
 V_{a2} &= -Z_2 I_{a2} = -\frac{Z_2 E}{Z_1 + Z_2 + 3Z} \\
 V_{a0} &= -Z_0 I_0 = 0
 \end{aligned}
 \tag{3.62}$$

and

$$V_{a0} = -Z_0 I_0 = 0$$

The phase voltages are therefore

$$\begin{aligned}
 V_a &= V_{a0} + V_{a1} + V_{a2} = \frac{3ZE}{Z_1 + Z_2 + 3Z} \\
 V_b &= V_{a0} + a^2 V_{a1} + a V_{a2} = \frac{[a(Z_2 + 3Z) - a^3 Z]E}{Z_1 + Z_2 + 3Z} \\
 V_c &= V_{a0} + a V_{a1} + a^2 V_{a2} = \frac{[a(Z_1 + 3Z) - 3Za^2]E}{Z_1 + Z_2 + 3Z}
 \end{aligned}
 \tag{3.63}$$

and

$$V_c = V_{a0} + a V_{a1} + a^2 V_{a2} = \frac{[a(Z_1 + 3Z) - 3Za^2]E}{Z_1 + Z_2 + 3Z}$$

The unbalance factor for the current is

$$\left| \frac{I_{a2}}{I_{a1}} \right| = 1$$

and that for the voltage is

$$\left| \frac{V_{a2}}{V_{a1}} \right| = \left| \frac{Z_2}{Z_2 + 3Z} \right|$$

### 3.2.3 Line-to-Line Loaded Generator

From the circuit diagram for a line-to-line loaded star-connected 3-phase synchronous generator shown in Figure 3.9, it is evident that

$$I_a = 0, \quad I_b = -I_c, \quad V_b = V_c - ZI_c \quad (3.64)$$

Hence

$$I_{a1} = \frac{1}{3} (I_a + aI_b + a^2I_c) = -j \frac{1}{\sqrt{3}} I_b$$

$$I_{a2} = \frac{1}{3} (I_a + a^2I_b + aI_c) = j \frac{1}{\sqrt{3}} I_b \quad (3.65)$$

$$I_{a0} = \frac{1}{3} (I_a + I_b + I_c) = 0$$

i.e.

$$I_{a1} = -I_{a2} = j \frac{I_b}{\sqrt{3}}$$

and the symmetrical components of the generator voltages are

$$\begin{aligned} V_{a1} &= \frac{1}{3} (V_a + aV_b + a^2V_c) = \frac{1}{3} [V_a - V_c - aZI_c] \\ & \quad (3.66) \\ V_{a2} &= \frac{1}{3} (V_a + a^2V_b + aV_c) = \frac{1}{3} [V_a - V_c - a^2ZI_c] \end{aligned}$$

It follows that

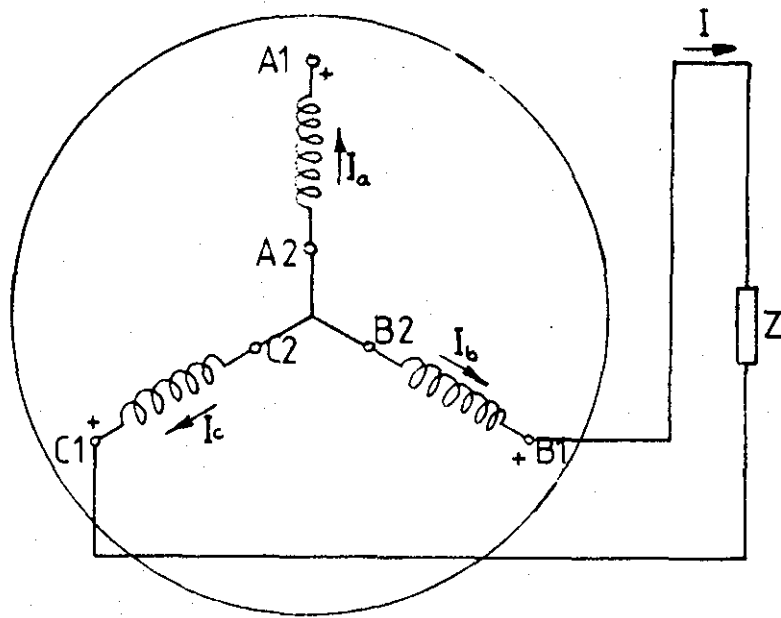


FIGURE 3.9: A line-to-line loaded star connected 3-phase synchronous generator

$$V_{a1} - V_{a2} = \frac{1}{3} (a_2 - a) I_c Z = I_{a1} Z$$

so that

$$V_{a1} = V_{a2} + Z I_{a1} \quad (3.67)$$

The equations for the phase sequence voltage drops are

$$V_{a1} = E - Z_1 I_{a1}$$

$$V_{a2} = - Z_2 I_{a2} \quad (3.68)$$

$$V_{a0} = - Z_0 I_{a0} = 0$$

so that

$$V_{a1} = - Z_2 I_{a2} + Z I_{a1} = (Z_2 + Z) I_{a1}$$

From equation (3.68)

$$E - Z_1 I_{a1} = (Z_2 + Z) I_{a2}$$

Therefore

$$I_{a1} = \frac{E}{Z_1 + Z_2 + Z}$$

and

$$I_{a2} = - I_{a1} = - \frac{E}{Z_1 + Z_2 + Z} \quad (3.69)$$

Having determined the symmetrical components of a phase current, the phase currents  $I_b$  and  $I_c$  are

$$I_b = I_{a0} + a_2 I_{a1} + a I_{a2} = - j \frac{\sqrt{3} E}{Z_1 + Z_2 + Z}$$

and

(3.70)

$$I_c = I_{a0} + aI_{a1} + a^2I_{a2} = \frac{j\sqrt{3} E}{Z_1 + Z_2 + Z}$$

respectively.

The symmetrical components of the generator voltages are

$$V_{a1} = (Z_2 + Z) I_{a1} = \frac{Z_2 + Z}{Z_1 + Z_2 + Z} E$$

and

(3.71)

$$V_{a2} = Z_2 I_{a2} = \frac{Z_2}{Z_1 + Z_2 + Z} E$$

respectively.

Hence the generator phase voltages are

$$\begin{aligned} V_a &= V_{a0} + V_{a1} + V_{a2} = \frac{(2Z_2 + Z)}{Z_1 + Z_2 + Z} E \\ V_b &= V_{a0} + a^2V_{a1} + aV_{a2} = \frac{a^2Z - Z_2}{Z_1 + Z_2 + Z} E \end{aligned} \quad (3.72)$$

and

$$V_c = V_{a0} + aV_{a1} + a^2V_{a2} = \frac{aZ - Z_2}{Z_1 + Z_2 + Z} E$$

With the unbalance factor being

$$\left| \frac{I_{a2}}{I_{a1}} \right| = 1$$

for the currents and

$$\left| \frac{V_{a2}}{V_{a1}} \right| = \left| \frac{Z_2}{Z_2 + Z} \right|$$

for the voltages.

### 3.2.4 Line-to-Neutral Loaded Generator

The terminal conditions which apply to the line-to-neutral loaded star-connected generator shown in Figure 3.10 are

$$I_b = 0, \quad I_c = 0, \quad V_a = ZI_a \quad (3.73)$$

Hence

$$\begin{aligned} I_{a1} &= \frac{1}{3} (I_a + aI_b + a^2I_c) = \frac{1}{3} I_a \\ I_{a2} &= \frac{1}{3} (I_a + a^2I_b + aI_c) = \frac{1}{3} I_a \end{aligned} \quad (3.74)$$

and 
$$I_{a0} = \frac{1}{3} (I_a + I_b + I_c) = \frac{1}{3} I_a$$

i.e. 
$$I_{a0} = I_{a1} = I_{a2}$$

and the phase sequence voltages are

$$\begin{aligned} V_{a1} &= E - Z_1 I_{a1} = E - \frac{1}{3} Z_1 I_a \\ V_{a2} &= -Z_2 I_{a2} = -\frac{1}{3} Z_2 I_a \end{aligned} \quad (3.75)$$

and 
$$V_{a0} = -I_{a0} Z_0 = -\frac{1}{3} Z_0 I_a$$

It follows from the terminal conditions that

$$\begin{aligned} V_a &= I_a Z = V_{a1} + V_{a2} + V_{a0} \\ &= -\frac{1}{3} Z_0 I_a + E - \frac{1}{3} Z_1 I_a - \frac{1}{3} Z_1 I_a \end{aligned}$$

so that

$$I_a = \frac{3E}{Z_0 + Z_1 + Z_2 + 3Z} \quad (3.76)$$

and the symmetrical components of the generator currents are

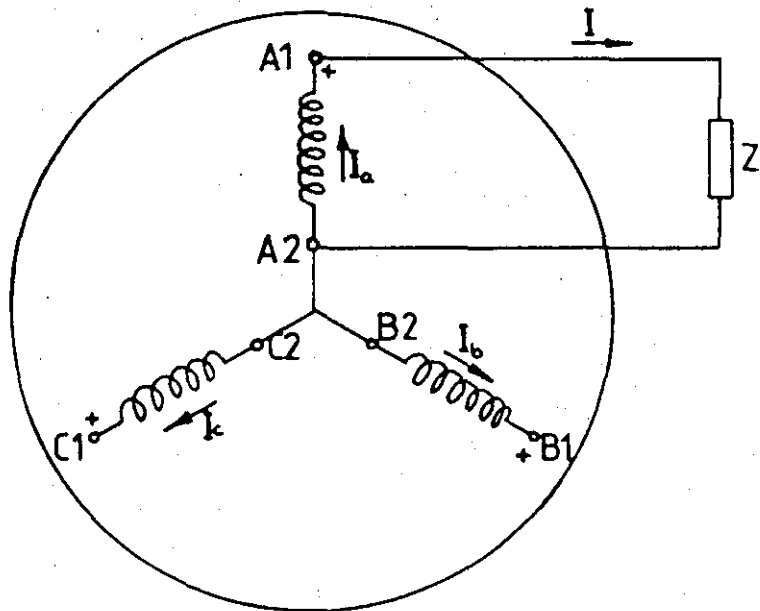


FIGURE 3.10: Line-to-neutral loaded star-connected synchronous generator

$$I_{a1} = I_{a2} = I_{a0} = \frac{E}{Z_0 + Z_1 + Z_2 + 3Z} \quad (3.77)$$

The corresponding symmetrical components of the voltages are

$$\begin{aligned} V_{a1} &= \frac{E(Z_0 + Z_2 + 3Z)}{Z_0 + Z_1 + Z_2 + 3Z} \\ V_{a2} &= \frac{-EZ_2}{Z_0 + Z_1 + Z_2 + 3Z} \\ V_{a0} &= \frac{-EZ_0}{Z_0 + Z_1 + Z_2 + 3Z} \end{aligned} \quad (3.78)$$

and those of the armature phase voltages are

$$\begin{aligned} V_a &= V_{a0} + V_{a1} + V_{a2} = \frac{3EZ}{Z_0 + Z_1 + Z_2 + 3Z} \\ V_b &= V_{a0} + a^2V_{a1} + aV_{a2} = \frac{(a^2-1)Z_0 + (a^2-a)Z_2 + 3a^2Z}{Z_0 + Z_1 + Z_2 + 3Z} E \\ V_c &= V_{a0} + aV_{a1} + a^2V_{a2} = \frac{(a-1)Z_0 + (a-a^2)Z_2 + 3aZ}{Z_0 + Z_1 + Z_2 + 3Z} E \end{aligned} \quad (3.79)$$

The unbalance factor for the generator currents is again

$$\left| \frac{I_{a2}}{I_{a1}} \right| = 1$$

while that for the voltage is now

$$\left| \frac{V_{a2}}{V_{a1}} \right| = \left| \frac{Z_0}{Z_0 + Z_2 + 3Z} \right|$$

### 3.3 CONCLUSIONS

The steady-state performance of various connections of a 3-phase synchronous generator have been investigated using a symmetrical component model. Mathematical expressions for the currents and voltages were derived and also expressions of unbalance factors for both currents and voltages were provided. Practical results using values of sequence reactances obtained experimentally were compared with theoretically derived results and these were found to agree reasonably satisfactorily. The discrepancy that exists is accounted for primarily by the presence of harmonics in the voltage and current waveforms. This is shown by the experimental voltage waveforms given later in Chapter 6, for various voltage settings. Other obvious reasons for these discrepancies are the use of unsaturated values for negative and zero sequence reactances, and the neglect of saliency in the development of the symmetrical component model for the 3-phase synchronous machine.

It is interesting to observe that the current unbalance factor for various single-phase connections is load independent and equal to unity. This is because any single-phase connected armature sets up a pulsating mmf which may be resolved into equal magnitude contra-rotating components. Since the magnitude of negative- and positive-sequence components is equal, the unbalance factor for currents for each case is unity.

CHAPTER 4PHASE MODEL FOR VARIOUS CONNECTIONS

Although both the transient and the steady-state performances of a conventional 3-phase synchronous generator have been investigated by many authors<sup>23,24</sup>, no attention appears to have been directed towards the performance of such a machine when the armature windings are arranged in a zig-zag or Edison-delta connection. The present chapter investigates therefore both the transient and the steady-state performance associated with these connections.

A prediction of either the transient or the steady-state performance of a generator requires the development of a mathematical model, in the form of a set of simultaneous ordinary differential equations. The standard simplifying assumptions which are involved in this development are:

- a) The air-gap mmf and the flux density are both sinusoidally distributed in space, so that the phase-to-phase mutual inductance coefficients and the phase self-inductance coefficients are simple trigonometric functions of the rotor position.
- b) The effect of magnetic saturation on both axes is negligible.
- c) There is only one damper winding on each axis.
- d) The effect of hysteresis and eddy currents is negligible.
- e) The speed of the generator is assumed to remain constant after any disturbance, i.e. the generator drive is stiff.

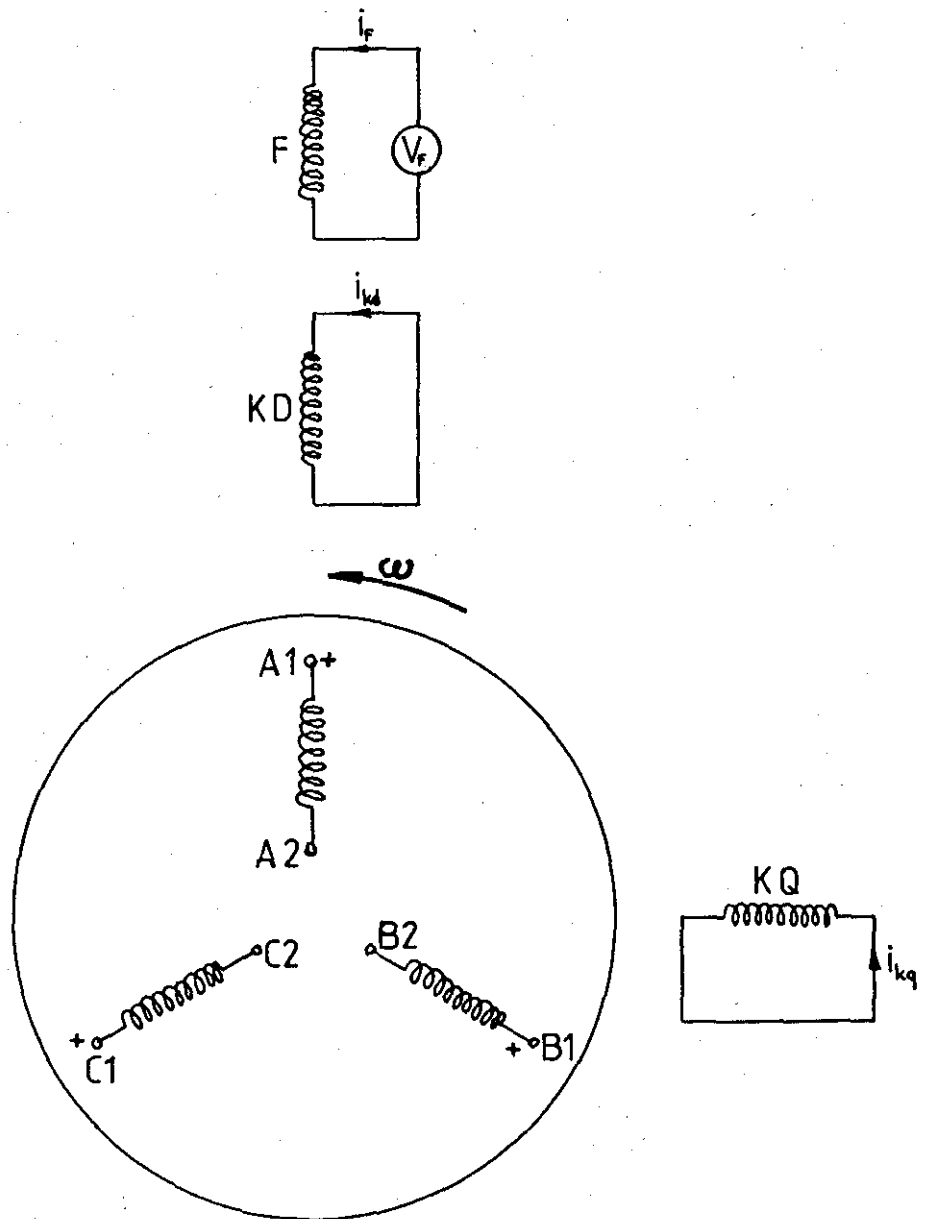


FIGURE 4.1: The primitive synchronous generator

$v_a$	$R + pL_{11}$	$pM_{12}$	$pM_{13}$	$pM_{14}$	$pM_{15}$	$pM_{16}$	$i_a$
$v_b$	$pM_{21}$	$R + pL_{22}$	$pM_{23}$	$pM_{24}$	$pM_{25}$	$pM_{26}$	$i_b$
$v_c$	$pM_{31}$	$pM_{32}$	$R + pL_{33}$	$pM_{34}$	$pM_{35}$	$pM_{36}$	$i_c$
$v_f$	$pM_{41}$	$pM_{42}$	$pM_{43}$	$R_{44} + pL_{44}$	$pM_{45}$	0	$i_f$
0	$pM_{51}$	$pM_{52}$	$pM_{53}$	$pM_{54}$	$R_{55} + pL_{55}$	0	$i_{kd}$
0	$pM_{61}$	$pM_{62}$	$pM_{63}$	0	0	$R_{66} + pL_{66}$	$i_{kq}$

EQUATION 4.1: Differential equation for the primitive synchronous generator

#### 4.1 STATE EQUATIONS FOR A 3-PHASE SYNCHRONOUS GENERATOR

The differential equations for various connections of a 3-phase generator may be obtained from the corresponding equations of the primitive machine shown in Figure 4.1. The associated differential equations, given in matrix form in equation 4.1, may be written in abbreviated form as:

$$[V] = p[L][I] + [R][I] \quad (4.2)$$

where  $V$  is the voltage vector

$I$  is the current vector

$R$  is the resistance matrix

$L$  is the inductance matrix.

Since some of the inductance terms are time variant, the general form of equation 4.2 is:

$$[V] = [L][pI] + [R+G][I] \quad (4.3)$$

where  $[G] = \frac{d}{dt} [L] = \frac{d}{d\theta} [L] \frac{d\theta}{dt}$

If the generator is driven at constant speed  $\omega = \frac{d\theta}{dt}$  - constant then

$$[G] = \omega \frac{d[L]}{dt} \quad (4.4)$$

and the state-variable form of equation 4.3 becomes

$$[pI] = [L]^{-1} [[V] - [R+G][I]] \quad (4.5)$$

where  $[G]$  is the time-rate-of-change of inductance matrix.

## 4.2 INDUCTANCE AND TIME-RATE-OF-CHANGE OF INDUCTANCE COEFFICIENTS

### 4.2.1 Inductance Coefficients

The inductance coefficients forming the  $[L]$  matrix of equations 4.2 and 4.3 are in general dependent on the rotor position, and they have therefore to be calculated at each step of a numerical integration of these equations. Since the model neglects any effects of saturation, the inductances are not functions of currents.

#### 4.2.1.1 Stator Self-Inductance

The phase winding self-inductances are<sup>25,26,27</sup>

$$\begin{aligned} L_{11} &= L_{A0} + L_2 \cos 2\theta \\ L_{22} &= L_{A0} + L_2 \cos (2\theta - 240^\circ) \\ L_{33} &= L_{A0} + L_2 \cos (2\theta - 120^\circ) \end{aligned} \quad (4.6)$$

where both  $L_{A0}$  and  $L_2$  are constant.

#### 4.2.1.2 Rotor self-inductance

The rotor self-inductances are<sup>25,26,27</sup>

$$L_{44} = L_f$$

$$L_{55} = L_{kd} \quad (4.7)$$

$$L_{66} = L_{kq}$$

#### 4.2.1.3 Stator mutual inductances

The phase-to-phase mutual inductances are<sup>25,26,27</sup>

$$M_{12} = M_{21} = -M_0 + M_2 \cos (2\theta - 120^\circ)$$

$$M_{23} = M_{32} = -M_0 + M_2 \cos 2\theta \quad (4.8)$$

$$M_{13} = M_{31} = -M_0 + M_2 \cos (2\theta - 240^\circ)$$

where both  $M_0$  and  $M_2$  are constant.

#### 4.2.1.4 Rotor mutual inductances

The mutual inductance between the field winding and the d-axis damper winding does not vary with the rotor position. So that<sup>25,26,27</sup>

$$M_{45} = M_{54} = M_{fkd}$$

$$M_{46} = M_{64} = 0 \quad (4.9)$$

$$M_{56} = M_{65} = 0$$

#### 4.2.1.5 Stator-to-rotor mutual inductances

Finally, we consider the mutual inductances between the stator and rotor windings, all of which are functions of the rotor position. The mutual inductances between the various phase windings and the field winding are<sup>25,26,27</sup>

$$\begin{aligned}
 M_{14} &= M_{41} = M_f \cos \theta \\
 M_{24} &= M_{42} = M_f \cos (\theta - 120^\circ) \\
 M_{34} &= M_{43} = M_f \cos (\theta - 240^\circ)
 \end{aligned} \tag{4.10}$$

The phase to d-axis damper winding mutual inductances are

$$\begin{aligned}
 M_{15} &= M_{51} = M_d \cos \theta \\
 M_{25} &= M_{52} = M_d \cos (\theta - 120^\circ) \\
 M_{35} &= M_{53} = M_d \cos (\theta - 240^\circ)
 \end{aligned} \tag{4.11}$$

and the mutual inductances between phase and q-axis damper winding are

$$\begin{aligned}
 M_{16} &= M_{61} = M_q \sin \theta \\
 M_{26} &= M_{62} = M_q \sin (\theta - 120^\circ) \\
 M_{36} &= M_{63} = M_q \sin (\theta - 240^\circ)
 \end{aligned} \tag{4.12}$$

#### 4.2.2 Time-Rate-of-Change of Inductance Coefficients

##### 4.2.2.1 Time-Rate-of-change of stator self-inductance

The time-rate-of-change of the self-inductances of the phase windings are obtained by differentiating the stator self inductances with respect to times

$$\begin{aligned} G_{11} &= -2\omega_0 L_2 \sin 2\theta \\ G_{22} &= -2\omega_0 L_2 \sin (2\theta - 240^\circ) \\ G_{33} &= -2\omega_0 L_2 \sin (2\theta - 120^\circ) \end{aligned} \quad (4.13)$$

##### 4.2.2.2 Time-Rate-of-change of rotor self-inductance

Since the rotor self-inductances are constant, their rates-of-change are zero:

$$\begin{aligned} G_{44} &= 0 \\ G_{55} &= 0 \\ G_{66} &= 0 \end{aligned} \quad (4.14)$$

##### 4.2.2.3 Time-Rate-of-change of stator mutual inductance

The rate-of-change of the phase-to-phase mutual inductances are obtained by differentiating the stator self inductances with respect to time

$$\begin{aligned} G_{12} = G_{21} &= -2\omega_0 M_2 \sin (2\theta - 120^\circ) \\ G_{23} = G_{32} &= -2\omega_0 M_2 \sin 2\theta \\ G_{13} = G_{31} &= -2\omega_0 M_2 \sin (2\theta - 240^\circ) \end{aligned} \quad (4.15)$$

#### 4.2.2.4 Time-Rate-of-change of rotor mutual inductances

The mutual inductance between the field and the d-axis damper winding does not vary with the rotor position and its time-rate-of-change is, therefore, zero. Similarly, since the mutual inductances between the d- and q-axes are also zero:

$$G_{45} = G_{54} = 0$$

$$G_{46} = G_{64} = 0 \quad (4.16)$$

$$G_{56} = G_{65} = 0$$

#### 4.2.2.5 Time-Rate-of-change of stator-to-rotor mutual inductances

The time-rate-of-change of the mutual inductance between the phase windings and the field winding are obtained from equation 4.10

$$G_{14} = G_{41} = -\omega_0 M_f \sin \theta$$

$$G_{24} = G_{42} = -\omega_0 M_f \sin(\theta - 120^\circ) \quad (4.17)$$

$$G_{34} = G_{43} = -\omega_0 M_f \sin(\theta - 240^\circ)$$

Similarly, the time-rate-of-change of the phase winding to d-axis damper winding mutual inductances are, obtained from equation 4.11

$$G_{15} = G_{51} = -\omega_0 M_d \sin \theta$$

$$G_{25} = G_{52} = -\omega_0 M_d \sin(\theta - 120^\circ) \quad (4.18)$$

$$G_{35} = G_{53} = -\omega_0 M_d \sin(\theta - 240^\circ)$$

and the rates-of-change of the phase winding to q-axis damper winding mutual inductances are, obtained from equation 4.12

$$\begin{aligned}
 G_{16} &= G_{61} = \omega_0 M_q \cos \theta \\
 G_{26} &= G_{62} = \omega_0 M_q \cos (\theta - 120^\circ) \\
 G_{36} &= G_{63} = \omega_0 M_q \cos (\theta - 240^\circ)
 \end{aligned} \tag{4.19}$$

#### 4.3 STATE EQUATIONS FOR VARIOUS CONNECTIONS

The connection matrix which relates the currents in the zig-zag connection to those of the primitive synchronous generator may be written from inspection of Figure 4.2 as

$$\begin{bmatrix} i_a \\ i_b \\ i_c \\ i_f \\ i_{kd} \\ i_{kq} \end{bmatrix} = \begin{bmatrix} 1 & & & & & \\ & -1 & & & & \\ & & -1 & & & \\ & & & 1 & & \\ & & & & 1 & \\ & & & & & 1 \end{bmatrix} \begin{bmatrix} i_1 \\ i_2 \\ i_f \\ i_{kd} \\ i_{kq} \end{bmatrix} \tag{4.20}$$

When written in abbreviated matrix form, equation 4.20 becomes

$$I = CI'$$

where the connection matrix C is given by



$$C = \begin{pmatrix} 1 & 1 & & & & \\ & 1 & & & & \\ & & 1 & & & \\ & & & 1 & & \\ & & & & 1 & \\ & & & & & 1 \end{pmatrix} \quad (4.23)$$

where,

$I = [i_a \ i_b \ i_c \ i_f \ i_{kd} \ i_{kq}]^t$ , denotes the currents in the primitive synchronous generator.

and

$I' = [i_1 \ i_2 \ i_f \ i_{kd} \ i_{kq}]^t$ , denotes the currents in the Edison-delta connected synchronous generator.

The matrix operational equation for various generator connections may be obtained by using the standard impedance transformation  $C^T Z C$  (where  $C^T$  is the transpose of  $C$ ). The matrix operational equation for various generator connections can be rearranged in the state-variable form

$$[pI'] = [L'][[V'] - [R'+G']I']$$

which can be solved using the numerical integration technique described in Appendix IV, to arrive at the machine currents.

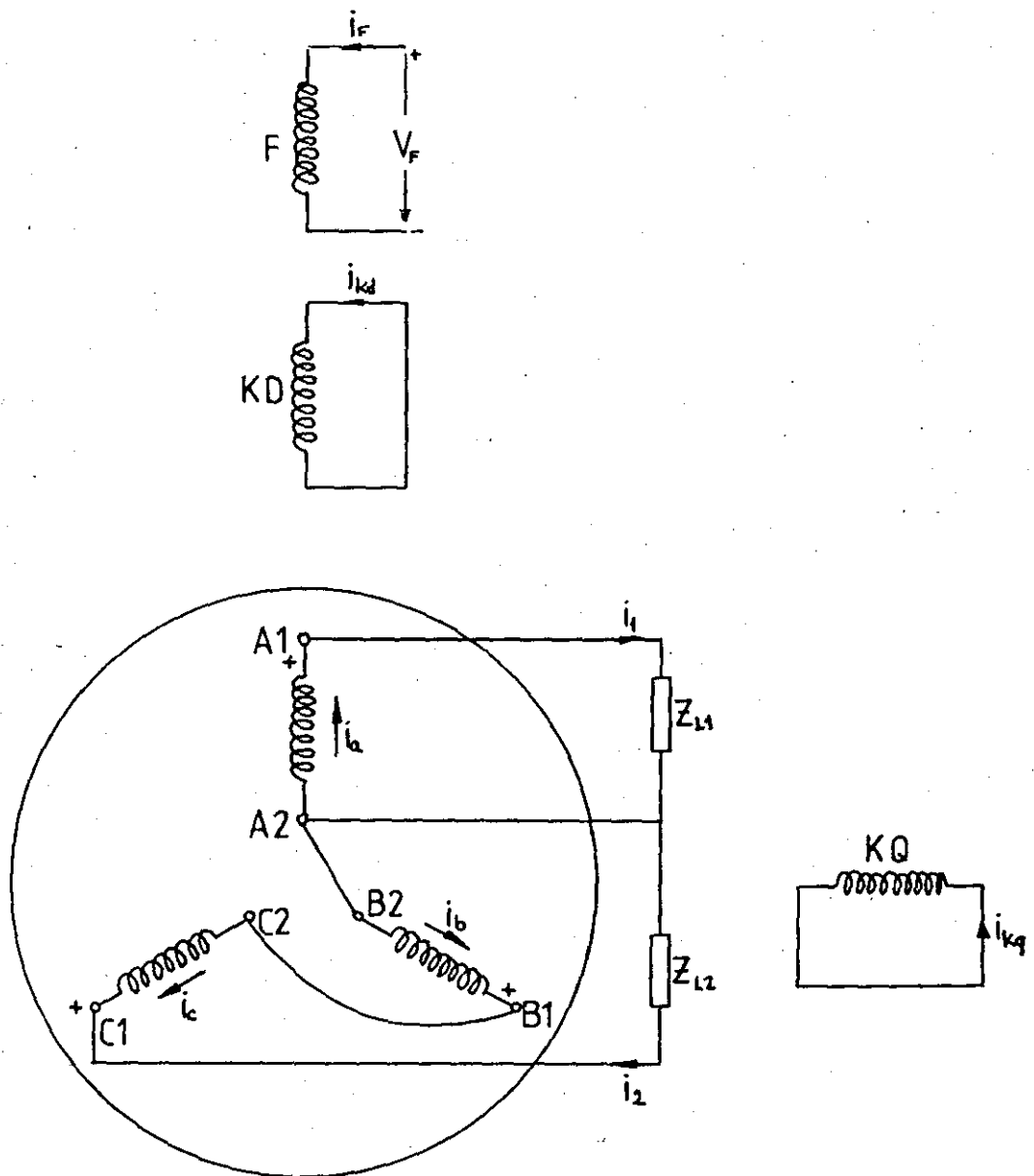


FIGURE 4.2: A zig-zag connected 3-phase synchronous generator in load

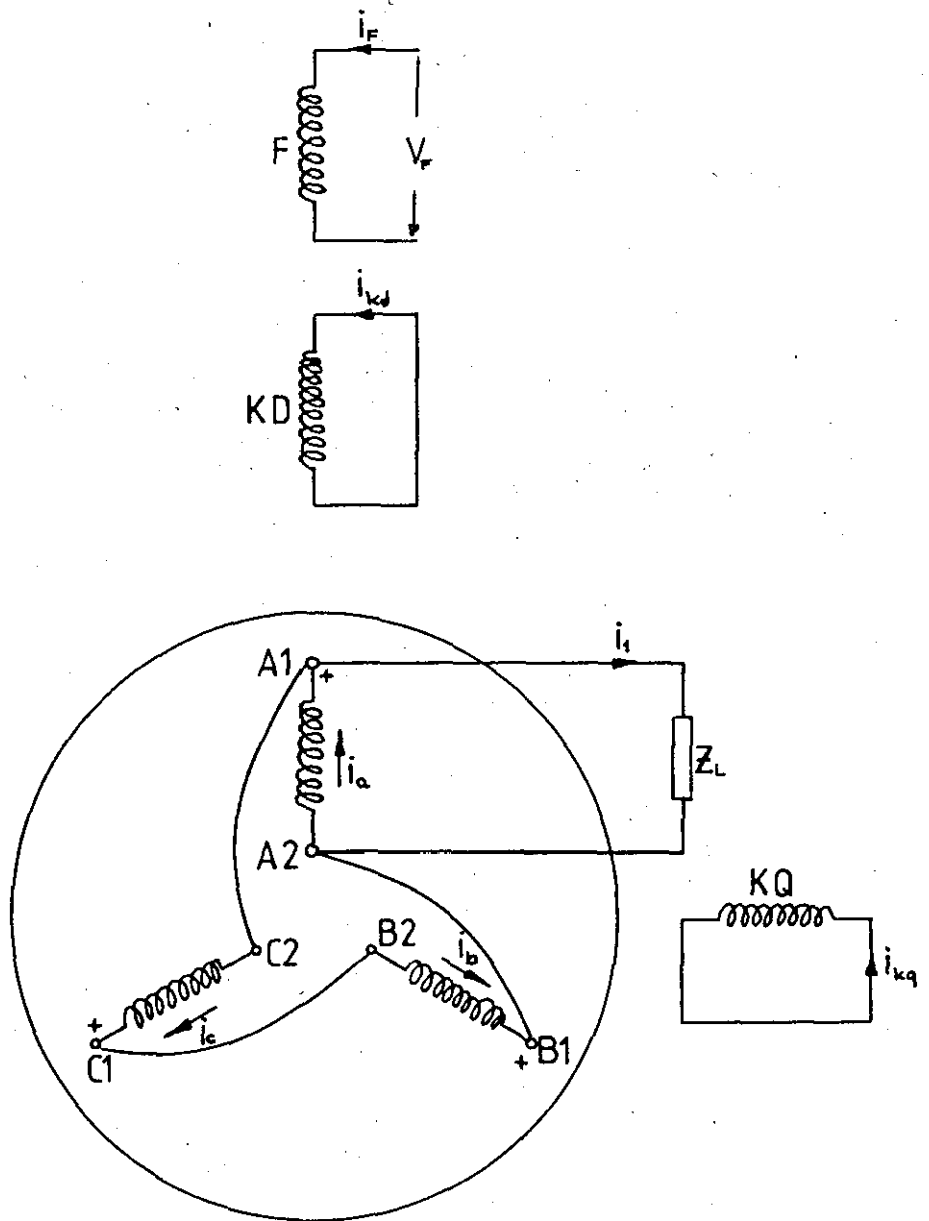


FIGURE 4.3: Edison-delta connected synchronous generator

0	$R + R_{L1}$ $+p(L_{11} + L_{L1})$	$-p(M_{12} + M_{13})$	$pM_{14}$	$pM_{15}$	$pM_{16}$	$i_1$	
0		$2R + R_{L2}$ $+p(L_{22} + L_{33} + 2L_{23} + L_{L2})$	$-p(M_{24} + M_{34})$	$-p(M_{25} + M_{35})$	$-p(M_{26} + M_{36})$	$i_2$	
$v_f$	Symmetrical about the leading diagonal		$R_{44} + pL_{44}$	$pM_{45}$	0	$i_f$	
0				$R_{55} + pL_{55}$	0	$i_{kd}$	
0						$R_{66} + pL_{66}$	$i_{kq}$

Equation 4.24: Differential equation for a zig-zag connected 3-phase synchronous generator

[L] =

$L_{A0} + L_{L1}$ $+ L_2 \cos 2\theta$	$2M_0 + M_2 \cos 2\theta$	$M_f \cos \theta$	$M_d \cos \theta$	$M_q \sin \theta$
	$L_{L2} + 2L_{A0} - 2M_0$ $+ (2M_2 - L_2) \cos 2\theta$	$M_f \cos \theta$	$M_d \cos \theta$	$M_q \sin \theta$
		$L_{44}$	$M_{45}$	0
			$L_{55}$	0
				$L_{66}$

Symmetrical about  
the leading diagonal

Equation 4.25: Inductance matrix for a zig-zag connected 3-phase synchronous generator

[G] =

$-2 \omega_0 L_2 \sin 2\theta$	$-2 \omega_0 M_2 \sin 2\theta$	$-\omega_0 M_f \sin \theta$	$-\omega_0 M_d \sin \theta$	$\omega_0 M_q \cos \theta$
	$-2 \omega_0 (2M_2 - L_2) \sin 2\theta$	$-\omega_0 M_f \sin \theta$	$-\omega_0 M_d \sin \theta$	$\omega_0 M_q \cos \theta$
Symmetrical about the leading diagonal		0	0	0
			0	0
				0

Equation 4.26 Time-Rate-of-change of the inductance matrix for a zig-zag connected 3-phase synchronous generator

[R] =

$R+R_{L1}$	0	0	0	0
	$2R+R_{L2}$	0	0	0
		$R_{44}$	0	0
			$R_{55}$	0
				$R_{66}$

Symmetrical about  
the leading diagonal

Equation 4.27: Resistance matrix for a zig-zag connected 3-phase synchronous generator

0	$R+R_L+p(L_{11}+L_L)$	$R+p(L_{11}+M_{12}+M_{13})$	$pM_{14}$	$pM_{15}$	$pM_{16}$	$i_1$
0		$3R+p(L_{11}+L_{22}+L_{33}+2M_{12}+2M_{13}+2M_{23})$	$p(M_{14}+M_{24}+M_{34})$	$p(M_{15}+M_{25}+M_{35})$	$p(M_{16}+M_{26}+M_{36})$	$i_2$
$v_f$	=		$R_{44}+pL_{44}$	$M_{45}$	0	$i_f$
0	Symmetrical about the leading diagonal			$R_{55}+pL_{55}$	0	$i_{kd}$
0					$R_{66}+pL_{66}$	$i_{kq}$

Equation 4.28: Differential equation for an Edison-delta connected synchronous generator

[L] =

$L_{A0} + L_L$ $+ L_2 \cos 2\theta$	$(L_{A0} - 2M_0)$ $+ (L_2 - M_2) \cos 2\theta$	$M_f \cos \theta$	$M_d \cos \theta$	$M_q \sin \theta$
	$3(L_{A0} - 2M_0)$	0	0	0
		$L_{44}$	$M_{45}$	0
			$L_{55}$	0
				$L_{66}$

Symmetrical about  
the leading diagonal

Equation 4.29: Inductance matrix for an Edison-delta connected synchronous generator

[G] =

$-2\omega L_2 \sin 2\theta$	$-2\omega(L_2 - M_2) \sin 2\theta$	$-\omega M_f \sin \theta$	$-\omega M_d \sin \theta$	$\omega M_q \cos \theta$
	0	0	0	0
		0	0	0
			0	0
				0

Symmetrical about  
the leading diagonal

Equation 4.30: Time-Rate-of-change of inductance matrix for an Edison-delta connected synchronous generator

[R] =

$R+R_L$	$R$	$0$	$0$	$0$
	$3R$	$0$	$0$	$0$
		$R_{44}$	$0$	$0$
			$R_{55}$	$0$
				$R_{66}$

Symmetrical about  
the leading diagonal

Equation 4.31: Resistance matrix for an Edison-delta connected synchronous generator

#### 4.4 TRANSIENT FAULT TESTS

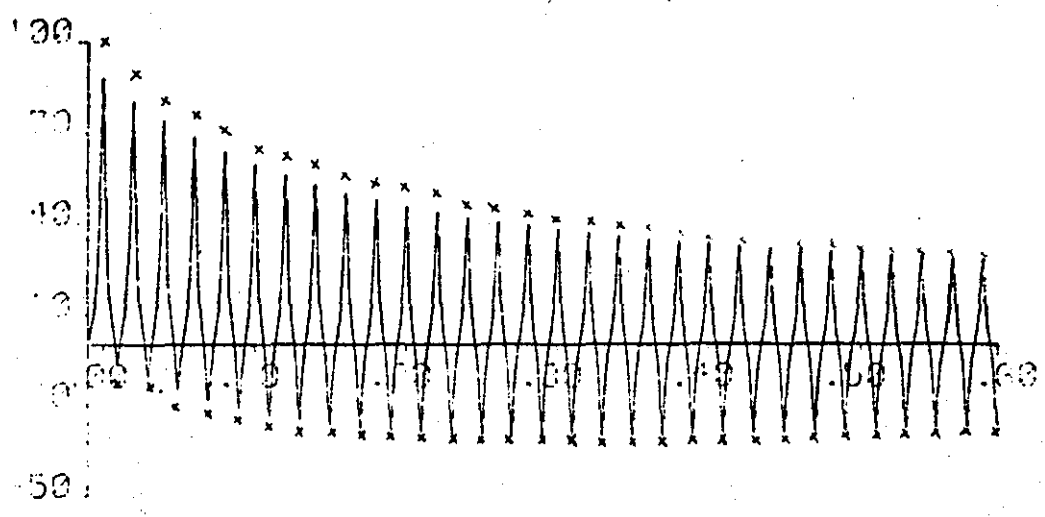
Short-circuit tests are useful for verifying the validity of the various assumptions made in Section 4 in the development of the machine model and also of the numerical technique described for predicting generator performance.

Various short-circuit fault tests were carried out on the experimental machine. During the short-circuit tests the generator was run at synchronous speed with its field winding excited to give rated voltage on open-circuit in the phase windings, with the armature windings connected in the different configurations considered previously. Various short-circuit faults were applied at the terminals of the unloaded generator and ultra-violet recordings of the armature and field currents were taken. Figures 4.4, 4.5 and 4.6 show both the experimental and computed results obtained when a line (1)-to-centre point, line (2)-to-centre point and double line-to-centre point fault of a zig-zag connected generator respectively. Figure 4.7 shows both the experimental and computed result when a line-to-line short-circuit fault of an Edison-delta connected generator.

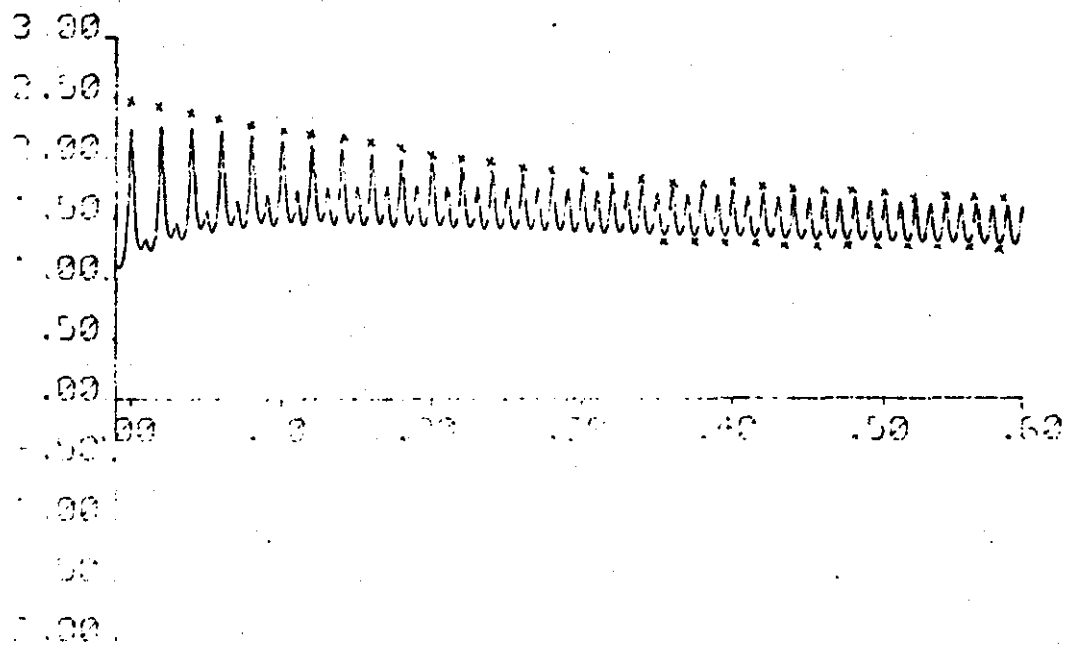
One feature of particular interest in the figures is that the unbalanced armature short-circuit currents contain substantial third-harmonic components, and the existence of these may be qualitatively explained by the following argument. The fault current in the armature winding sets up a pulsating field, which can be resolved into two counter-rotating mmf fields in the air-gap of the alternator. There is no relative motion between the positively-rotating field (which is the source of the single-phase armature reaction) and the field winding, but the negatively-rotating field travels relatively to the field winding at twice synchronous speed. Double-frequency voltages are thereby induced in the field winding, and since this is assumed to be supplied from a source of zero impedance, a substantial double-frequency current will result. This will in turn establish a field pulsating at double frequency along

the axis of the field winding which may be resolved into two counter-rotating air-gap fields. The negatively-rotating field travels backwards relatively to the armature winding at synchronous speed and thereby gives rise to negative-sequence voltages of fundamental frequency in the armature windings. The positively-rotating field travels relatively to the armature windings at three times synchronous speed, and thereby generates third-harmonic voltages of zero sequence in the armature windings.

The close agreement between the experimental and predicted results gives a high degree of confidence in the techniques employed.

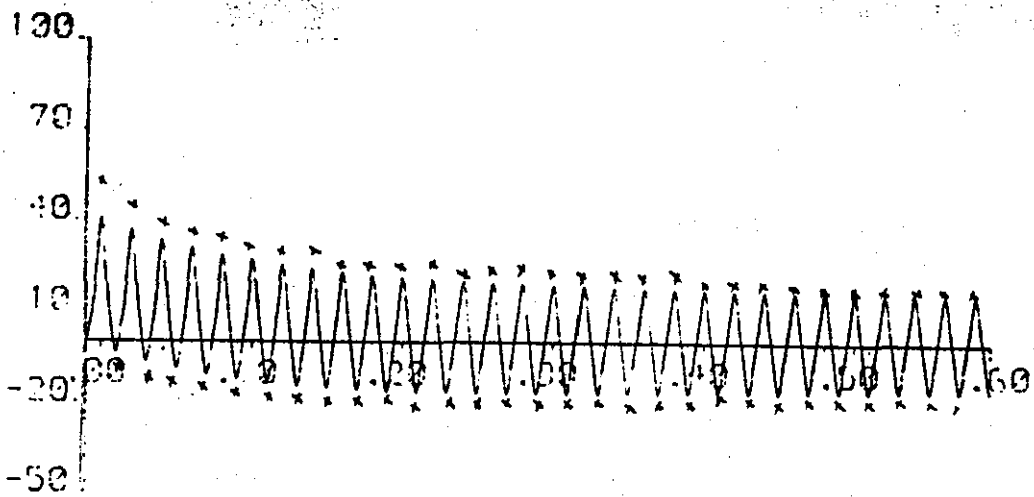


Armature current

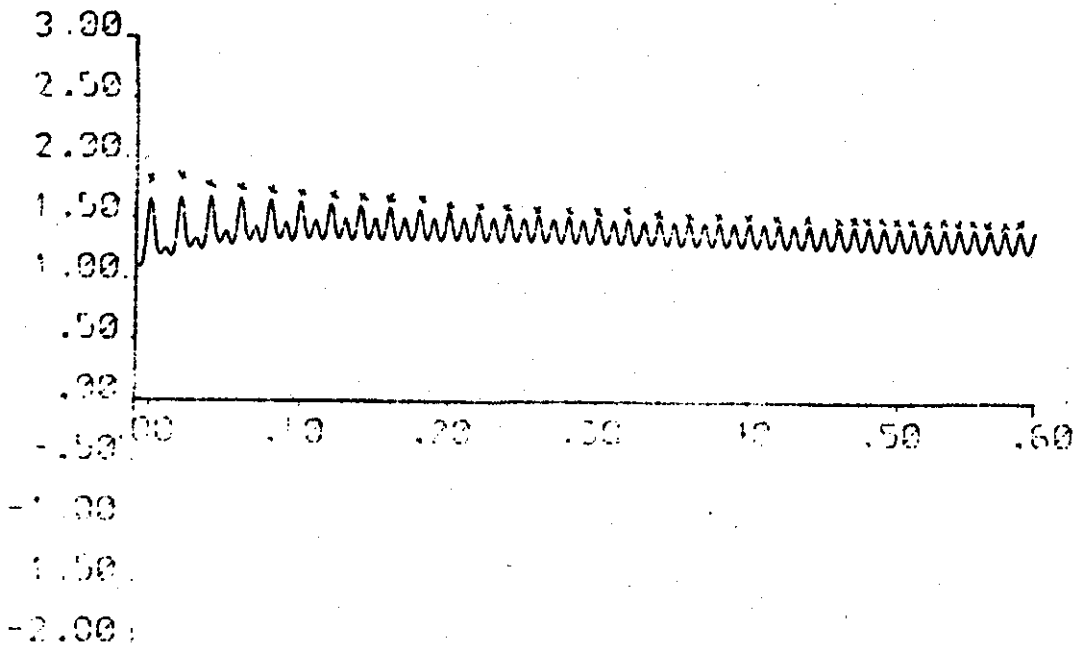


Field current

FIGURE 4.4: Line (1)-to-centre point fault for zig-zag connected synchronous generator

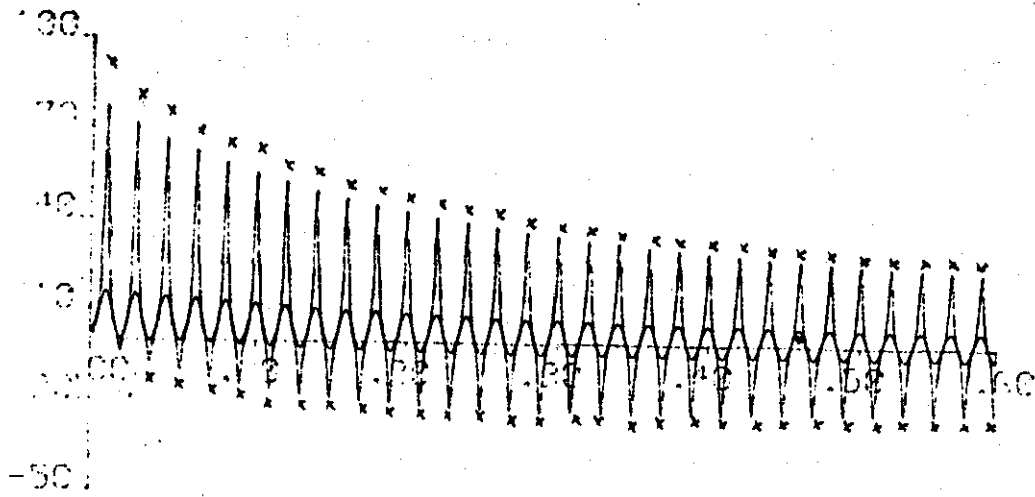


Armature current

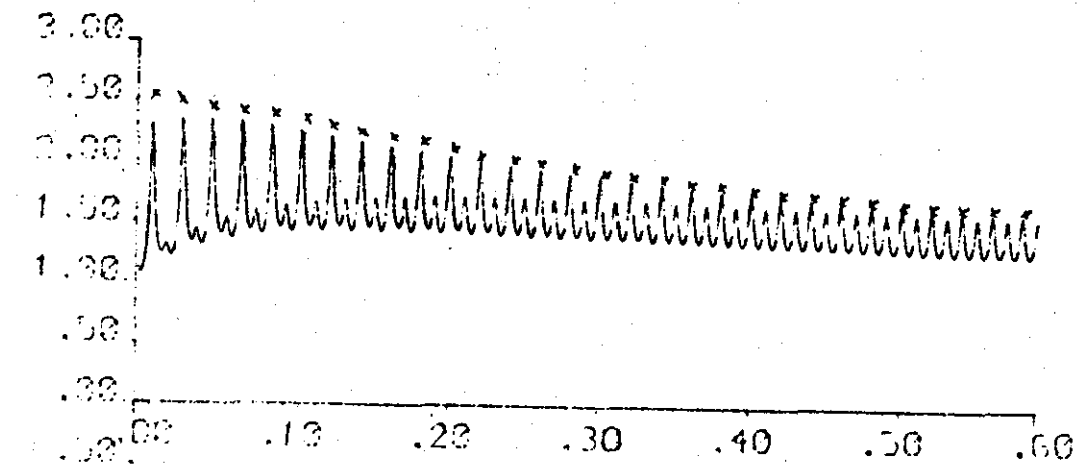


Field current

FIGURE 4.5: : Line (2)-to-center point fault for zig-zag connected synchronous generator

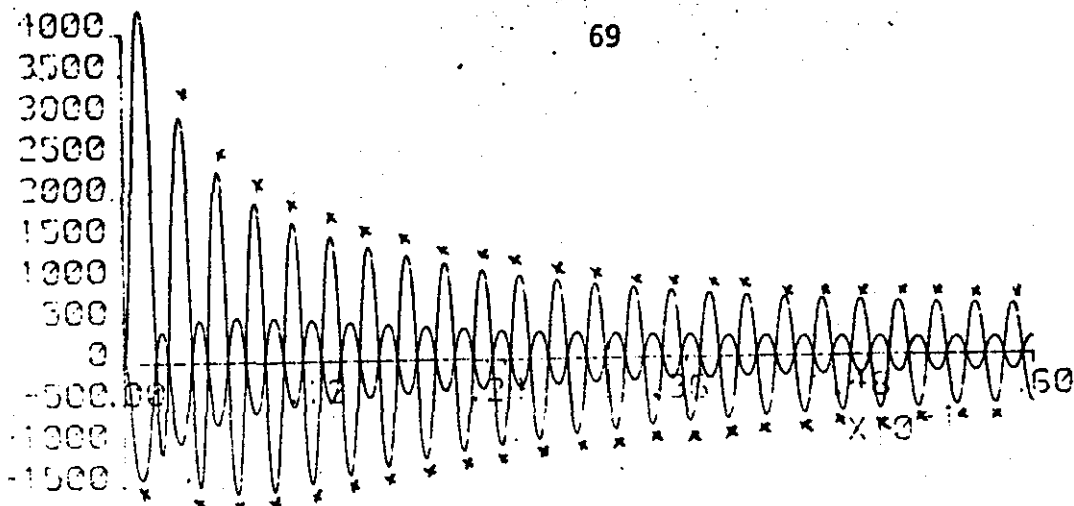


Armature current

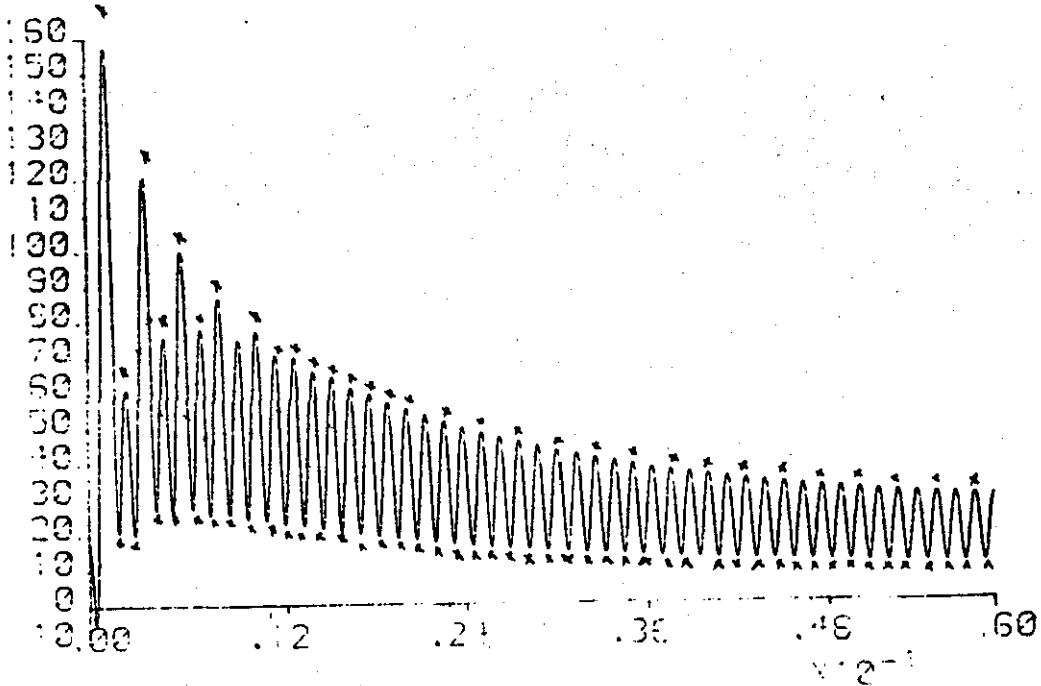


Field current

FIGURE 4.6: Double line-to-centre point fault for zig-zag connected generator



Armature current



Field current

FIGURE 4.7: Line-to-line fault for an Edison delta connected generator

CHAPTER 5 $\alpha, \beta, \gamma$  COMPONENT MODEL FOR VARIOUS GENERATOR CONNECTIONS

This chapter deals with an analytical solution for the short-circuit situation in a zig-zag or an Edison-delta connected generator. For this purpose, the direct phase equations are written down for an ideal salient-pole synchronous machine<sup>28,29</sup>, and a modified d-q-0 transformation<sup>30,31</sup> followed by an  $\alpha, \beta, \gamma$  transformation<sup>32,33,34,35,36</sup> is subsequently applied. The advantage of the modified d-q-0 transformation over the conventional d-q-0 transformation<sup>37,38</sup> is that it results in a symmetrical inductance matrix with reciprocal mutual inductances. The  $\alpha, \beta, \gamma$  transformation has the advantage of being power invariant, unlike the  $\alpha, \beta, 0$  transformation<sup>39,40,41</sup>. These various transformations are presented in Appendix VII.

The ideal generator considered in this chapter comprises a stator with three physically-identical armature windings a, b and c, displaced mutually by  $120^\circ$  (electrical) degrees. On the rotor there is a field circuit, symmetrical about the d-axis. Damper windings are not considered here, since these increase the complexity of the mathematical manipulations involved, and also necessitate a questionable extra simplifying assumption<sup>35</sup>. Assuming the machine to be ideal means that all the assumptions given in Chapter 4 are valid, although the additional assumption must be made that the second-harmonic components of the armature phase inductance and the phase-to-phase mutual inductance are equal. Under these conditions the application of either a conventional or a modified d-q-0 transformation yields equations in the d-q reference frame with no time-varying coefficients and thereby enables an analytical solution to be produced.

In an ideal synchronous machine, the flux linkages of the phase and field windings<sup>28,29</sup> are

$$\begin{aligned}
 \psi_a &= L_{11}i_a + M_{12}i_b + M_{13}i_c + M_{14}i_f \\
 \psi_b &= M_{21}i_a + L_{22}i_b + M_{23}i_c + M_{24}i_f \\
 \psi_c &= M_{31}i_a + M_{32}i_b + L_{33}i_c + M_{34}i_f \\
 \psi_f &= M_{41}i_a + M_{42}i_b + M_{43}i_c + L_{44}i_f
 \end{aligned} \tag{5.1}$$

while the various self-inductances are

$$\begin{aligned}
 L_{11} &= L_{A0} + L_m \cos 2\theta \\
 L_{22} &= L_{A0} + L_m \cos (2\theta - 240^\circ) \\
 L_{33} &= L_{A0} + L_m \cos (2\theta - 120^\circ) \\
 L_{44} &= L_f \\
 M_{12} &= M_{21} = -M_0 + L_m \cos (2\theta - 120^\circ) \\
 M_{23} &= M_{32} = -M_0 + L_m \cos 2\theta \\
 M_{13} &= M_{31} = -M_0 + L_m \cos (2\theta - 240^\circ) \\
 M_{14} &= M_{41} = M_f \cos \theta \\
 M_{24} &= M_{42} = M_f \cos (\theta - 120^\circ) \\
 M_{34} &= M_{43} = M_f \cos (\theta - 240^\circ)
 \end{aligned} \tag{5.2}$$

Park's transformation, as modified by Lewis<sup>30,31</sup> is

$$\begin{aligned}
 f_d &= \sqrt{\frac{2}{3}} [f_a \cos \theta + f_b \cos (\theta - 120^\circ) + f_c \cos (\theta - 240^\circ)] \\
 f_q &= \sqrt{\frac{2}{3}} [f_a \sin \theta + f_b \sin (\theta - 120^\circ) + f_c \sin (\theta - 240^\circ)] \\
 f_o &= \frac{1}{3} [f_a + f_b + f_c]
 \end{aligned}
 \tag{5.3}$$

where  $f$  may represent the currents  $i$ , voltages  $v$  or flux linkages  $\psi$  of the generator.

After much mathematical manipulation, application of the modified Park transformation to the flux/current equations leads to the flux-linkage equation<sup>30</sup>

$$\begin{aligned}
 \psi_d &= L_d i_d + \sqrt{\frac{3}{2}} M_f i_f \\
 \psi_q &= L_q i_q \\
 \psi_o &= L_\gamma i_o \\
 \psi_f &= \sqrt{\frac{3}{2}} M_f i_d + L_f i_f
 \end{aligned}
 \tag{5.4}$$

where

$$\begin{aligned}
 L_d &= L_{AO} + M_o + \frac{3}{2} L_m \\
 L_q &= L_{AO} + M_o - \frac{3}{2} L_m \\
 L_\gamma &= L_{AO} - 2M_o
 \end{aligned}
 \tag{5.5}$$

The advantage of the modified d-q transformation is evident from the reciprocal form of the mutual inductances in the flux linkage equation (5.4). The circuit representation of a synchronous generator by d-axis, q-axis and zero-sequence windings is given in Figure 5.1.

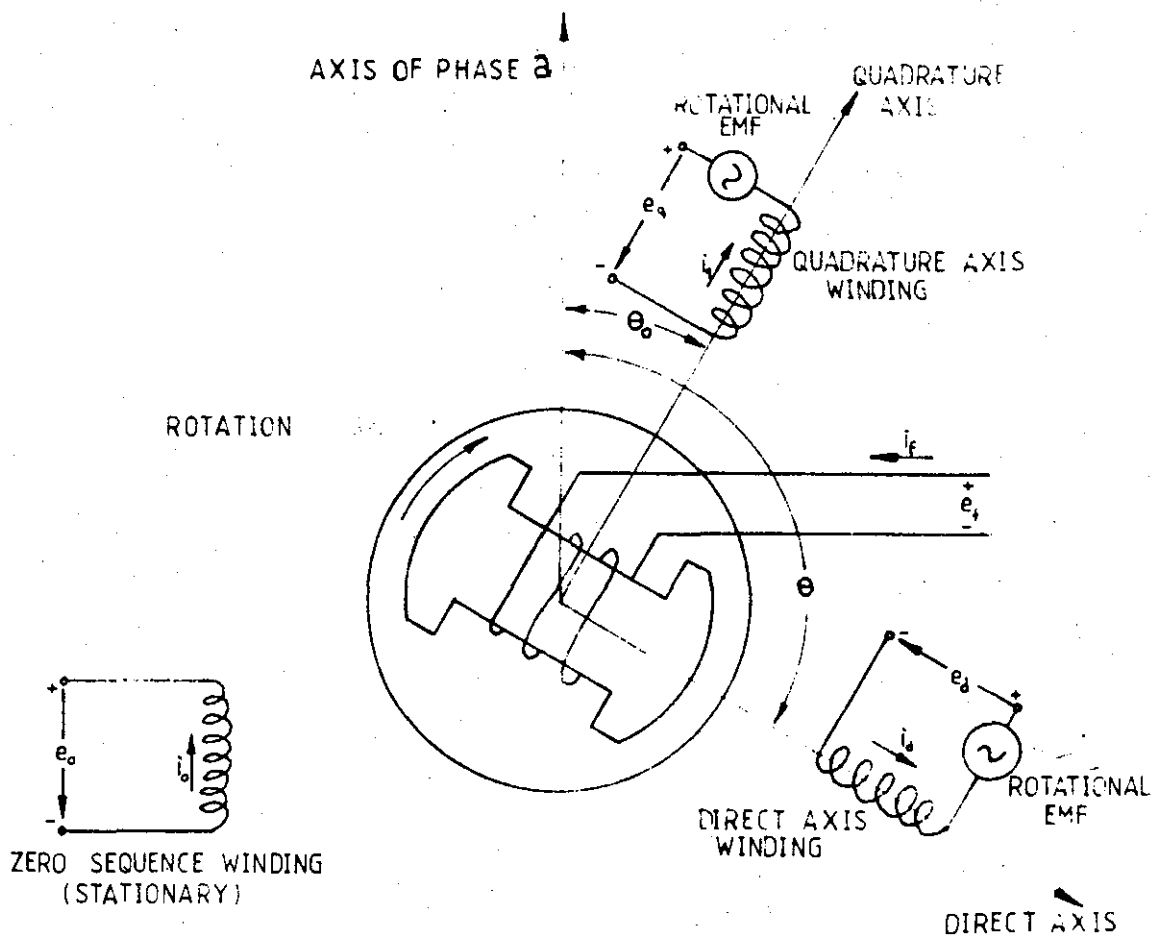


FIGURE 5.1: Representation of a synchronous generator by direct-axis, quadrature axis and zero-sequence windings

### 5.1 MACHINE EQUATIONS IN TERMS OF $\alpha, \beta, \gamma$ COMPONENTS

In a series of papers, Hwang<sup>32,33,34,35,36</sup> has demonstrated the mathematical convenience of the  $\alpha, \beta, \gamma$  transformation and successive approximation technique. In the analysis of unsymmetrical short-circuit faults applied to a conventional star-connected 3-phase synchronous generator. In this section, the relationships between  $\alpha, \beta$  components and d-q components as well as phase quantities are established, and synchronous machine equations in terms of  $\alpha, \beta, \gamma$  components are also provided.

The transformations from d-q to  $\alpha, \beta$  components<sup>32</sup> are

$$\begin{aligned} f_{\alpha} &= f_d \cos\theta + f_q \sin\theta \\ f_{\beta} &= -f_d \sin\theta + f_q \cos\theta \end{aligned}$$

or conversely

$$\begin{aligned} f_d &= f_{\alpha} \cos\theta - f_{\beta} \sin\theta \\ f_q &= f_{\alpha} \sin\theta + f_{\beta} \cos\theta \end{aligned}$$

The transformation from phase quantities to  $\alpha, \beta, \gamma$  components<sup>32</sup> are

$$\begin{aligned} f_{\alpha} &= \sqrt{\frac{2}{3}} f_a - \frac{1}{\sqrt{6}} f_b - \frac{1}{\sqrt{6}} f_c \\ f_{\beta} &= -\frac{1}{\sqrt{2}} f_b + \frac{1}{\sqrt{2}} f_c \\ f_{\gamma} &= \frac{1}{\sqrt{3}} f_a + \frac{1}{\sqrt{3}} f_b + \frac{1}{\sqrt{3}} f_c \end{aligned} \tag{5.8}$$

or conversely

$$\begin{aligned} f_a &= \sqrt{\frac{2}{3}} f_{\alpha} + \frac{1}{\sqrt{3}} f_{\gamma} \\ f_b &= -\frac{1}{\sqrt{6}} f_{\alpha} - \frac{1}{\sqrt{2}} f_{\beta} + \frac{1}{\sqrt{3}} f_{\gamma} \\ f_c &= \frac{1}{\sqrt{6}} f_{\alpha} + \frac{1}{\sqrt{2}} f_{\beta} + \frac{1}{\sqrt{3}} f_{\gamma} \end{aligned} \tag{5.9}$$

where  $f$  may represent the currents  $i$ , voltages  $v$  or flux linkages  $\psi$  of the machine.

The  $\alpha$ ,  $\beta$ ,  $\gamma$  components of the various flux linkages may be expressed in terms of the  $\alpha$ ,  $\beta$ ,  $\gamma$  components of the phase currents<sup>32</sup> by

$$\psi_{\alpha} = \sqrt{\frac{3}{2}} M_f i_f \cos\theta + \left[ \frac{L_d+L_q}{2} + \frac{L_d-L_q}{2} \cos 2\theta \right] i_{\alpha} - \frac{L_d-L_q}{2} \sin\theta i_{\beta}$$

$$\psi_{\beta} = -\sqrt{\frac{3}{2}} M_f i_f \sin\theta - \frac{L_d-L_q}{2} \sin 2\theta i_{\alpha} + \left[ \frac{L_d+L_q}{2} - \frac{L_d-L_q}{2} \cos 2\theta \right] i_{\beta}$$

$$\psi_{\gamma} = L_{\gamma} i_{\gamma} \quad (5.10)$$

$$\psi_f = \sqrt{\frac{3}{2}} M_f (i_{\alpha} \cos\theta - i_{\beta} \sin\theta) + L_f i_f$$

which may be re-written as

$$\psi_{\alpha} = M_{af} i_f \cos\theta + (A + B \cos 2\theta) i_{\alpha} - B \sin 2\theta i_{\beta}$$

$$\psi_{\beta} = -M_{af} i_f \sin\theta - B \sin 2\theta i_{\alpha} + (A - B \cos 2\theta) i_{\beta}$$

(5.11)

$$\psi_{\gamma} = L_{\gamma} i_{\gamma}$$

$$\psi_f = L_f i_f + M_{af} \cos\theta i_{\alpha} - M_{af} \sin\theta i_{\beta}$$

where

$$\begin{aligned}
 A &= \frac{L_d + L_q}{2} \\
 B &= \frac{L_d - L_q}{2} \\
 M_{af} &= \sqrt{\frac{3}{2}} M_f
 \end{aligned}
 \tag{5.12}$$

In terms of  $\alpha$ ,  $\beta$ ,  $\gamma$  components, the voltage-current relationships of the generator are

$$\begin{aligned}
 e_\alpha &= -Ri_\alpha - \frac{d\psi_\alpha}{dt} \\
 e_\beta &= -Ri_\beta - \frac{d\psi_\beta}{dt} \\
 e_\gamma &= -Ri_\gamma - \frac{d\psi_\gamma}{dt} \\
 e_f &= R_f i_f + \frac{d\psi_f}{dt}
 \end{aligned}
 \tag{5.13}$$

or, when the results of equation 5.13 are introduced

$$\begin{aligned}
 e_\alpha &= -(R+p(A+B \cos 2\theta))i_\alpha + pB \sin 2\theta i_\beta - pM_{af} \cos\theta i_f \\
 e_\beta &= pB \sin 2\theta i_\alpha - (R+p(A-B \cos 2\theta))i_\beta + pM_{af} \sin\theta i_f \\
 e_\gamma &= -(R+pL_\gamma)i_\gamma \\
 e_f &= (R_f+pL_f)i_f + pM_{af} \cos\theta i_\alpha - pM_{af} \sin\theta i_\beta
 \end{aligned}
 \tag{5.14}$$

The circuit representation of a synchronous generator by  $\alpha$ ,  $\beta$  and  $\gamma$  component windings is illustrated in Figure 5.2.

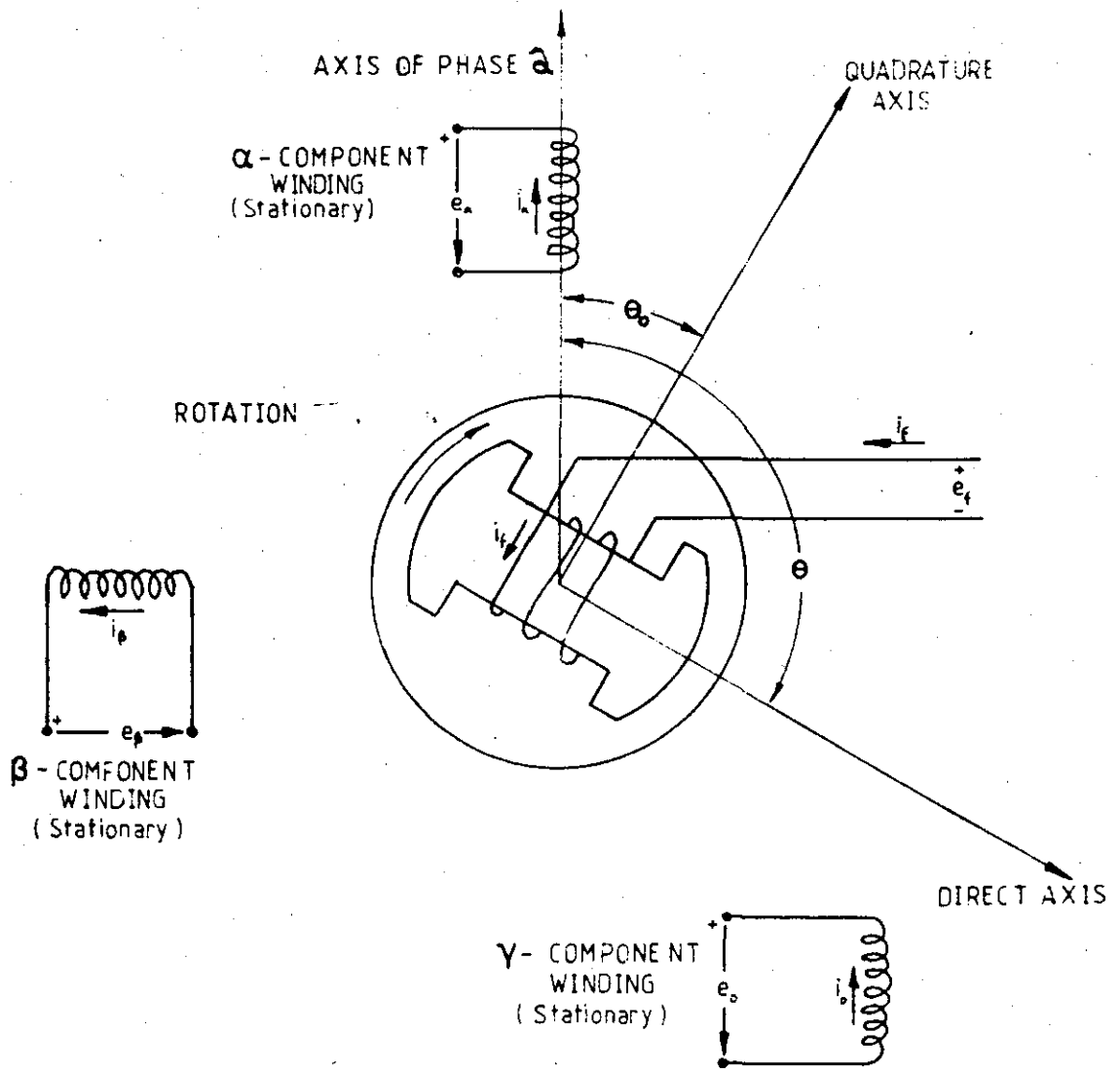


FIGURE 5.2: Representation of a synchronous generator by  $\alpha$ -component,  $\beta$ -component,  $\gamma$ -component windings

## 5.2 SYNCHRONOUS GENERATOR ON NO-LOAD

When a short circuit from no-load is considered, it is necessary to know both the flux linkages and the voltage conditions prior to the fault. On no-load, the field and the armature currents of the generator are

$$\begin{aligned}
 i_a &= 0 \\
 i_b &= 0 \\
 i_c &= 0 \\
 i_f &= I_{f0}
 \end{aligned}
 \tag{5.15}$$

where the field current  $I_{f0}$  produces rated armature voltage on open-circuit.

From equations (5.15), the  $\alpha$ ,  $\beta$ ,  $\gamma$  components of the armature currents are

$$\begin{aligned}
 i_\alpha &= 0 \\
 i_\beta &= 0 \\
 i_\gamma &= 0
 \end{aligned}
 \tag{5.16}$$

The flux linkages for an unloaded generator are found by substituting equations (5.16) into equation (5.11) as

$$\begin{aligned}
 \psi_{\alpha 0} &= M_{af} I_{f0} \cos \theta \\
 \psi_{\beta 0} &= -M_{af} I_{f0} \sin \theta \\
 \psi_{\gamma 0} &= 0
 \end{aligned}
 \tag{5.17}$$

The actual phase flux linkages for an unloaded generator are found by substituting equation (5.17) into (5.9)

$$\begin{aligned}\psi_{a0} &= \sqrt{\frac{2}{3}} M_{af} I_{f0} \cos\theta \\ \psi_{b0} &= -\frac{1}{\sqrt{6}} M_{af} I_{f0} \cos\theta + \frac{1}{\sqrt{2}} M_{af} I_{f0} \sin\theta \\ \psi_{c0} &= -\frac{1}{\sqrt{6}} M_{af} I_{f0} \cos\theta - \frac{1}{\sqrt{2}} M_{af} I_{f0} \sin\theta\end{aligned}\quad (5.18)$$

In terms of  $\alpha$ ,  $\beta$ ,  $\gamma$  components, the phase voltages for an unloaded generator are

$$\begin{aligned}e_{\alpha 0} &= -p M_{af} \cos\theta I_{f0} \\ &= \omega_0 M_{af} \sin\theta I_{f0} \\ &= \omega_0 \sqrt{\frac{3}{2}} M_f \sin\theta I_{f0} \\ &= \sqrt{\frac{3}{2}} E_0 \sin\theta\end{aligned}\quad (5.19)$$

$$\begin{aligned}e_{\beta 0} &= p M_{af} \sin\theta I_{f0} \\ &= \omega_0 M_{af} \cos\theta I_{f0} \\ &= \omega_0 \sqrt{\frac{3}{2}} M_f \cos\theta I_{f0} \\ &= \sqrt{\frac{3}{2}} E_0 \cos\theta\end{aligned}\quad (5.20)$$

$$\text{and } e_{\gamma 0} = 0 \quad (5.21)$$

$$\text{where } E_0 = \omega_0 M_f I_{f0} \quad (5.22)$$

So that the actual phase voltages are

$$\begin{aligned}
 e_{a0} &= \sqrt{\frac{2}{3}} e_{\alpha 0} + \sqrt{\frac{2}{3}} e_{\gamma 0} \\
 &= -\sqrt{\frac{2}{3}} \cdot \sqrt{\frac{3}{2}} E_0 \sin \theta + \frac{1}{\sqrt{3}} 0 \\
 &= -E_0 \sin \theta
 \end{aligned} \tag{5.23}$$

$$\begin{aligned}
 e_{b0} &= -\frac{1}{\sqrt{6}} e_{\alpha 0} - \frac{1}{\sqrt{2}} e_{\beta 0} + \frac{1}{\sqrt{3}} e_{\gamma 0} \\
 &= \frac{1}{\sqrt{6}} \sqrt{\frac{3}{2}} E_0 \sin \theta - \frac{1}{\sqrt{2}} \sqrt{\frac{3}{2}} E_0 \cos \theta + \frac{1}{\sqrt{3}} 0 \\
 &= \frac{1}{2} E_0 \sin \theta - \frac{\sqrt{3}}{2} E_0 \cos \theta
 \end{aligned} \tag{5.24}$$

and

$$\begin{aligned}
 e_{c0} &= -\frac{1}{\sqrt{6}} e_{\alpha 0} + \frac{1}{\sqrt{2}} e_{\beta 0} + \frac{1}{\sqrt{3}} e_{\gamma 0} \\
 &= \frac{1}{\sqrt{6}} \sqrt{\frac{3}{2}} E_0 \sin \theta + \frac{1}{\sqrt{2}} \sqrt{\frac{3}{2}} E_0 \cos \theta + \frac{1}{\sqrt{3}} 0 \\
 &= \frac{1}{2} E_0 \sin \theta + \frac{\sqrt{3}}{2} E_0 \cos \theta
 \end{aligned} \tag{5.25}$$

### 5.3 SIMULATION OF DISTURBANCES

During any disturbance, the voltages and currents at the various points in a system can be determined by superimposing the components resulting from the disturbance upon those which would exist if the disturbance had not occurred. The components of the voltages and currents due to a disturbance (such as an unsymmetrical short-circuit) which reduces the phase voltage to zero, can be determined by applying a component of the voltage at the point of fault equal in magnitude but opposite in sign to that which existed at the instant the fault occurred.

#### 5.4 TERMINAL (1)-TO-CENTRE POINT FAULT FOR ZIG-ZAG CONNECTION

A terminal (1)-to-centre point fault for a zig-zag connected generator is illustrated in Figure 5.3. The corresponding terminal conditions are

$$\begin{aligned} i_b &= 0 \\ i_c &= 0 \\ e_a &= 0 \end{aligned} \quad (5.26)$$

or, in terms of  $\alpha, \beta, \gamma$  quantities,

$$\begin{aligned} e_\alpha &= \sqrt{\frac{2}{3}} e_a - \frac{1}{\sqrt{6}} e_b - \frac{1}{\sqrt{6}} e_c \\ &= -\frac{1}{\sqrt{6}} (e_b + e_c) \end{aligned} \quad (5.27)$$

$$\begin{aligned} e_\beta &= -\frac{1}{\sqrt{2}} e_b + \frac{1}{\sqrt{2}} e_c \\ &= -\frac{1}{\sqrt{2}} (e_b - e_c) \end{aligned} \quad (5.28)$$

and

$$\begin{aligned} e_\gamma &= \frac{1}{\sqrt{3}} e_a + \frac{1}{\sqrt{3}} e_b + \frac{1}{\sqrt{3}} e_c \\ &= \frac{1}{\sqrt{3}} (e_b + e_c) \end{aligned} \quad (5.29)$$

$$\text{i.e.} \quad e_\alpha = -\frac{1}{\sqrt{2}} e_\gamma \quad (5.30)$$

Similarly, the terminal conditions for the currents in terms of their  $\alpha, \beta, \gamma$  components are

$$\begin{aligned} i_\alpha &= \sqrt{\frac{2}{3}} i_a - \frac{1}{\sqrt{6}} i_b - \frac{1}{\sqrt{6}} i_c \\ &= \sqrt{\frac{2}{3}} i_a \end{aligned} \quad (5.31)$$

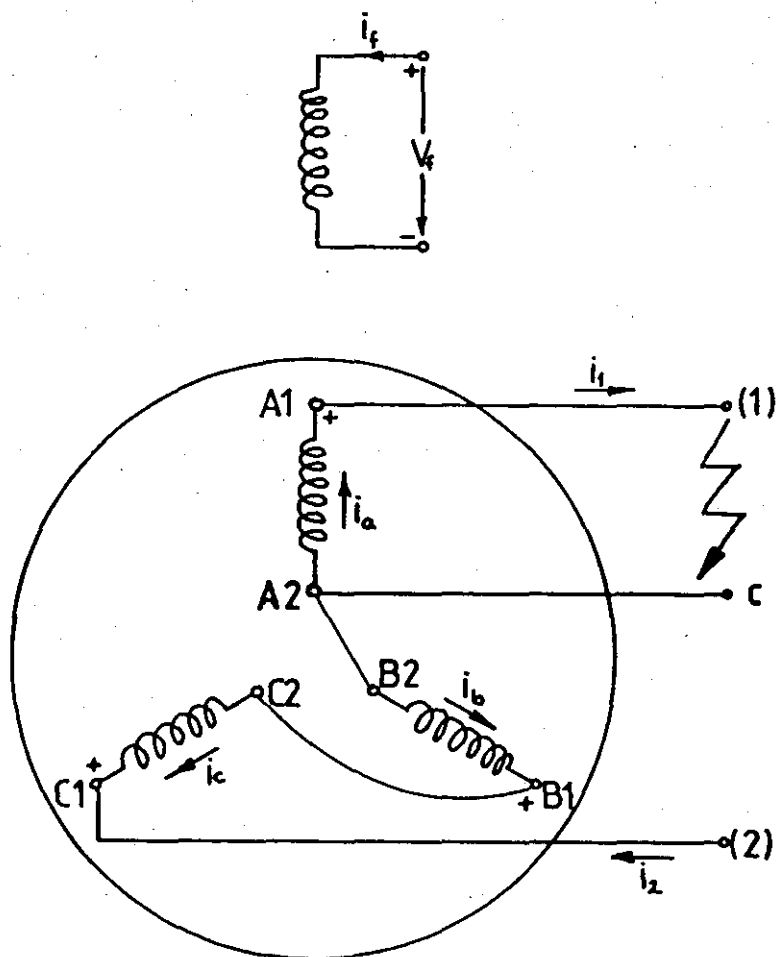


FIGURE 5.3: Terminal (1)-to-centre point fault for a zig-zag connected synchronous generator

and

$$\begin{aligned} i_{\beta} &= -\frac{1}{\sqrt{2}} i_b + \frac{1}{\sqrt{2}} i_c \\ &= 0 \end{aligned} \quad (5.32)$$

and

$$\begin{aligned} i_Y &= \frac{1}{\sqrt{3}} i_a + \frac{1}{\sqrt{3}} i_b + \frac{1}{\sqrt{3}} i_c \\ &= \frac{1}{\sqrt{3}} i_a \end{aligned} \quad (5.33)$$

i.e.

$$i_Y = \frac{1}{\sqrt{2}} i_{\alpha} \quad (5.34)$$

The change in voltage due to the short circuit is

$$\Delta e_{\alpha} = -\frac{1}{\sqrt{2}} e_Y - \sqrt{\frac{3}{2}} E_0 \sin \theta$$

The effect of the short circuit on phase a may be simulated by applying a step voltage  $\Delta e_{\alpha}$  to the armature, with the field voltage  $e_f$  equal to zero, whence from equation (5.14)

$$-\frac{1}{\sqrt{2}} e_Y - \sqrt{\frac{3}{2}} E_0 \sin \theta = -pM_{af} \cos \theta i_f - (R + (A+B \cos 2\theta)) i_{\alpha} \quad (5.35)$$

$$\begin{aligned} e_Y &= -(R + pL_Y) i_Y \\ &= -(R + pL_Y) \frac{i_{\alpha}}{\sqrt{2}} \end{aligned} \quad (5.36)$$

and

$$0 = (R_f + pL_f) i_f + pM_{af} \cos \theta i_{\alpha} \quad (5.37)$$

Substituting equation (5.36) into equation (5.35) and simplifying yields

$$\sqrt{\frac{3}{2}} E_0 \sin \theta = pM_{af} \cos \theta i_f + (r + p(A+B \cos 2\theta)) i_{\alpha} \quad (5.38)$$

where

$$r = \frac{3}{2} R$$

Equations (5.37) and (5.38) can be solved only by the method of successive approximations<sup>42,43</sup>. In the first approximation, all resistances are neglected and the equations solved simultaneously to give

$$i_{\alpha} = - \frac{\sqrt{6} E_0 (\cos\theta - \cos\theta_0)}{(A'+B') + (A'-B') \cos 2\theta} \quad (5.39)$$

and

$$\begin{aligned} i_f &= - \frac{M_{af}}{L_f} \cos\theta i_{\alpha} \\ &= \sqrt{6} \frac{M_{af}}{L_f} \frac{E_0 (\cos\theta - \cos\theta_0) \cos\theta}{A'+B'+(A'-B') \cos 2\theta} \end{aligned} \quad (5.40)$$

where

$$X'_d = \omega (L_d - \frac{M_{af}^2}{L_f})$$

$$X_0 = \omega L_Y$$

$$X_q = \omega L_q$$

$$A' = X'_d + \frac{X_0}{2}$$

$$B' = X_q + \frac{X_0}{2}$$

and  $\theta_0$  is the angle between the  $\alpha$  and  $d$  axes at  $t = 0$ .

Applying the formulae given in Appendix VI,  $i_{\alpha}$  and  $i_f$  may be resolved into the Fourier series

$$\begin{aligned} i_{\alpha} &= - \frac{\sqrt{6} E_0}{A' + \sqrt{A'B'}} [\cos\theta + \sum_{n=1}^{\infty} b^n \cos(2n+1)\theta] \\ &+ \frac{\sqrt{6} E_0 \cos\theta_0}{\sqrt{A'B'}} \left[ \frac{1}{2} + \sum_{n=1}^{\infty} b^n \cos 2n\theta \right] \end{aligned} \quad (5.41)$$

and

and

$$\begin{aligned}
 i_f = & \frac{\sqrt{6}}{2} \frac{M_{af}}{L_f} \frac{E_o}{A' + \sqrt{A'B'}} \left[ 1 + \frac{(1+b)}{b} \sum_{n=1}^{\infty} b^n \cos 2n\theta \right] \\
 & - \frac{\sqrt{6}}{2} \frac{M_{af}}{L_f} \frac{E_o \cos \theta_o (1+b)}{\sqrt{A'B'}} \left[ \cos \theta + \sum_{n=1}^{\infty} b^n \cos (2n+1)\theta \right]
 \end{aligned} \tag{5.42}$$

respectively, where

$$b = \frac{\sqrt{B'} - \sqrt{A'}}{\sqrt{B'} + \sqrt{A'}}$$

A correction for resistance is now made by multiplying each corresponding series for each current expression by a decrement factor which is a function of time. The modified currents are

$$\begin{aligned}
 i_\alpha = & - \frac{\sqrt{6} E_o}{A' + \sqrt{A'B'}} F_1(t) \left[ \cos \theta + \sum_{n=1}^{\infty} b^n \cos (2n+1)\theta \right] \\
 & + \frac{\sqrt{6} E_o \cos \theta_o}{\sqrt{A'B'}} F_2(t) \left[ \frac{1}{2} + \sum_{n=1}^{\infty} b^n \cos 2n\theta \right]
 \end{aligned} \tag{5.43}$$

and

$$\begin{aligned}
 i_f = & I_f(t) + \frac{\sqrt{6}}{2} \frac{M_{af}}{L_f} \frac{E_o}{A' + \sqrt{A'B'}} F_1(t) \left[ 1 + \frac{1+b}{b} \sum_{n=1}^{\infty} b^n \cos 2n\theta \right] \\
 & - \frac{\sqrt{6}}{2} \frac{M_{af}}{L_f} \frac{E_o \cos \theta_o}{\sqrt{A'B'}} (1+b) F_2(t) \left[ \cos \theta + \sum_{n=1}^{\infty} b^n \cos (2n+1)\theta \right]
 \end{aligned} \tag{5.44}$$

where  $F_1(t)$  and  $F_2(t)$  are undetermined decrement factors, each equal to unity at  $t = 0$ , and  $I_f(t)$  is a transient DC component introduced to include the effect of the field resistance. At  $t = 0$   $I_f(t)$  is obviously equal to zero.

$F_1(t)$ ,  $F_2(t)$  and  $I_f(t)$  may be found by substituting equations (5.43) and (5.44) into equations (5.37) and (5.38), expanding the resulting trigonometric expressions, and equating the coefficients of the corresponding terms on both sides of the equations. To ensure that

the mathematical manipulations are manageable, the relatively small resistances in the coefficients of the harmonic terms are neglected but those in the DC terms are retained. This results in three independent equations with three unknowns (the mathematical manipulations involved are given in Appendix VIII).

$$\begin{aligned}
 (R_f + pL_f) I_f(t) + \sqrt{\frac{3}{2}} R_f \frac{M_{af}}{L_f} \frac{E_0}{A' + \sqrt{A'B'}} &= 0 \\
 -\sqrt{\frac{3}{2}} E_0 &= M_{af} I_f(t) - \sqrt{\frac{3}{2}} E_0 F_1(t) \\
 0 &= r F_2(t) + p \frac{\sqrt{A'B'}}{\omega} F_2(t)
 \end{aligned} \tag{5.45}$$

Solving (5.45) for the decrement factors yield

$$\begin{aligned}
 F_2(t) &= e^{-t/\tau_a} \\
 F_1(t) &= \frac{X'_d + X_0 + X_2}{X'_d + X_0 + X_2} \left[ \frac{X'_d - X'_d}{X'_d + X_0 + X_2} e^{-t/\tau_{d'}} + 1 \right] \\
 I_f(t) &= \frac{\sqrt{3}}{2} \frac{E_0}{\omega M_{af}} \frac{X'_d - X'_d}{X'_d + X_0 + X_2} [e^{-t/\tau_{d'}} - 1] \\
 &= \sqrt{\frac{3}{2}} E_0 \frac{M_{af}}{L_f} \frac{1}{X'_d + X_0 + X_2} [e^{-t/\tau_{d'}} - 1]
 \end{aligned} \tag{5.46}$$

where

$$\begin{aligned}
 \tau_a &= \frac{\sqrt{A'B'}}{\omega r} \\
 \tau_{d'} &= \tau_{d0} \frac{X'_d - X_0 + X_2}{X'_d + X_0 + X_2} \\
 \tau_{d0} &= \frac{L_f}{R_f} \\
 X_2 &= \sqrt{A'B'} - 0.5 X_0
 \end{aligned} \tag{5.47}$$

The final short-circuit current expressions then become

$$i_{\alpha} = -\sqrt{6} E_0 \left[ \left( \frac{1}{X'_d + X_0 + X_2} - \frac{1}{X_d + X_0 + X_2} \right) e^{-t/\tau_{d'}} + \frac{1}{X_d + X_0 + X_2} \right] (\cos\theta + \sum_{n=1}^{\infty} b^n \cos(2n+1)\theta) \\ + \sqrt{6} \frac{E_0 \cos \theta_0}{X_2 + 0.5 X_0} \left[ \frac{1}{2} + \sum_{n=1}^{\infty} b^n \cos 2n\theta \right] e^{-t/\tau_a} \quad (5.48)$$

and

$$i_f = I_{f0} + \sqrt{\frac{3}{2}} \frac{M_{af}}{L_f} E_0 \frac{e^{-t/\tau_{d'}} - 1}{X_d + X_0 + X_2} \\ + \sqrt{\frac{3}{2}} \frac{M_{af}}{L_f} E_0 \left[ \left( \frac{1}{X'_d + X_0 + X_2} - \frac{1}{X_d + X_0 + X_2} \right) e^{-t/\tau_{d'}} + \frac{1}{X_d + X_0 + X_2} \right] \left( 1 + \frac{1+b}{b} \sum_{n=1}^{\infty} b^n \cos 2n\theta \right) \\ - \sqrt{\frac{3}{2}} \frac{M_{af}}{L_f} \frac{E_0 \cos \theta_0}{X_2 + 0.5 X_0} (1+b) \left( \cos\theta + \sum_{n=1}^{\infty} b^n \cos(2n+1)\theta \right) e^{-t/\tau_a} \quad (5.49)$$

where  $I_{f0}$  is the field current existing before the fault.

For convenience in calculating the terms in the series for  $i_{\alpha}$  and  $i_f$ , equations (5.48) and (5.49) are summed using the formulae presented in Appendix VI, to give

$$i_{\alpha} = -\frac{\sqrt{6} E_0 (F_1(t) \cos\theta - F_2(t) \cos\theta_0)}{X'_d + X_q + (X'_d - X_q) \cos 2\theta + X_0} \quad (5.50)$$

$$i_f = I_{f0} + \sqrt{\frac{3}{2}} \frac{M_{af}}{L_f} E_0 \frac{e^{-t/\tau_{d'}} - 1}{X_d + X_0 + X_2} - \frac{2(F_1(t) \cos\theta - F_2(t) \cos\theta_0) \cos\theta}{X'_d + X_q + (X'_d - X_q) \cos 2\theta + X_0} \\ = I_{f0} + I_f(t) - \frac{M_{af}}{L_f} \cos\theta i_{\alpha} \quad (5.51)$$

These equations are obviously more convenient than equations (5.48) and (5.49) when numerical calculations are to be made.

The phase currents for a terminal (1)-to-centre point short-circuit fault are now readily obtained as

$$\begin{aligned}
 i_a &= \sqrt{\frac{3}{2}} i_\alpha \\
 &= - \frac{3 E_o (F_1(t) \cos\theta - F_2(t) \cos\theta_o)}{X'_d + X_q + (X'_d - X_q) \cos 2\theta + X_o} \\
 i_b &= 0 \\
 i_c &= 0
 \end{aligned} \tag{5.52}$$

### 5.5 TERMINAL (2)-TO-CENTRE POINT FAULT FOR ZIG-ZAG CONNECTION

The terminal conditions for the terminal (2)-to-centre point fault illustrated in Figure 5.4 are

$$\begin{aligned}
 i_a &= 0 \\
 i_b &= -i_2 \\
 i_c &= -i_2 \\
 e_b + e_c &= 0
 \end{aligned} \tag{5.53}$$

or in terms of the  $\alpha, \beta, \gamma$  quantities

$$\begin{aligned}
 i_\alpha &= \sqrt{\frac{2}{3}} i_a - \frac{1}{\sqrt{6}} i_b - \frac{1}{\sqrt{6}} i_c \\
 &= \sqrt{\frac{2}{3}} i_2
 \end{aligned} \tag{5.54}$$

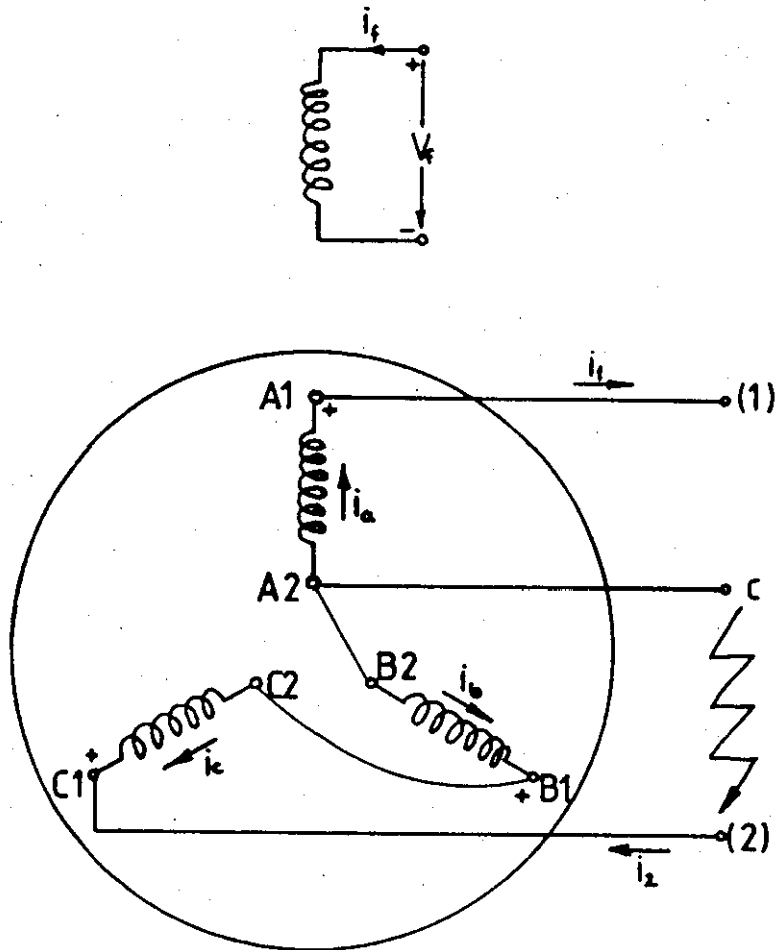


FIGURE 5.4: Terminal (2)-to-centre point fault for zig-zag connected generator

and

$$\begin{aligned} i_{\beta} &= -\frac{1}{\sqrt{2}} i_b + \frac{1}{\sqrt{2}} i_c \\ &= 0 \end{aligned} \quad (5.55)$$

and

$$\begin{aligned} i_{\gamma} &= \frac{1}{\sqrt{3}} i_a + \frac{1}{\sqrt{3}} i_b + \frac{1}{\sqrt{3}} i_c \\ &= -\frac{2}{\sqrt{3}} i_2 \end{aligned} \quad (5.56)$$

From equations (5.54) and (5.56)

$$i_{\gamma} = -\sqrt{2} i_{\alpha} \quad (5.57)$$

The  $\alpha$ ,  $\beta$ ,  $\gamma$  components of the voltage are

$$\begin{aligned} e_{\alpha} &= \sqrt{\frac{2}{3}} e_a - \frac{1}{\sqrt{6}} e_b - \frac{1}{\sqrt{6}} e_c \\ &= \sqrt{\frac{2}{3}} e_a \end{aligned} \quad (5.58)$$

and

$$\begin{aligned} e_{\gamma} &= \frac{1}{\sqrt{3}} e_a + \frac{1}{\sqrt{3}} e_b + \frac{1}{\sqrt{3}} e_c \\ &= \frac{1}{\sqrt{3}} e_a \end{aligned} \quad (5.59)$$

$$\text{i.e.} \quad e_{\alpha} = \sqrt{2} e_{\gamma} \quad (5.60)$$

The change in voltage due to the short-circuit is

$$\Delta e_{\alpha} = \sqrt{2} e_{\gamma} - \sqrt{\frac{3}{2}} E_0 \sin\theta \quad (5.61)$$

The effect of the short-circuit is again simulated by applying  $\Delta e_{\alpha}$  to the  $\alpha$ -axis component of the voltage, with the field voltage  $e_f$  equal to zero. Thus

$$\sqrt{2} e_Y - \sqrt{\frac{3}{2}} E_0 \sin\theta = -p M_{af} \cos\theta i_f - (R + p(A + B \cos 2\theta)) i_\alpha \quad (5.62)$$

$$\begin{aligned} e_Y &= -(R + pL_Y) i_Y \\ &= (R + pL_Y) \sqrt{2} i_\alpha \end{aligned} \quad (5.63)$$

$$0 = (R_f + pL_f) i_f + p M_{af} \cos\theta i_\alpha \quad (5.64)$$

Substituting equation (5.63) into equation (5.62) and simplifying the result yields

$$\sqrt{\frac{3}{2}} E_0 \sin\theta = p M_{af} \cos\theta i_f + [3R + p(A + L_Y + B \cos 2\theta)] i_\alpha \quad (5.65)$$

Equations (5.64) and (5.65) can again only be solved by the method of successive approximation. In the first approximation, with resistances neglected, equations (5.34) and (5.65) may be solved simultaneously to give

$$i_\alpha(t) = - \frac{\sqrt{6} E_0 (\cos\theta - \cos\theta_0)}{(C' + D') + (C' - D') \cos 2\theta} \quad (5.66)$$

and

$$\begin{aligned} i_f(t) &= - \frac{M_{af}}{L_f} \cos\theta i_\alpha \\ &= \sqrt{6} \frac{M_{af}}{L_f} \frac{E_0 (\cos\theta - \cos\theta_0) \cos\theta}{(C' + D') + (C' - D') \cos 2\theta} \end{aligned} \quad (5.67)$$

where

$$\begin{aligned} X'_d &= \omega(L_d - \frac{M_{af}^2}{L_f}) \\ X_q &= \omega L_q \\ X_0 &= \omega L_Y \end{aligned} \quad (5.68)$$

$$C' = X'_d + 2X_0$$

$$D' = X_q + 2X_0$$

and  $\theta_0$  is the angle between the  $\alpha$ - and  $d$ -axes at  $t = 0$ .

Applying the formulae given in Appendix VI,  $i_\alpha$  and  $i_f$  may be resolved respectively into the Fourier series

$$i_\alpha = -\frac{\sqrt{6} E_0}{C'+\sqrt{C'D'}} [\cos\theta + \sum_{n=1}^{\infty} b^n \cos(2n+1)\theta] + \frac{\sqrt{6} E_0 \cos\theta_0}{\sqrt{C'D'}} \left[ \frac{1}{2} + \sum_{n=1}^{\infty} \cos 2n\theta \right] \quad (5.69)$$

and

$$i_f = \frac{\sqrt{6}}{2} \frac{M_{af}}{L_f} \frac{E_0}{C'+\sqrt{C'D'}} \left[ 1 + \frac{(1+b)}{b} \sum_{n=1}^{\infty} b^n \cos 2n\theta \right] - \frac{\sqrt{6}}{2} \frac{M_{af}}{L_f} \frac{E_0 \cos\theta_0 (1+b)}{\sqrt{C'D'}} \left[ \cos\theta + \sum_{n=1}^{\infty} b^n \cos(2n+1)\theta \right] \quad (5.70)$$

Taking resistance into account, by introducing decrement factors as in Section 5.4, gives the modified current expressions

$$i_\alpha = -\frac{\sqrt{6} E_0}{C'+\sqrt{C'D'}} F_1(t) [\cos\theta + \sum_{n=1}^{\infty} b^n \cos(2n+1)\theta] + \frac{\sqrt{6} E_0 \cos\theta_0}{\sqrt{C'D'}} F_2(t) \left[ \frac{1}{2} + \sum_{n=1}^{\infty} b^n \cos 2n\theta \right] \quad (5.71)$$

and

$$i_f = I_f(t) + \frac{\sqrt{6}}{2} \frac{M_{af}}{L_f} \frac{E_0}{C'+\sqrt{C'D'}} F_1(t) \left[ 1 + \frac{(1+b)}{b} \sum_{n=1}^{\infty} b^n \cos 2n\theta \right] - \frac{\sqrt{6}}{2} \frac{M_{af}}{L_f} \frac{E_0 \cos\theta_0}{\sqrt{C'D'}} (1+b) F_2(t) \left[ \cos\theta + \sum_{n=1}^{\infty} b^n \cos(2n+1)\theta \right] \quad (5.72)$$

The decrement factors may be found in the same way as in Section 5.4. After the mathematical manipulations which are given in Appendix IX, the resulting three independent equations are

$$(R_f + pL_f)I_f(t) + \frac{\sqrt{6}}{2} R_f \frac{M_{af}}{L_f} E_0 \frac{1}{C' + \sqrt{C'D'}} = 0$$

$$\sqrt{\frac{3}{2}} E_0 = -\omega M_{af} I_f(t) + \sqrt{\frac{3}{2}} E_0 F_1(t) \quad (5.73)$$

$$3R F_2(t) + p \frac{\sqrt{C'D'}}{\omega} F_2(t) = 0$$

Solving equations (5.73) gives

$$F_2(t) = e^{-t/\tau_b} \quad (5.74)$$

$$F_1(t) = \frac{X'_d + 4X_0 + X_2}{X'_d + 4X_0 + X_2} \left[ \frac{X'_d - X'_d}{X'_d + 4X_0 + X_2} e^{-t/\tau_{d'}} + 1 \right]$$

and

$$I_f(t) = \sqrt{\frac{3}{2}} E_0 \frac{M_{af}}{L_f} \frac{1}{X'_d + 4X_0 + X_2} [e^{-t/\tau_{d'}} - 1]$$

$$= \sqrt{\frac{3}{2}} \frac{E_0}{\omega M_{af}} \frac{X'_d - X'_d}{X'_d + 4X_0 + X_2} [e^{-t/\tau_{d'}} - 1] \quad (5.75)$$

where

$$\tau_b = \frac{\sqrt{C'D'}}{3R\omega}$$

$$\tau_{d'} = \tau'_{do} \frac{X'_d + 4X_0 + X_2}{X'_d + 4X_0 + X_2} \quad (5.76)$$

$$\tau'_{do} = \frac{L_f}{R_f}$$

$$X_2 = \sqrt{C'D'} - 2X_0$$

The final current expressions are therefore

$$i_{\alpha} = -\sqrt{6} E_0 \left[ \left( \frac{1}{X'_d + 4X_0 + X_2} - \frac{1}{X_d + 4X_0 + X_2} \right) e^{-t/\tau_d} + \frac{1}{X_d + 4X_0 + X_2} \right] (\cos\theta + \sum_{n=1}^{\infty} b^n \cos(2n+1)\theta) \\ + \frac{\sqrt{6} E_0 \cos \theta_0}{X_2 + 2X_0} e^{-t/\tau_b} \left( \frac{1}{2} + \sum_{n=1}^{\infty} b^n \cos 2n\theta \right) \quad (5.77)$$

and

$$i_f = I_{f0} + \sqrt{\frac{3}{2}} E_0 \frac{M_{af}}{L_f} \frac{e^{-t/\tau'_d} - 1}{X_d + 4X_0 + X_2} \\ + \sqrt{\frac{3}{2}} \frac{M_{af}}{L_f} E_0 \left[ \left( \frac{1}{X'_d + 4X_0 + X_2} - \frac{1}{X_d + 4X_0 + X_2} \right) e^{-t/\tau'_d} + \frac{1}{X_d + 4X_0 + X_2} \right] (1 + \frac{1+b}{b} \sum_{n=1}^{\infty} b^n \cos 2n\theta) \\ - \sqrt{\frac{3}{2}} \frac{M_{af}}{L_f} \frac{E_0 \cos \theta_0}{X_2 + 2X_0} (1+b) e^{-t/\tau_b} (\cos\theta + \sum_{n=1}^{\infty} b^n \cos(2n+1)\theta) \quad (5.78)$$

where  $I_{f0}$  is the constant field current existing before the fault.

Because of the inconvenience in calculating  $i_{\alpha}$  and  $i_f$  term-by-term, these are summed using the formulae given in Appendix VI, to give

$$i_{\alpha} = -\frac{\sqrt{6} E_0 (F_1(t) \cos\theta - F_2(t) \cos \theta_0)}{X'_d + X_q + (X'_d - X_q) \cos 2\theta + 4X_0} \quad (5.79)$$

and

$$i_f = I_{f0} + \sqrt{\frac{3}{2}} \frac{M_{af}}{L_f} E_0 \left[ \frac{e^{-t/\tau'_d} - 1}{X_d + 4X_0 + X_2} + \frac{2(F_1(t) \cos\theta - F_2(t) \cos \theta_0)}{X'_d + X_q + (X'_d - X_q) \cos 2\theta + 4X_0} \right] \quad (5.80)$$

All the phase currents for a terminal (2)-to-centre point fault are now readily obtained as

$$i_a = 0$$

$$i_b = - \frac{3 E_o (F_1(t) \cos \theta - F_2(t) \cos \theta_o)}{X'_d + X_q + (X'_d - X_q) \cos 2\theta + 4X_o} \quad (5.81)$$

$$i_c = - \frac{3 E_o (F_1(t) \cos \theta - F_2(t) \cos \theta_o)}{X'_d + X_q + (X'_d - X_q) \cos 2\theta + 4X_o}$$

### 5.6 DOUBLE LINE-TO-CENTRE POINT FAULT FOR ZIG-ZAG CONNECTION

Figure 5.5 illustrates a double line-to-centre point fault for a zig-zag connected generator, with the terminal conditions imposed by the fault being

$$i_a = i_1$$

$$i_b = -i_2$$

$$i_c = -i_2 \quad (5.82)$$

$$e_a = 0$$

$$e_b + e_c = 0$$

or in terms of the  $\alpha$ ,  $\beta$ ,  $\gamma$  quantities

$$\begin{aligned} e_\alpha &= \sqrt{\frac{2}{3}} e_a - \frac{1}{\sqrt{6}} e_b - \frac{1}{\sqrt{6}} e_c \\ &= 0 \end{aligned} \quad (5.83)$$

and

$$\begin{aligned} e_\gamma &= \frac{1}{\sqrt{3}} e_a + \frac{1}{\sqrt{3}} e_b + \frac{1}{\sqrt{3}} e_c \\ &= 0 \end{aligned} \quad (5.84)$$

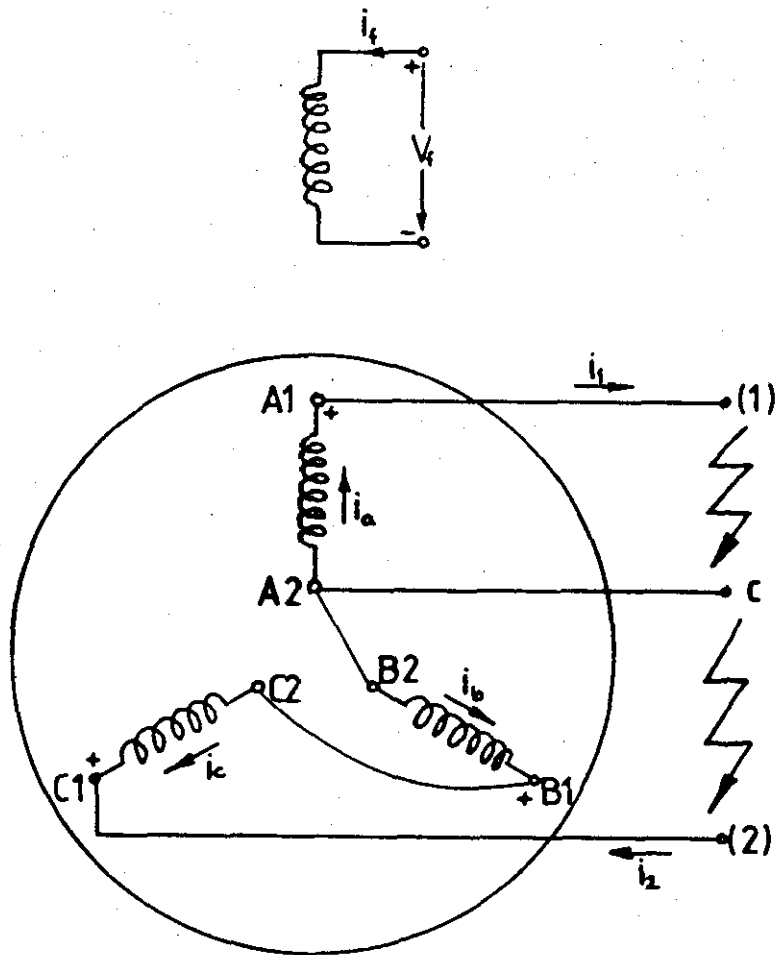


FIGURE 5.5: Double line-to-centre point fault for zig-zag connected generator

i.e.  $i_Y = 0$  (5.85)

$$i_Y = \frac{1}{\sqrt{3}} i_a + \frac{1}{\sqrt{3}} i_b + \frac{1}{\sqrt{3}} i_c$$

$$= \frac{1}{\sqrt{3}} (i_1 - 2i_2)$$

Since  $i_Y = 0$

$$i_1 = 2i_2 \quad (5.86)$$

and

$$i_\alpha = \sqrt{\frac{2}{3}} i_a - \frac{1}{\sqrt{3}} i_b - \frac{1}{\sqrt{3}} i_c$$

$$= \sqrt{\frac{2}{3}} (i_1 + i_2) \quad (5.87)$$

and substituting equation (5.86) into (5.87)

$$i_\alpha = \sqrt{\frac{3}{2}} (3i_2)$$

$$i_\alpha = \sqrt{6} i_2 \quad (5.88)$$

or

$$i_\alpha = \sqrt{\frac{3}{2}} i_1 \quad (5.89)$$

and

$$i_\beta = -\frac{1}{\sqrt{2}} i_b + \frac{1}{\sqrt{2}} i_c$$

$$= 0 \quad (5.90)$$

The change in voltage due to the short-circuit is

$$\Delta e_\alpha = -\sqrt{\frac{3}{2}} E_0 \sin \theta$$

With the effect of the fault simulated by a step voltage applied to the armature, with the field voltage equal to zero

$$\sqrt{\frac{3}{2}} E_0 \sin \theta = p M_{af} \cos \theta i_f + (R + (A + B \cos 2\theta)) i_\alpha \quad (5.91)$$

and

$$0 = (R_f + pL_f) i_f + pM_{af} \cos \theta i_\alpha \quad (5.92)$$

As before, equations (5.91) and (5.92) are solved using the method of successive approximations. The first approximation with all resistances neglected, gives

$$i_\alpha = - \frac{\sqrt{6} E_0 (\cos \theta - \cos \theta_0)}{(G' + H') + (G' - H') \cos 2\theta} \quad (5.93)$$

and

$$\begin{aligned} i_f &= - \frac{M_{af}}{L_f} \cos \theta i_\alpha \\ &= \sqrt{6} \frac{M_{af}}{L_f} \frac{E_0 (\cos \theta - \cos \theta_0) \cos \theta}{(G' + H') + (G' - H') \cos 2\theta} \end{aligned} \quad (5.94)$$

where

$$\begin{aligned} G' &= X_d' \\ H' &= X_q \\ X_d' &= \omega (L_d - \frac{M_{af}^2}{L_f}) \\ X_q &= \omega L_q \end{aligned} \quad (5.95)$$

Applying the formulae given in Appendix VI,  $i_\alpha$  and  $i_f$  may be resolved into the Fourier series

$$\begin{aligned} i_\alpha &= - \frac{\sqrt{6} E_0}{G' + \sqrt{G'H'}} (\cos \theta + \sum_{n=1}^{\infty} b^n \cos (2n+1)\theta) \\ &\quad + \frac{\sqrt{6} E_0 \cos \theta_0}{\sqrt{G'H'}} (\frac{1}{2} + \sum_{n=1}^{\infty} b^n \cos 2n\theta) \end{aligned} \quad (5.96)$$

and

$$\begin{aligned}
 i_f = & \frac{\sqrt{6}}{2} \frac{M_{af}}{L_f} \frac{E_o}{G' + \sqrt{G'H'}} \left( 1 + \frac{1+b}{b} \sum_{n=1}^{\infty} b^n \cos 2n\theta \right) \\
 & - \frac{\sqrt{6}}{2} \frac{M_{af}}{L_f} E_o \frac{(1+b) \cos \theta}{\sqrt{G'H'}} \left( \cos \theta + \sum_{n=1}^{\infty} b^n \cos (2n+1)\theta \right)
 \end{aligned} \tag{5.97}$$

where

$$b = \frac{\sqrt{H'} - \sqrt{G'}}{\sqrt{H'} + \sqrt{G'}}$$

Introducing a decrement factor as a correction for the resistances, gives the modified currents

$$\begin{aligned}
 i_\alpha = & - \frac{\sqrt{6} E_o}{G' + \sqrt{G'H'}} F_1(t) \left( \cos \theta + \sum_{n=1}^{\infty} b^n \cos (2n+1)\theta \right) \\
 & + \frac{\sqrt{6} E_o \cos \theta}{\sqrt{G'H'}} F_2(t) \left( \frac{1}{2} + \sum_{n=1}^{\infty} b^n \cos 2n\theta \right)
 \end{aligned} \tag{5.98}$$

and

$$\begin{aligned}
 i_f = & I_f(t) + \frac{\sqrt{6}}{2} \frac{M_{af}}{L_f} \frac{E_o}{G' + \sqrt{G'H'}} F_1(t) \left( 1 + \frac{1+b}{b} \sum_{n=1}^{\infty} b^n \cos (2n+1)\theta \right) \\
 & - \frac{\sqrt{6}}{2} \frac{M_{af}}{L_f} E_o \frac{(1+b) \cos \theta}{\sqrt{G'H'}} F_2(t) \left( \cos \theta + \sum_{n=1}^{\infty} b^n \cos (2n+1)\theta \right)
 \end{aligned} \tag{5.99}$$

The decrement factors in equations (5.98) and (5.99) are determined in the same way as described in Section 5.4. After the mathematical manipulations given in Appendix X, the resulting three independent equations are

$$(R_f + pL_f) I_f(t) + \frac{\sqrt{6}}{2} R_f E_0 \frac{1}{G' + \sqrt{G'H'}} = 0$$

$$\sqrt{\frac{3}{2}} E_0 = -\omega M_{af} I_f(t) + \sqrt{\frac{3}{2}} E_0 F_1(t) \quad (5.100)$$

$$RF_2(t) + p \frac{\sqrt{G'H'}}{\omega} F_2(t) = 0$$

Solving equation (5.100) gives

$$F_2(t) = e^{-t/\tau_c}$$

$$F_1(t) = \frac{X'_d + X_2}{X_d + X_2} \left[ \frac{X_d - X'_d}{X_d + X_2} e^{-t/\tau'_d} - 1 \right] \quad (5.101)$$

and

$$\begin{aligned} I_f(t) &= \sqrt{\frac{3}{2}} E_0 \frac{M_{af}}{L_f} \frac{1}{X_d - X_2} [e^{-t/\tau'_d} - 1] \\ &= \sqrt{\frac{3}{2}} \frac{E_0}{\omega M_{af}} \frac{X_d - X'_d}{X_d + X_2} [e^{-t/\tau'_d} - 1] \end{aligned}$$

where

$$\tau_c = \frac{\sqrt{G'H'}}{\omega R}$$

$$\tau'_d = \tau_{d0} \frac{X'_d + X_2}{X_d + X_2}$$

(5.102)

$$\tau_{d0} = \frac{L_f}{R_f}$$

$$X_2 = \sqrt{G'H'}$$

The final current expressions are obtained by substituting equation (5.101) into equation (5.98) and equation (5.99) to give

$$i_{\alpha} = -\sqrt{6} E_0 \left[ \left( \frac{1}{X'_d + X_2} - \frac{1}{X_d + X_2} \right) e^{-t/\tau'_d} + \frac{1}{X_d + X_2} \right] (\cos\theta + \sum_{n=1}^{\infty} b^n \cos(2n+1)\theta) \\ + \frac{\sqrt{6} E_0 \cos \theta_0}{X_2} e^{-t/\tau_c} \left( \frac{1}{2} + \sum_{n=1}^{\infty} b^n \cos 2n\theta \right) \quad (5.103)$$

and

$$i_f = I_{f0} + \sqrt{\frac{3}{2}} \frac{M_{af}}{L_f} \frac{e^{-t/\tau'_d} - 1}{X_d + X_2} \\ + \sqrt{\frac{3}{2}} \frac{M_{af}}{L_f} E_0 \left[ \left( \frac{1}{X'_d + X_2} - \frac{1}{X_d + X_2} \right) e^{-t/\tau'_d} + \frac{1}{X_d + X_2} \right] \left( 1 + \frac{1+b}{b} \sum_{n=1}^{\infty} b^n \cos 2n\theta \right) \\ - \sqrt{\frac{3}{2}} \frac{M_{af}}{L_f} \frac{E_0 \cos \theta_0}{X_2} (1+b) e^{-t/\tau_c} (\cos\theta + \sum_{n=1}^{\infty} b^n \cos(2n+1)\theta) \quad (5.104)$$

where  $I_{f0}$  is the constant field current existing before the fault.

Summing equations (5.103) and (5.104), term-by-term, using the formulae given in Appendix VI, yields

$$i_{\alpha} = - \frac{\sqrt{6} E_0 (F_1(t) \cos\theta - F_2(t) \cos\theta_0)}{X'_d + X_q + (X'_d - X_q) \cos 2\theta} \quad (5.105)$$

and

$$i_f = I_{f0} + \sqrt{\frac{3}{2}} \frac{M_{af}}{L_f} E_0 \left[ \frac{e^{-t/\tau'_d} - 1}{X_d + X_2} + \frac{2(F_1(t) \cos\theta - F_2(t) \cos\theta_0) \cos\theta}{X'_d + X_q + (X'_d - X_q) \cos 2\theta} \right] \quad (5.106)$$

All the short-circuit currents for a double line-to-centre point fault are now readily obtained as

$$i_1 = - \frac{2 E_0 (F_1(t) \cos \theta - F_2(t) \cos \theta_0)}{X'_d + X_q + (X'_d - X_q) \cos 2\theta}$$

$$i_2 = - \frac{E_0 (F_1(t) \cos \theta - F_2(t) \cos \theta_0)}{X'_d + X_q + (X'_d - X_q) \cos 2\theta}$$

$$i_a = - \frac{2 E_0 (F_1(t) \cos \theta - F_2(t) \cos \theta_0)}{X'_d + X_q + (X'_d - X_q) \cos 2\theta} \quad (5.107)$$

$$i_b = \frac{E_0 (F_1(t) \cos \theta - F_2(t) \cos \theta_0)}{X'_d + X_q + (X'_d - X_q) \cos 2\theta}$$

$$i_c = \frac{E_0 (F_1(t) \cos \theta - F_2(t) \cos \theta_0)}{X'_d + X_q + (X'_d - X_q) \cos 2\theta}$$

### 5.7 LINE-TO-LINE FAULT FOR AN EDISON DELTA CONNECTION

Figure 5.6 illustrates a line-to-line fault for an Edison-delta connected generator, with the terminal conditions imposed by the fault being

$$i = i_a - i_b$$

$$i_c = i_b \quad (5.108)$$

$$e_a = 0$$

$$e_b + e_c = 0$$

or in terms of the  $\alpha$ ,  $\beta$ ,  $\gamma$  quantities

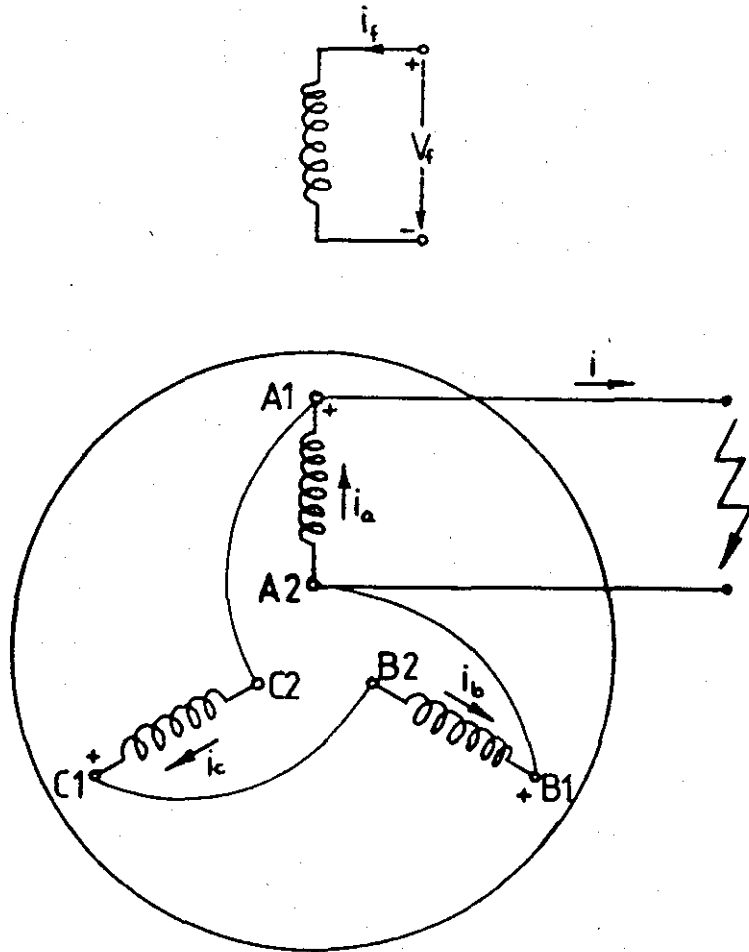


FIGURE 5.6: Line-to-line fault for an Edison-delta connected generator

$$\begin{aligned}
 e_{\alpha} &= \sqrt{\frac{2}{3}} e_a - \frac{1}{\sqrt{6}} e_b - \frac{1}{\sqrt{6}} e_c \\
 &= \sqrt{\frac{2}{3}} e_a - \frac{1}{\sqrt{6}} (e_b + e_c) \\
 &= \sqrt{\frac{2}{3}} (0) - \frac{1}{\sqrt{6}} (0) = 0
 \end{aligned} \tag{5.109}$$

and

$$\begin{aligned}
 e_{\gamma} &= \frac{1}{\sqrt{3}} e_a + \frac{1}{\sqrt{3}} e_b + \frac{1}{\sqrt{3}} e_c \\
 &= \frac{1}{\sqrt{3}} e_a + \frac{1}{\sqrt{3}} (e_b + e_c) \\
 &= \frac{1}{\sqrt{3}} 0 + \frac{1}{\sqrt{3}} 0 \\
 e_{\gamma} &= 0
 \end{aligned} \tag{5.110}$$

i.e.

$$i_{\gamma} = 0 \tag{5.111}$$

$$\begin{aligned}
 i_{\gamma} &= \frac{1}{\sqrt{3}} i_a + \frac{1}{\sqrt{3}} i_b + \frac{1}{\sqrt{3}} i_c \\
 &= \frac{1}{\sqrt{3}} (i_a + 2i_b)
 \end{aligned} \tag{5.112}$$

Since

$$i_{\gamma} = 0$$

$$i_a = -2i_b \tag{5.113}$$

and

$$\begin{aligned}
 i_{\alpha} &= \sqrt{\frac{2}{3}} i_a - \frac{1}{\sqrt{6}} i_b - \frac{1}{\sqrt{6}} i_c \\
 &= -\sqrt{6} i_b
 \end{aligned} \tag{5.114}$$

or

$$i_{\alpha} = \sqrt{\frac{3}{2}} i_a \tag{5.115}$$

and

$$\begin{aligned}
 i_{\beta} &= -\frac{1}{\sqrt{2}} i_b + \frac{1}{\sqrt{2}} i_c \\
 &= \frac{1}{\sqrt{2}} (-i_b + i_c)
 \end{aligned}$$

$$i_{\beta} = 0 \tag{5.116}$$

The change in voltage due to the short-circuit is

$$\Delta e_{\alpha} = -\sqrt{\frac{3}{2}} E_0 \sin \theta \tag{5.117}$$

Simulating again the effect of the line-to-line fault by a step voltage  $\Delta e_{\alpha}$  applied to the  $\alpha$ -axis component of the voltage, with the field voltage  $e_f$  equal to zero:

$$\sqrt{\frac{3}{2}} E_0 \sin \theta = pM_{af} \cos \theta i_f + (R+p(A+B \cos 2\theta))i_{\alpha} \tag{5.118}$$

$$0 = (R_f + pL_f)i_f + pM_{af} \cos \theta i_{\alpha} \tag{5.119}$$

Equations (5.118) and (5.119) are linear differential equations with periodically time-varying coefficient, which can only be solved by the use of successive approximations. With all resistances neglected in the first approximation, equations (5.118) and (5.119) are solved simultaneously to give

$$i_{\alpha} = - \frac{\sqrt{6} E_0 (\cos\theta - \cos\theta_0)}{(M'+N')+(M'-N')\cos 2\theta} \quad (5.120)$$

and

$$\begin{aligned} i_f &= - \frac{M_{af}}{L_f} \cos\theta i_{\alpha} \\ &= \sqrt{6} \frac{M_{af}}{L_f} \frac{E_0 (\cos\theta - \cos\theta_0) \cos\theta}{(M'+N')+(M'-N')\cos 2\theta} \end{aligned} \quad (5.121)$$

where

$$\begin{aligned} M' &= X_d' \\ N' &= X_q \\ X_d' &= \omega \left( L_d - \frac{M_{af}^2}{L_f} \right) \\ X_q &= \omega L_q \end{aligned} \quad (5.122)$$

Applying the formulae given in Appendix VI,  $i_{\alpha}$  and  $i_f$  may be resolved into the Fourier series

$$\begin{aligned} i_{\alpha} &= - \frac{\sqrt{6} E_0}{M'+\sqrt{M'N'}} \left( \cos\theta + \sum_{n=1}^{\infty} b^n \cos (2n+1)\theta \right) \\ &\quad + \frac{\sqrt{6} E_0 \cos\theta_0}{\sqrt{M'N'}} \left( \frac{1}{2} + \sum_{n=1}^{\infty} b^n \cos 2n\theta \right) \end{aligned} \quad (5.123)$$

and

$$\begin{aligned} i_f &= \sqrt{\frac{3}{2}} \frac{M_{af}}{L_f} \frac{E_0}{M'+\sqrt{M'N'}} \left( 1 + \frac{(1+b)}{b} \sum_{n=1}^{\infty} b^n \cos 2n\theta \right) \\ &\quad - \sqrt{\frac{3}{2}} \frac{M_{af}}{L_f} \frac{E_0 \cos\theta_0 (1+b)}{\sqrt{M'N'}} \left( \cos\theta + \sum_{n=1}^{\infty} b^n \cos (2n+1)\theta \right) \end{aligned} \quad (5.124)$$

where

$$b = \frac{\sqrt{M'} - \sqrt{N'}}{\sqrt{M'} + \sqrt{N'}}$$

Introducing a correction for the resistances is made by multiplying each corresponding harmonic series by a decrement factor which is a function of time, gives

$$i_{\alpha} = -\frac{\sqrt{6} E_0}{M' + \sqrt{M'N'}} F_1(t) [\cos\theta + \sum_{n=1}^{\infty} b^n \cos(2n+1)\theta] \\ + \frac{\sqrt{6} E_0 \cos\theta_0}{\sqrt{M'N'}} F_2(t) \left[ \frac{1}{2} + \sum_{n=1}^{\infty} b^n \cos 2n\theta \right] \quad (5.125)$$

and

$$i_f = I_f(t) + \sqrt{\frac{3}{2}} \frac{M_{af}}{L_f} \frac{E_0}{M' + \sqrt{M'N'}} F_1(t) \left[ 1 + \frac{1+b}{b} \sum_{n=1}^{\infty} b^n \cos(2n+1)\theta \right] \\ - \sqrt{\frac{3}{2}} \frac{M_{af}}{L_f} \frac{E_0 \cos\theta_0}{\sqrt{M'N'}} (1+b) F_2(t) \left[ \cos\theta + \sum_{n=1}^{\infty} b^n \cos(2n+1)\theta \right] \quad (5.126)$$

The method for obtaining the decrement factors is described in Section 5.4. After the mathematical manipulations given in Appendix XI, the resulting three independent equations are

$$(R_f + pL_f) I_f(t) + \frac{\sqrt{6}}{2} R_f \frac{M_{af}}{L_f} E_0 \frac{1}{M' + \sqrt{M'N'}} = 0$$

$$\sqrt{\frac{3}{2}} E_0 = -\omega M_{af} I_f(t) + \sqrt{\frac{3}{2}} E_0 F_1(t) \quad (5.127)$$

$$RF_2(t) + p \frac{\sqrt{M'N'}}{\omega} F_2(t) = 0$$

Solving equations(5.127)

$$F_2(t) = e^{-t/\tau_e}$$

and

$$F_1(t) = \frac{X'_d + X_2}{X'_d + X_2} \left[ \frac{X'_d - X'_d}{X'_d + X_2} e^{-t/\tau'_d} + 1 \right] \quad (5.128)$$

and

$$I_f(t) = \sqrt{\frac{3}{2}} E_0 \frac{M_{af}}{L_f} \frac{1}{X'_d + X_2} [e^{-t/\tau'_d} - 1]$$

$$= \sqrt{\frac{3}{2}} \frac{E_0}{\omega M_{af}} \frac{X'_d - X'_d}{X'_d + X_2} [e^{-t/\tau'_d} - 1]$$

where

$$\tau_e = \frac{\sqrt{M'N'}}{R}$$

$$\tau'_d = \tau'_{do} \frac{X'_d + X_2}{X'_d + X_2} \quad (5.129)$$

$$\tau'_{do} = \frac{L_f}{R_f}$$

$$X_2 = \sqrt{M'N'}$$

The final current expressions are

$$i_\alpha = -\sqrt{6} E_0 \left[ \left( \frac{1}{X'_d + X_2} - \frac{1}{X'_d + X_2} \right) e^{-t/\tau'_d} + \frac{1}{X'_d + X_2} \right] (\cos\theta + \sum_{n=1}^{\infty} b^n \cos(2n+1)\theta)$$

$$+ \frac{\sqrt{6} E_0 \cos\theta_0}{X_2} e^{-t/\tau_e} \left( \frac{1}{2} + \sum_{n=1}^{\infty} b^n \cos 2n\theta \right) \quad (5.130)$$

and

$$\begin{aligned}
i_f &= I_{f0} + \sqrt{\frac{3}{2}} E_0 \frac{M_{af}}{L_f} \frac{e^{-t/\tau'_d} - 1}{X'_d + X_2} \\
&+ \sqrt{\frac{3}{2}} \frac{M_{af}}{L_f} E_0 \left[ \left( \frac{1}{X'_d + X_2} - \frac{1}{X'_d + X_2} \right) e^{-t/\tau'_d} + \frac{1}{X'_d + X_2} \right] \left( 1 + \frac{1+b}{b} \sum_{n=1}^{\infty} b^n \cos 2n\theta \right) \\
&- \sqrt{\frac{3}{2}} \frac{M_{af}}{L_f} \frac{E_0 \cos \theta_0}{X_2} (1+b) e^{-t/\tau_e} \left( \cos \theta + \sum_{n=1}^{\infty} b^n \cos (2n+1)\theta \right)
\end{aligned} \tag{5.131}$$

where  $I_{f0}$  is the constant field current existing before the fault.

Summing equations (5.130.) and (5.131) term-by-term, using the formulae given in Appendix VI yields

$$i_\alpha = - \frac{\sqrt{6} E_0 (F_1(t) \cos \theta - F_2(t) \cos \theta_0)}{X'_d + X_q + (X'_d - X_q) \cos 2\theta} \tag{5.132}$$

$$i_f = I_{f0} + \sqrt{\frac{3}{2}} \frac{M_{af}}{L_f} E_0 \left[ \frac{e^{-t/\tau'_d} - 1}{X'_d + X_2} + \frac{2(F_1(t) \cos \theta - F_2(t) \cos \theta_0) \cos \theta}{X'_d + X_q + (X'_d - X_q) \cos 2\theta} \right] \tag{5.133}$$

All the short-circuit currents for a line-to-line fault are now readily obtained as

$$\begin{aligned}
i &= - \frac{3E_0 (F_1(t) \cos \theta - F_2(t) \cos \theta_0)}{X'_d + X_q + (X'_d - X_q) \cos 2\theta} \\
i_a &= \frac{2 E_0 (F_1(t) \cos \theta - F_2(t) \cos \theta_0)}{X'_d + X_q + (X'_d - X_q) \cos 2\theta} \\
i_b &= \frac{E_0 (F_1(t) \cos \theta - F_2(t) \cos \theta_0)}{X'_d + X_q + (X'_d - X_q) \cos 2\theta} \\
i_c &= \frac{E_0 (F_1(t) \cos \theta - F_2(t) \cos \theta_0)}{X'_d + X_q + (X'_d - X_q) \cos 2\theta}
\end{aligned} \tag{5.134}$$

## 5.8 SUMMARY AND COMMENTS

Analytical solutions for the short-circuit fault conditions in unloaded zig-zag and Edison delta connected generators have been achieved by utilising modified Clarke transformations, together with a successive approximation technique. For this purpose, the flux-linkage equations for an ideal machine were written down and a modified Park transformation was applied to these equations, so that flux-linkage equations were obtained in a d-q fixed axis reference frame. Then flux-linkage/current equations are expressed in an  $\alpha, \beta$  moving axis reference frame using the relationship between  $\alpha, \beta$  components and d,q components. Alternatively, the flux-linkage equations could have been expressed directly in the  $\alpha, \beta$  moving axis reference frame, using the relationship between direct-phase quantities and  $\alpha, \beta$  quantities, although this makes the trigonometric manipulation longer. The voltage-current equations in terms of  $\alpha, \beta, \gamma$  components were obtained from the flux-linkage equations by utilising Faraday's voltage law. Various fault conditions for unloaded zig-zag and Edison-delta connections have been simulated by application of the superposition principle. When terminal constraints for the various short-circuit cases were expressed in the form of  $\alpha, \beta, \gamma$  components, and substituted into the voltage-current equation, a set of ordinary linear time-varying differential equations for the armature and field currents resulted. Although these are linear and ordinary, the coefficients are periodically time varying. A direct analytical solution is not therefore possible and they can only be solved by the method of successive approximations. On this basis, analytical expressions for the initial short-circuit currents were found by neglecting the resistances of both field and armature circuits. The effect of resistances was subsequently introduced through decrement factors for both the field and armature currents. It was assumed that the even harmonics in the field current and the odd harmonics in the armature currents had the same factor, and odd harmonics in the field current and even harmonics in the armature currents also had the same decrement factors. Modified expressions were obtained by re-writing the current expressions to involve these

factors, as determined by substituting the modified current expressions into the original differential equations, and equating the corresponding terms is on the two sides of the equations. When doing this, relatively small resistances appearing in the coefficients of the harmonic terms are neglected, although those in the DC terms are retained.

A close examination of the armature and field current expressions shows that the armature currents contain a fundamental frequency component together with odd harmonics, while the field current contains a DC component together with even harmonics. As the absolute value of  $b$  is less than unity, each successive harmonic is less than the preceding one.

Since the process outlined above requires long and tedious mathematical manipulations, it does not appear to be a practical proposition in the modern computer age. However, harmonic production and the effects of initial rotor position on the short circuit current can clearly be seen in the analytical expressions, and the methods also provide simple formulae for the short-circuit currents.

It is interesting to observe that the  $\beta$ -axis components of the armature currents under various short-circuit conditions for a zig-zag or Edison-delta connected generator are always to zero.

## CHAPTER 6

### EXPERIMENTAL PROCEDURE USED WITH THE VARIOUS GENERATOR CONNECTIONS AND RESULTS

Any armature winding re-connection not only affects the dynamic and steady-state performance of the generator but also changes the available power output, the losses both in the rotor and the stator and the efficiency, as well as the voltage and current waveforms both in the field and the armature windings. These quantities were determined on a test machine, the name-plate details of which are given in Appendix I.

#### 6.1 AVAILABLE POWER OUTPUT

Based simply on the voltage and current rating of the armature windings, the output available from the experimental machine with its rated voltage  $E$  of 127 V/ph rated current  $I$  of 7.8 A/ph and rated power factor  $\cos\phi$  of 0.8 are presented in Table 6.1 for the different winding arrangements under consideration. As the table clearly shows, the power output is considerably reduced by any re-connection. A zig-zag connected generator provides the largest available power output, while line-to-neutral loaded generators provide the lowest available power output among the single-phase connections for 3-phase generator.

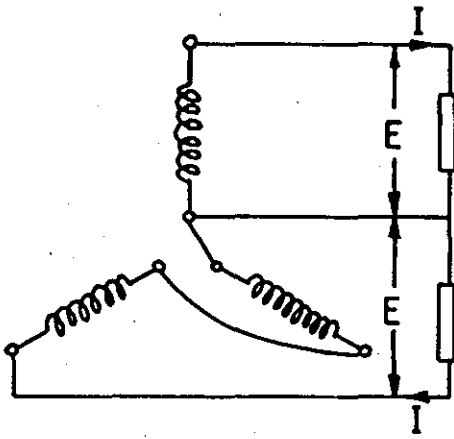


FIGURE 6.1(a) Zig-zag connected generator

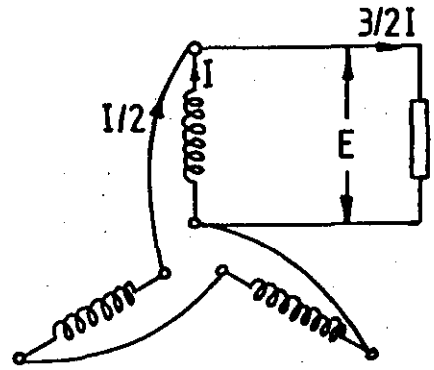


FIGURE 6.1(b) Edison-delta connected generator

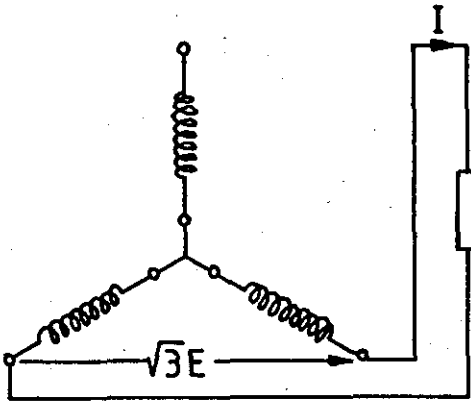


FIGURE 6.1(c) Line-to-line loaded generator

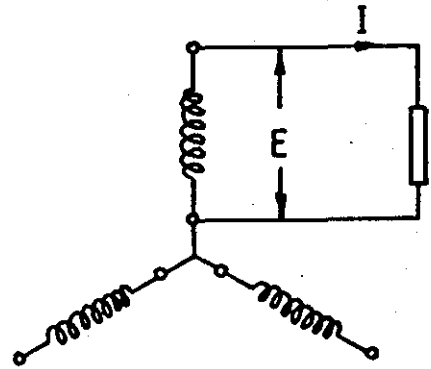


FIGURE 6.1(d) Line-to-neutral loaded generator

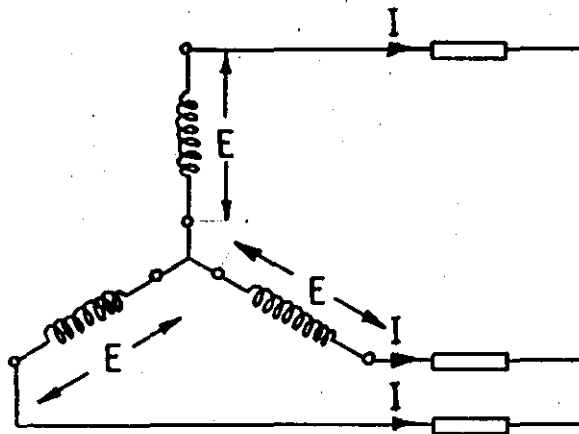


FIGURE 6.1(e) Star connected 3-phase generator

	Star Connection	Zig-Zag Connection	Edison-Delta Connection	Line-to-Line Loading	Line-to-Neutral Loading
a	$3EI \cos \phi$	$2EI \cos \phi$	$1.5EI \cos \phi$	$3EI \cos \phi$	$EI \cos \phi$
b	2377W	1585W	1189W	1371W	792W

TABLE 6.1: Available power outputs of re-connected generator:  
 a) Mathematical expressions  
 b) Numerical values

## 6.2 VOLTAGE WAVEFORMS

Any user of electric power normally desires a sinusoidal voltage waveform free from harmonic distortion. In practice however the voltage waveform supplied by a power utility may sometimes contain a certain amount of harmonic distortion. Some of the major effects resulting from the presence of harmonics in a power system are<sup>44,45</sup>:

- a) Capacitor bank failure, from dielectric breakdown or reactive power overload
- b) Interference with ripple control and power line carrier systems, causing mis-operation of systems which accomplish remote switching, load control, and metering
- c) Excessive losses in and heating of synchronous and induction machines
- d) Over-voltages and excessive currents on the system due to harmonic resonance

- e) Dielectric breakdown of insulated cables resulting from harmonic over-voltages on the system
- f) Inductive interference with telecommunication systems
- g) Error in induction kWh meters
- h) Signal interference and relay malfunction, particularly in solid-state and microprocessor control system
- i) Interferences with large motor controllers and power excitation system
- j) Mechanical oscillations of synchronous generator and induction motors
- k) Unstable operation of firing circuits based on zero voltage crossing detection or latching.

Voltage waveforms for both the field and the load are recorded in Figures 6.2-6.10 for the experimental machine supplying rated armature current at rated voltage and rated power factor. Clearly, these waveforms contain considerable harmonic distortion when the generator winding is re-connected in any abnormal configuration. Any re-connected armature sets up a pulsating mmf, which may be resolved into two contra-rotating components. The component in the opposite direction to normal rotation induces a second-harmonic component in the field, which produces further harmonics across the air-gap by inducing a third harmonic in the armature voltage. Both armature and field voltages contain an infinite series of progressively decaying harmonics

Harmonic production in the field and armature currents can clearly be seen in the analytical expressions for the currents which were obtained in Chapter 5.

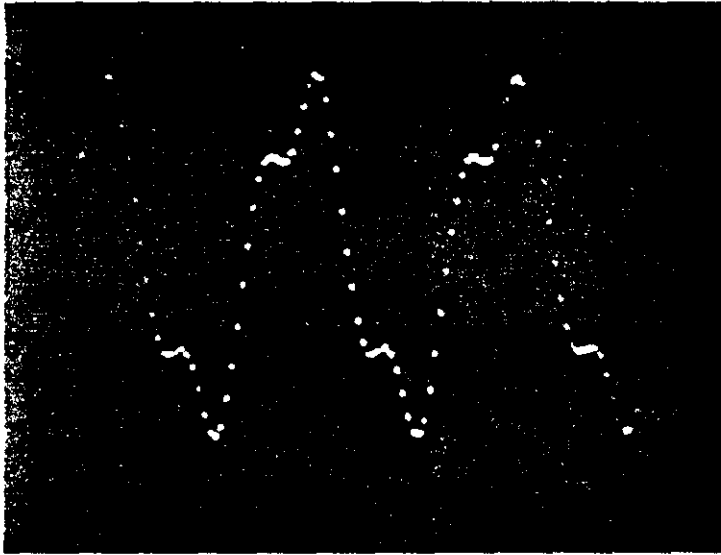


FIGURE 6.2: Load voltage ( $V_1$ ) for a zig-zag connected generator supplying rated load ( $V_1$  is the voltage of the first load)

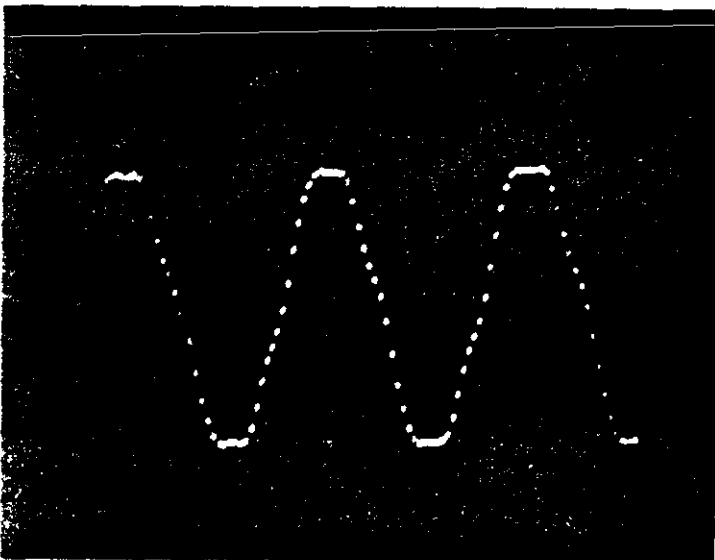


FIGURE 6.3: Load voltage ( $V_2$ ) for a zig-zag connected generator supplying rated load ( $V_2$  is the voltage of second load)

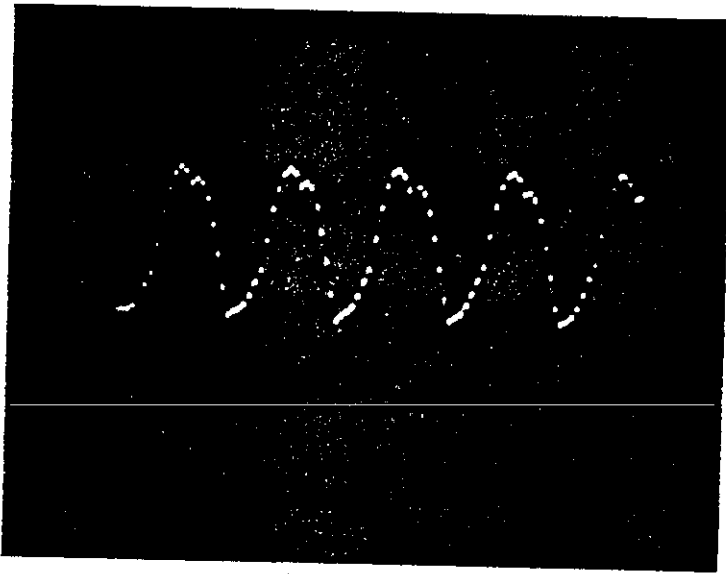


FIGURE 6.4: Field voltage for a zig-zag connected generator under rated load

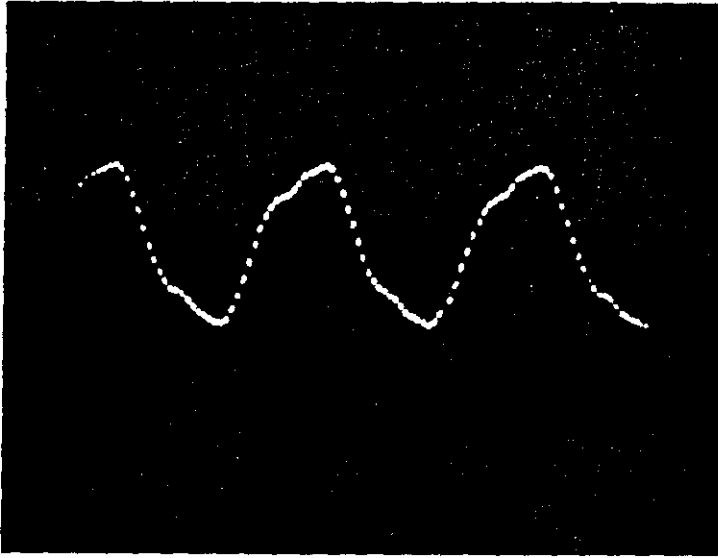


FIGURE 6.5: Load voltage for an Edison-delta connected generator supplying rated load

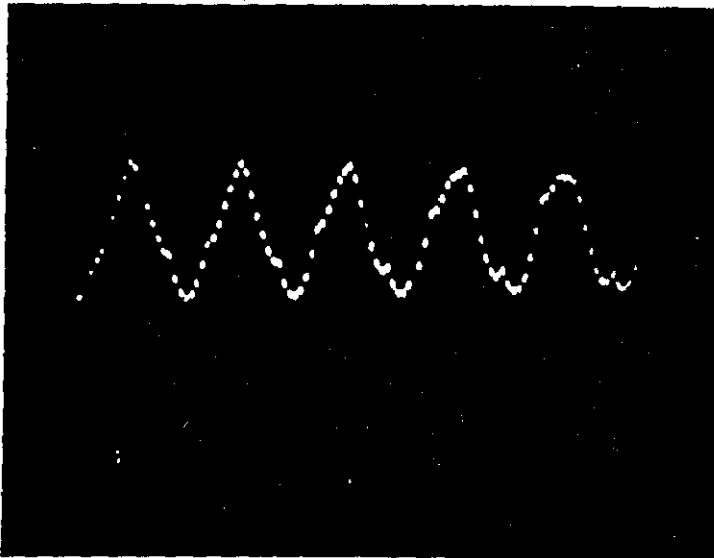


FIGURE 6.6: Field voltage for an Edison-delta connected generator supplying rated load

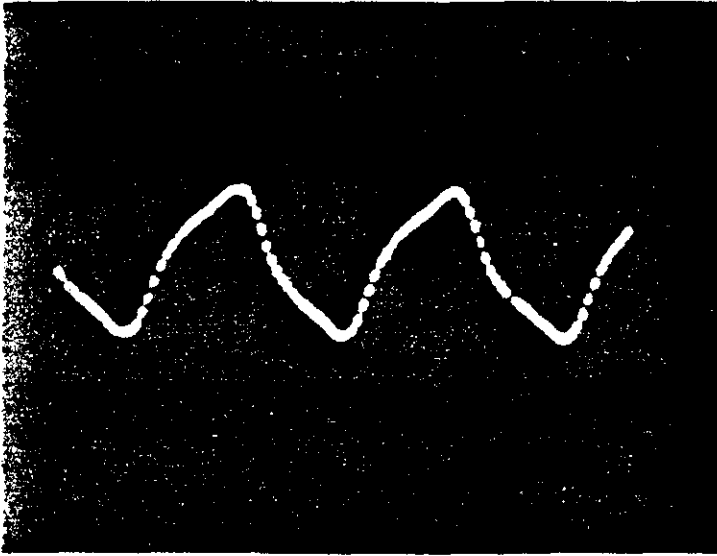


FIGURE 6.7: Load voltage for line-to-line loaded generator supplying rated load

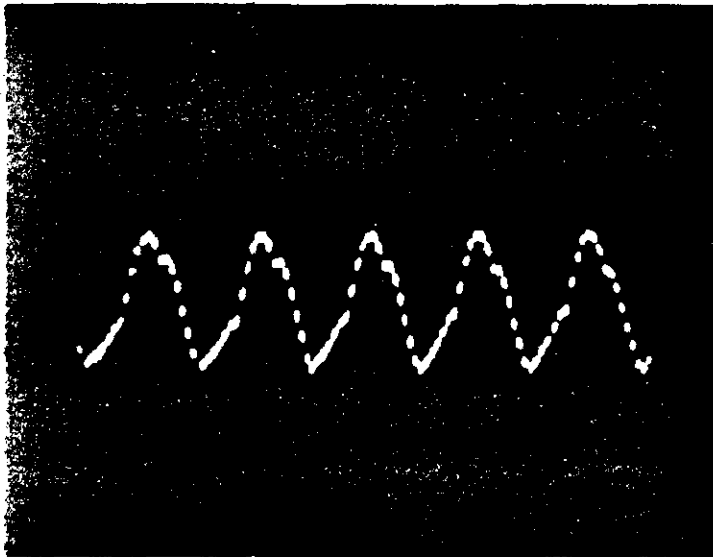


FIGURE 6.8: Field voltage for line-to-neutral loaded generator supplying rated load

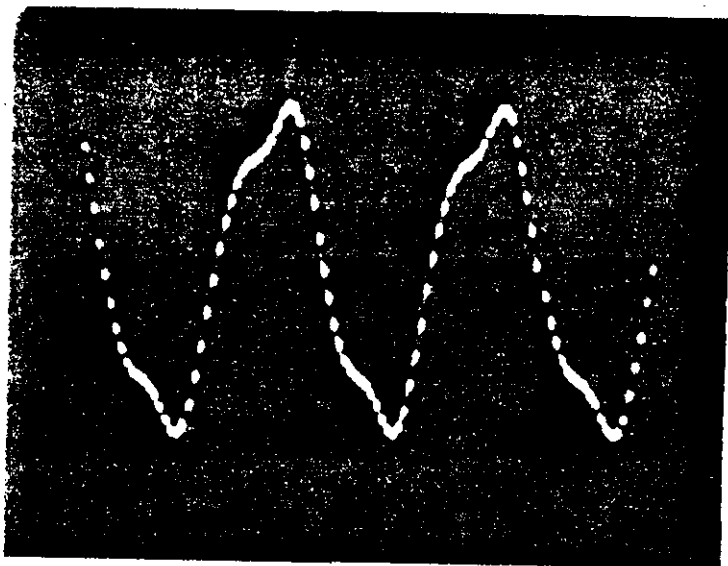


FIGURE 6.9: Load voltage for line-to-neutral loaded generator supplying rated load

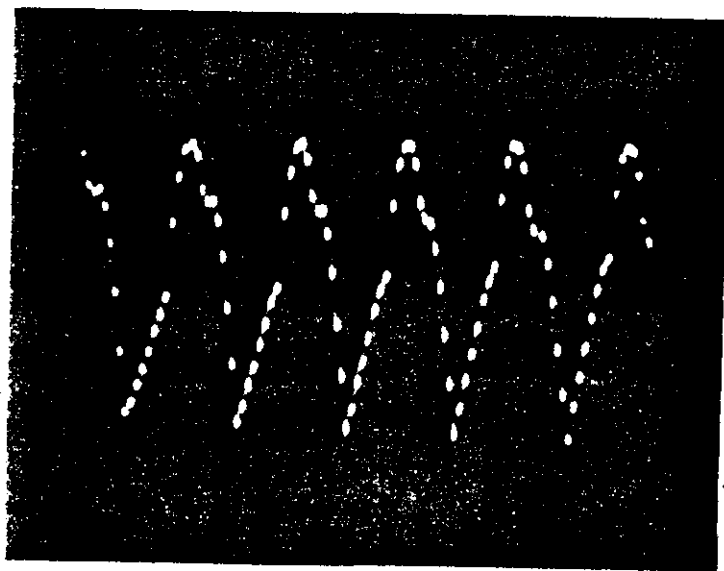


FIGURE 6.10: Field voltage for line-to-neutral loaded generator supplying rated load

### 6.3 LOSSES

Losses in a generator are very important, since they determine the efficiency and heating of the machine, and also appreciably influence its operating cost. The various losses in a synchronous generator may be summarised as:

- a) Copper losses which occur in the armature and field windings
- b) Core losses which comprise eddy current and hysteresis losses in the pole face, teeth, and stator core
- c) Friction and windage losses which are due to bearing and brush friction, and to the power required to circulate the cooling air
- d) Load loss attributed to the armature leakage flux, which causes eddy current and hysteresis heating in the iron surrounding the armature conductor.

There are four methods<sup>46</sup> available for measuring the losses in a synchronous machine:

- a) Separate-Drive Method
- b) Electric-Input Method
- c) Retardation Method
- d) Cooler Method

In the present investigation, the separate-drive method was used to determine the losses of the experimental machine, and the technique is explained briefly in Appendix III.

The sum of the armature copper losses, the iron loss and the friction and windage losses of the drive motor is shown in Figure 6.11 as a function of the driving motor speed, and the sum of the friction and

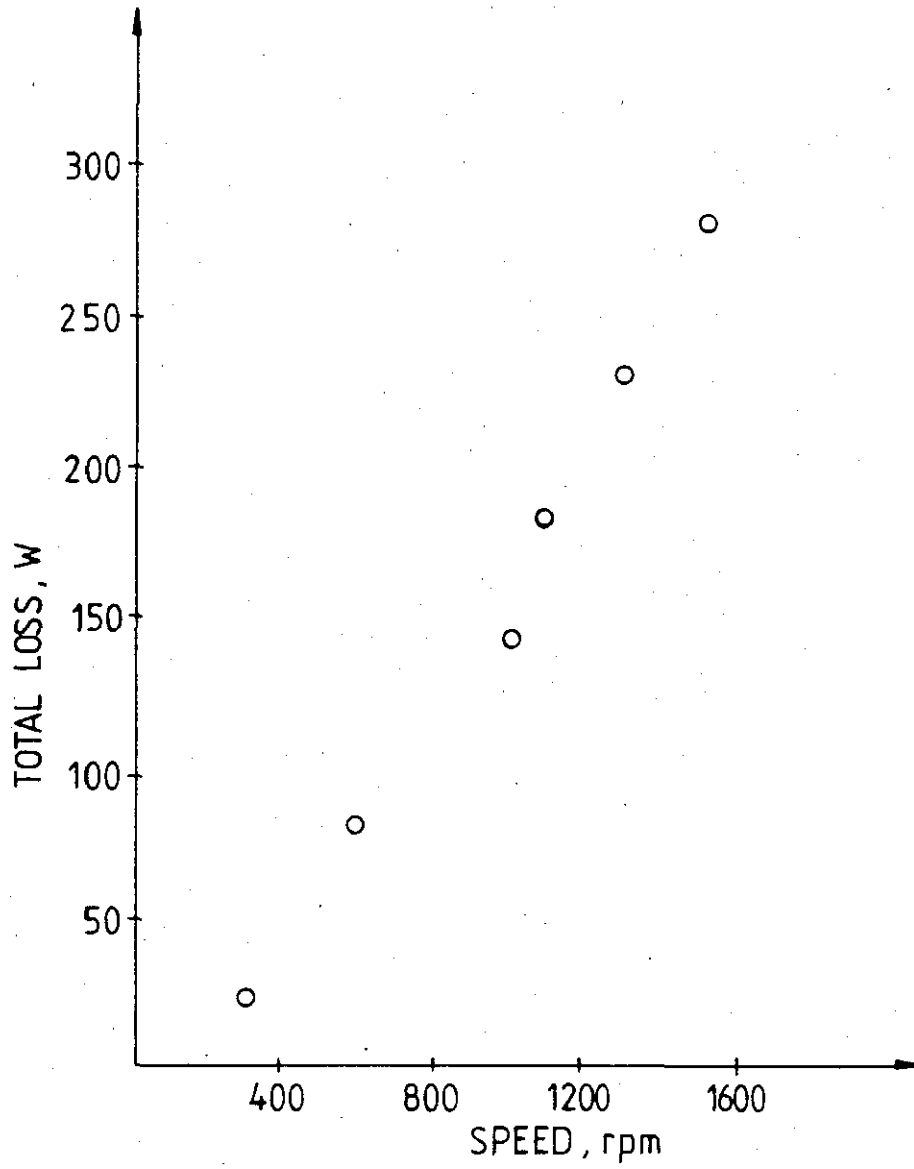


FIGURE 6.11: Variation of total losses of driving machine with speed (on no-load)

windage loss of the experimental generator is shown in Figure 6.12 as a function of its speed. The experimental generator core loss when the generator is on no load at rated speed is shown in Figure 6.13 as a function of the field current.

The armature copper loss for the various connections of the experimental machine with rated armature current and rated voltage are given in Table 6.2. The total losses of the generator were determined using the method explained in Appendix III and these are shown in Table 6.3, for the various connection and rated voltage and current conditions.

	Star Connection	Zig-Zag Connection	Edison-Delta Connection	Line-to-Line Loading	Line-to-Neutral Loading
a	$3RI^2$	$3RI^2$	$1.5RI^2$	$2RI^2$	$RI^2$
b	14.96W	14.96W	7.48W	9.97W	4.98W

TABLE 6.2: Armature copper losses for various generator connections  
 a) Mathematical expressions  
 b) Numerical values

#### 6.4 EFFICIENCY

The efficiency of the generator is defined as

$$\text{Efficiency} = \frac{P_{\text{out}}}{P_{\text{inp}}}$$

which can also be expressed in terms of power output and losses as

$$\text{Efficiency} = \frac{P_{\text{out}}}{P_{\text{out}} + P_{\text{losses}}} = \frac{P_{\text{inp}} - P_{\text{losses}}}{P_{\text{inp}}}$$

The generator efficiencies for the various armature connections were

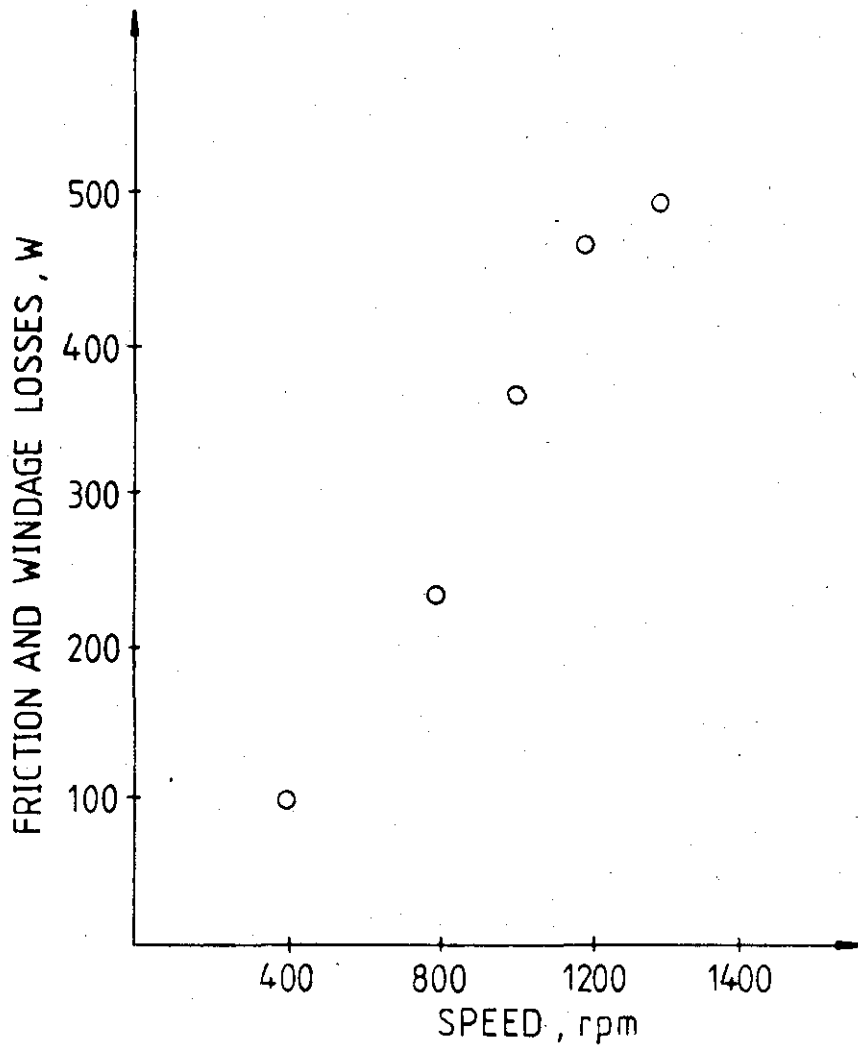


FIGURE 6.12: Variation of generator friction and windage loss with speed

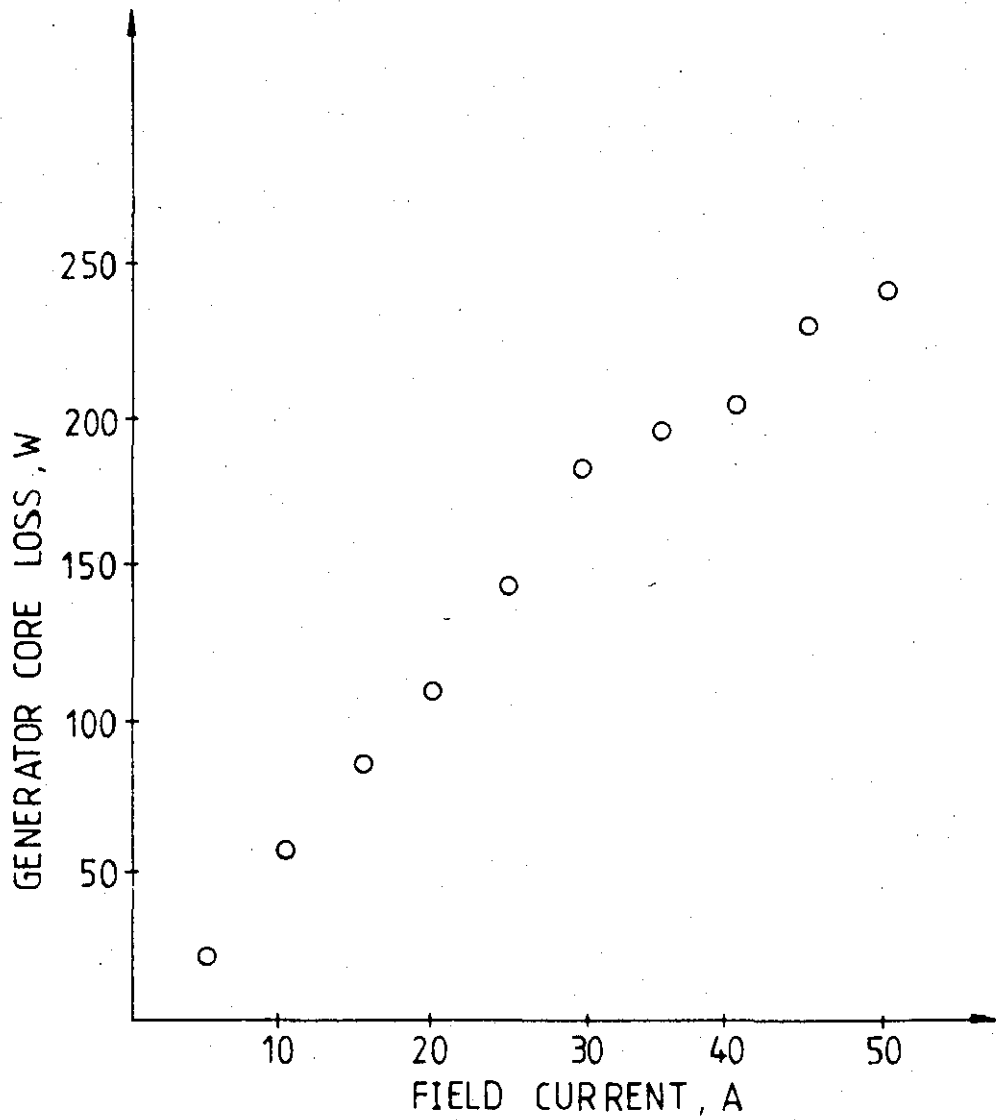


FIGURE 6.13: Variation of generator core loss with excitation current

determined at rated armature current and voltage and the results are given in Table 6.3. Clearly, the generator efficiency is reduced by re-connection, with the line-to-neutral loaded generator having the lowest efficiency among the single-phase connections.

	Star Connection	Zig-Zag Connection	Edison- Delta Connection	Line- to- Line Loading	Line- to- Neutral Loading
a	980	1002	918.5	962.8	792.5
b	71.0	57.8	58.0	58.0	50.8

TABLE 6.3: Total losses and efficiencies for the various generator connections at rated voltage and rated armature current and at rated power factor  
 a) Total losses, W  
 b) Efficiencies, %

CHAPTER 7CONCLUSIONS AND SUGGESTIONS7.1 CONCLUSIONS

The armature windings of a 3-phase generator are often capable of being connected in various configurations, in order to provide a single-phase supply for standby or emergency purposes. In this thesis, the different methods of obtaining a single-phase supply have been examined, and performance comparisons between these options have been made on a 3 kVA microalternator. The different single-phase connections investigated were:

- a) When the neutral point of a generator is unavailable and line-to-line loading is the only possibility.
- b) When the neutral point of a generator is available and both line-to-line and line-to-neutral loading are possible.
- c) When all the armature terminals are available and line-to-line loading, line-to-neutral loading, zig-zag connection and Edison-delta connection all become possible.

As a result of the work presented in this thesis, the following conclusions can be drawn.

1. A re-connected generator always produces a negative-sequence component in the armature current. In every possible single-phase connection the magnitude of this component is always equal to the positive-sequence component. This is because any single-phase connected armature sets up a pulsating mmf which may be resolved into equal magnitude contra-rotating components.

2. The available power output of a generator is considerably reduced by any re-connection of the armature windings. This reduction is smallest in the case of a zig-zag connection and greatest for line-to-neutral loading.
3. The current in the centre line of a zig-zag connected generator is very small when the two loads are identical since the two load currents are almost equal.
4. The unbalance factor for current is always independent of the load, for every single-phase connection, since the magnitudes of positive and negative-sequence components of the armature current are equal.
5. When rated current flows at rated voltage, the armature copper losses in a conventional star-connected and a zig-zag connected generator are equal, with this loss being clearly lower in the case of line-to-line loading and lowest for line-to-neutral loading.
6. The efficiency of the generator is reduced by armature winding re-connection. When rated current flows at rated voltage, the reduction is greatest in the case of line-to-neutral loading and smallest in the case of line-to-line loading.

Based on the theoretical and experimental results provided in this thesis the following comments can be made:

- a) Symmetrical components are easy to apply to unsymmetrical fault and unbalanced load conditions, since they require neither long and tedious mathematical manipulation nor computer programming. In addition, the parameters required for the analysis are readily measured by three straightforward tests. However, the accuracy of predictions based on this form of analysis are often poor, since the voltage and current waveforms both contain harmonic components. Nevertheless a symmetrical component model gives the

magnitude of the negative-sequence component in the armature current, and enables the temperature rise within the machine and eddy current losses within the rotor body to be assessed. The model also provides mathematical expressions for the unbalance factors of both current and voltage.

- b) A phase model for a generator can predict accurately both the steady-state and the transient performance of the machine during either balanced or unbalanced loading, as well as symmetrical and unsymmetrical fault conditions. To obtain the numerical results requires a digital computer simulation, with the consequent possibility of numerical instability. Another disadvantage of the phase model is that the measurement of the machine parameters which are involved is a time-consuming process. In addition to this, the model requires the inversion of a periodically time varying inductance matrix at each step of the numerical integration, which clearly increases the computation time.
- c) An  $\alpha$ ,  $\beta$ ,  $\gamma$  component model involves many questionable simplifications throughout the long and tedious mathematical manipulations which are involved in its development. On the other hand, harmonic production both in the field and the armature currents can be clearly seen in the analytical expressions which are obtained. The model also provides simple formulae for the time constants of the various short-circuit currents.

## 7.2 SUGGESTIONS FOR FURTHER INVESTIGATIONS

The investigations reported in this thesis have raised several interesting points, which could not be investigated further in the time available.

1. In the development of the phase model for the generator, several simplifying assumptions were made. Saturation was neglected, with the open-circuit characteristic of the generator assumed to be a straight-line within the operating region. If it is desired to include the effect of saturation, Smith and Snider<sup>47</sup> have described a technique which allows the winding inductance variations with machine currents to be determined, and thereby enables the complete nonlinear inductance matrix of the machine to be specified. Saturation effects may be accounted for in the prediction of the transient performance of a generator by employing the techniques described by Smith and Snider, although the computation time required for the investigation of any given situation will necessarily be increased.
2. It was also assumed in the development of the phase model that the armature phase mmf is sinusoidally distributed which led to no harmonics higher than the second appearing in the angular variation of the machine inductances. However, it is known<sup>48</sup> that the winding mmf and air-gap permeance harmonics may have a significant effect on the winding inductances. Smith and Snider<sup>19</sup> have shown that space harmonics may be included in a generator model and their approach may clearly be used with the model developed in this thesis.
3. It has been shown<sup>49,50,51</sup> that synchronous machine models employing only one damper winding on each axis may not be adequate for representing machine performance over a wide range of operating conditions due to eddy currents in the rotor structure. For more accurate predictions, the phase model developed in this thesis may need to be extended to include the

damping effect of the rotor iron, by introducing multiple damper circuits on each axis.

4. Temperature changes inside the generator may have a significant effect on its performance, since under no-load conditions the temperature is typically  $20^{\circ}$ - $30^{\circ}$  whereas under full-load conditions it can exceed  $120^{\circ}\text{C}$ . The corresponding increase in the resistance of the generator windings will affect both the steady-state operating point of the system as well as the transients which follow the application or rejection of load. Sollectio and Swann<sup>52</sup> investigated the effects of temperature changes on generator performance. Similar investigation can also be carried out using the mathematical model described in this thesis.
5. Certain protective devices in an electrical power system work on the basis of the presence of negative-sequence current in a supply line. Since both a zig-zag and an Edison-delta connected generator produce negative-sequence current, which may clearly cause problems, this should therefore be a subject for further investigation.
6. Generators are probably the most expensive item of plant in an AC power system. Winding re-connection will cause an increased temperature rise within the generator, which may reduce the expected life of the insulation. Protection of zig-zag or Edison-delta connected generators against overheating may thus be a subject for investigation.
7. Since standby generators are used in a wide variety of applications, it is important that the harmonic content of their output voltage waveforms should be minimized and that they meet any relevant industrial standards. Moore<sup>53</sup> has examined the possibilities of harmonic reduction in star-connected standby generators from a design point of view. Similar consideration should be given to generators which may operate as standby

generators in either a zig-zag or an Edison-delta connection.

8. Within the last few years, the advent of high-speed computers has allowed finite-difference and finite-element methods to be used extensively in the solution of field problems in electrical machines. The magnetic field distribution of a zig-zag or an Edison-delta connected generator may be plotted and the eddy currents in the rotor structure may be investigated using these numerical techniques. The temperature distribution within a re-connected generator, with particular reference to any potential hot spots, may be a subject of further investigation.
9. The phase model developed in this thesis could readily be extended to include the excitation circuit, and the automatic voltage regulator (AVR). Transient and steady-state performance characteristics, the effect of the AVR parameters on the overall stability and the optimisation of the transient performance should also be the subject of further investigation.
10. Eddy currents in the rotor structure of a synchronous generator affect both the transient and the steady-state performance. Although this effect was neglected in the development of the phase model, Rogers and Smith<sup>54</sup> have shown that eddy current effects can easily be included by an application of Green's functions. The model developed in the thesis can similarly be extended to include the effect of eddy currents.
11. The power output of a re-connected generator is reduced by the nature of the connection itself, as well as the increased losses which arise consequently from the re-connection. Clearly the cost of the energy supplied by a re-connected generator should be a subject of investigation.

APPENDICES

APPENDIX IMEASUREMENT OF D-Q PARAMETERS1. THE EXPERIMENTAL MACHINE

Conventional tests were performed to determine the parameters of a 3-phase salient-pole synchronous generator with the following name-plate details:

Rating	3 kVA, 0.8 pf
Phase voltage	220V
Speed	1500 rpm
Number of poles	4
Frequency	50 Hz
Field excitation for rated current at rated voltage	7.8A

The generator was mechanically coupled to a large 1500 rpm shunt-connected DC machine, which could act as a prime-mover or a load as required.

2. RESISTANCE MEASUREMENT

A Kelvin double bridge was used to measure the armature phase resistance. At an ambient temperature of 20°C the mean of the three phase resistances was 0.074 $\Omega$ . Since the effect of 50 Hz current is to increase the effective resistance by about 10%<sup>55</sup>, the armature phase resistance was assumed to be 0.082 $\Omega$  (0.005 pu) for calculation purposes.

The field resistance measured using a sub-standard DC voltmeter and ammeter, was found to be 4.23 $\Omega$  (0.259 pu), again at 20°C.

### 3. REACTANCE MEASUREMENT

#### 3.1 Direct-axis Synchronous Reactance ( $X_d$ )

The d-axis synchronous reactance  $X_d$  was obtained from both open-circuit and short-circuit tests<sup>46</sup>, as well as from a slip test<sup>46</sup>. The values of  $X_d$  determined by these two tests were:

From open and short-circuit tests:	21.3 $\Omega$ /phase (1.31 pu)
From slip test:	20.8 $\Omega$ /phase (1.28 pu)

The close agreement between these figures indicates that a reasonable value for  $X_d$  is 1.30 pu.

#### 3.2 Quadrature-axis Synchronous Reactance ( $X_q$ )

The q-axis synchronous reactance was obtained from both a slip test<sup>56</sup> and a maximum-lagging-current test<sup>56</sup>. The values of  $X_q$  determined by these two tests were:

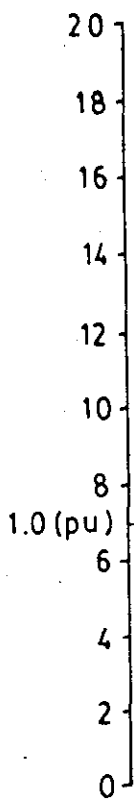
From the slip test:	12.9 $\Omega$ /phase (0.79 pu)
From the maximum-lagging-current test:	12.3 $\Omega$ /phase (0.77 pu)

The close agreement between these figures indicates that a reasonable value for  $X_q$  is 0.78 pu.

#### 3.3 Armature Leakage Reactance ( $X_a$ )

The armature leakage reactance of a synchronous machine is extremely difficult to measure and it is usually assumed to be equal to the Potier reactance. This latter reactance, as determined from open-circuit and zero power factor rated-current characteristics, was obtained as 0.05 pu.

ARMATURE PHASE CURRENT, (AMPS)



ARMATURE PHASE VOLTAGE, (VOLTS)

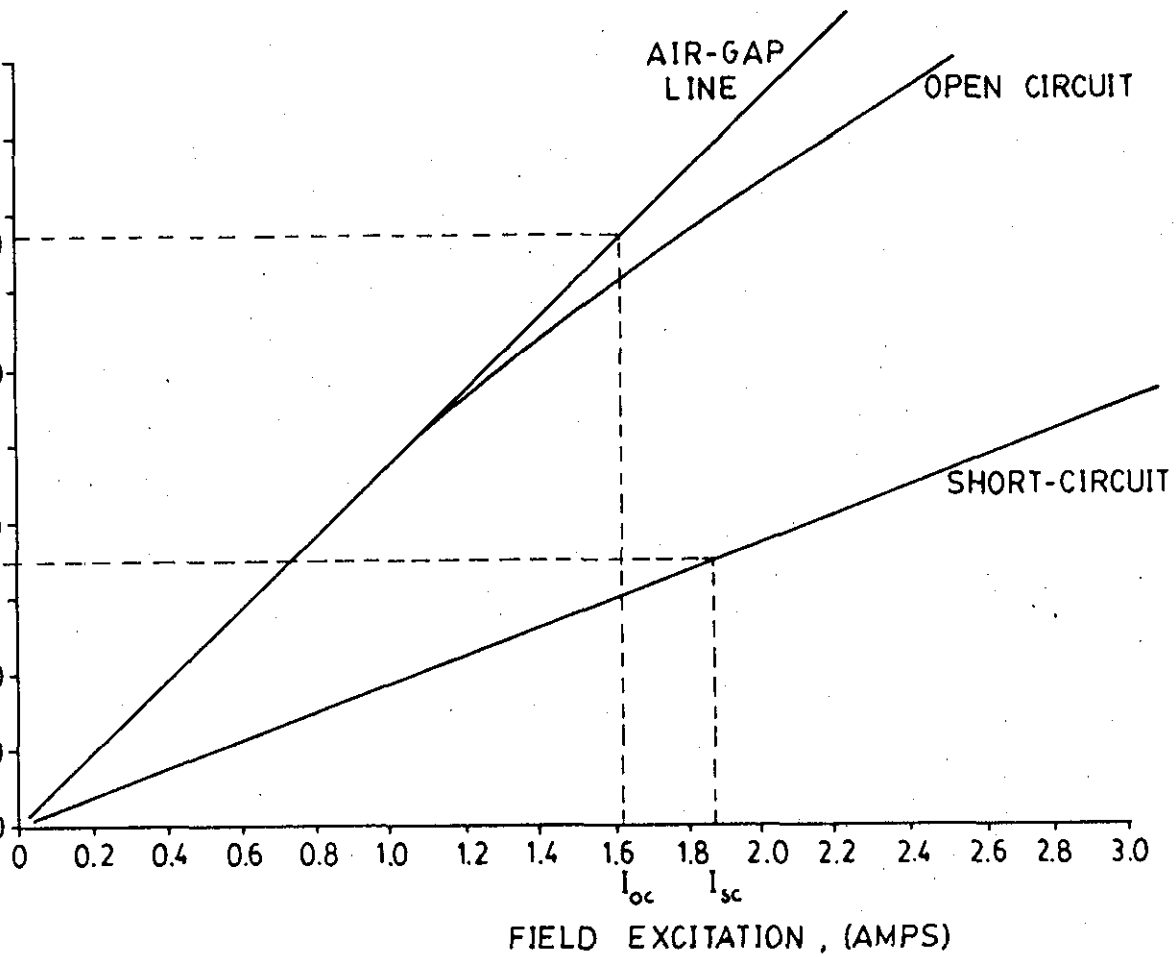
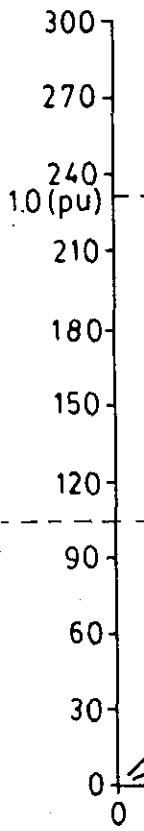


FIGURE A1.1: Open-circuit, short-circuit characteristics

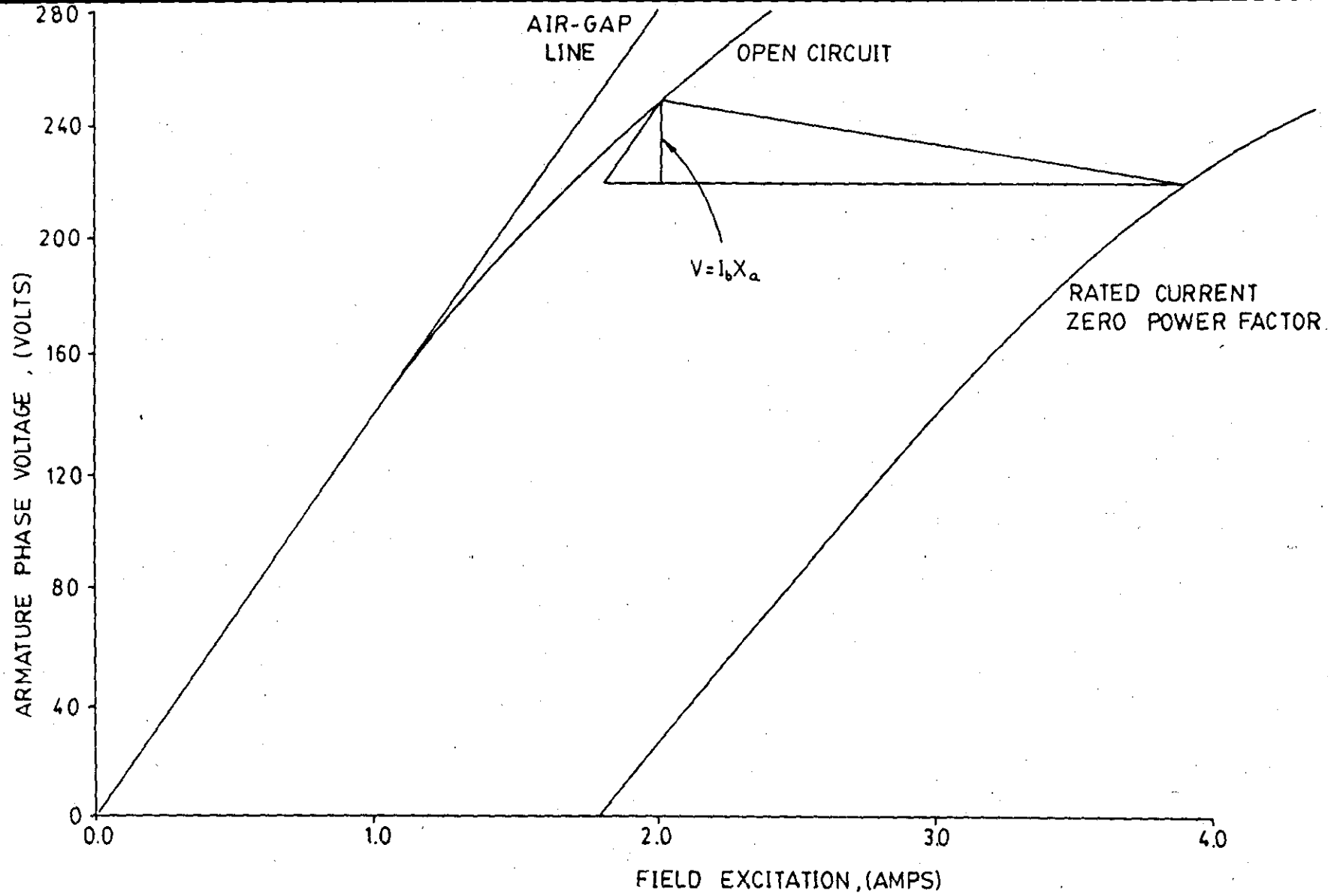
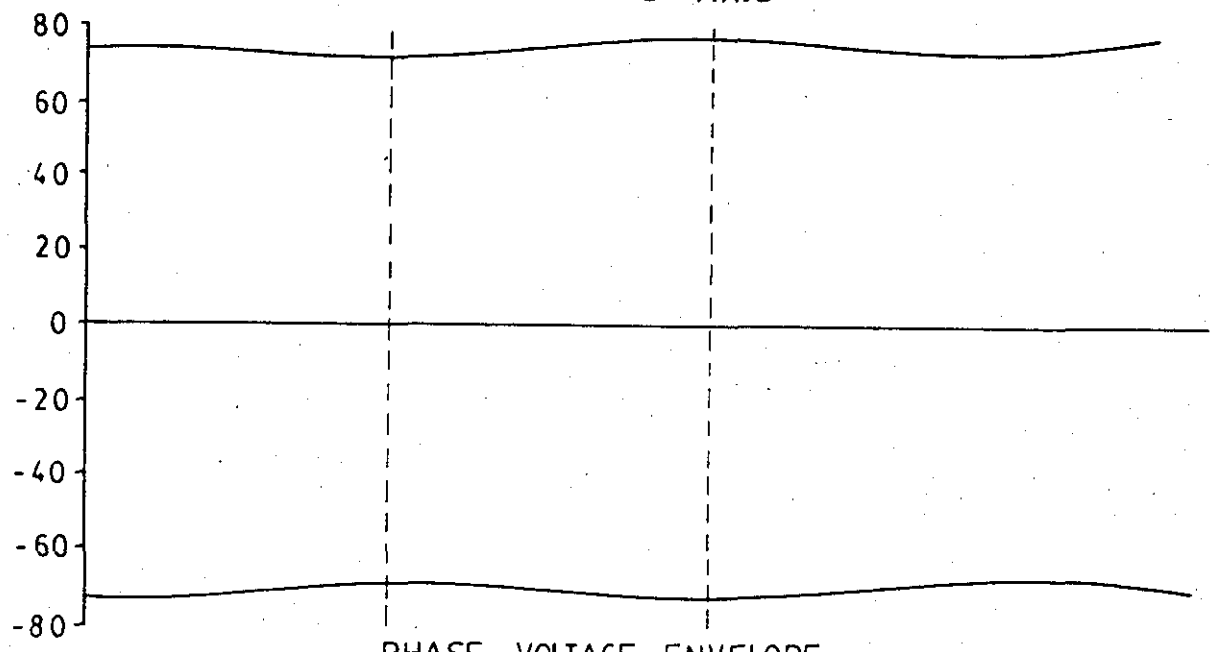


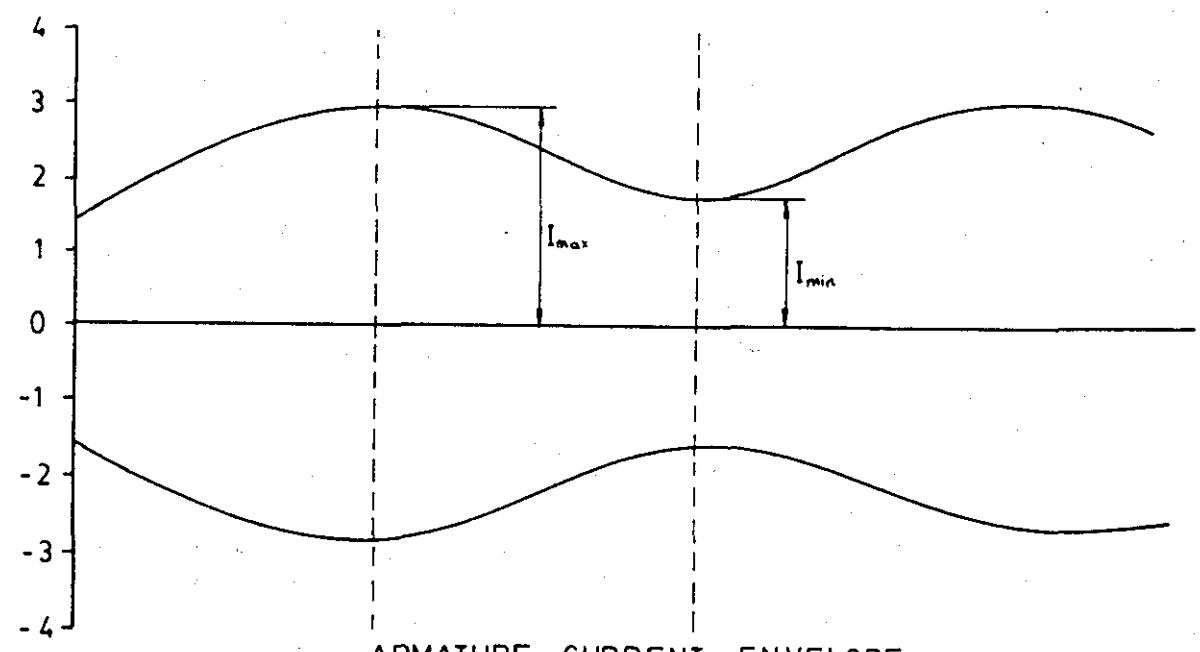
FIGURE A1.2: Open circuit and rated current zero power factor characteristics

Q - AXIS

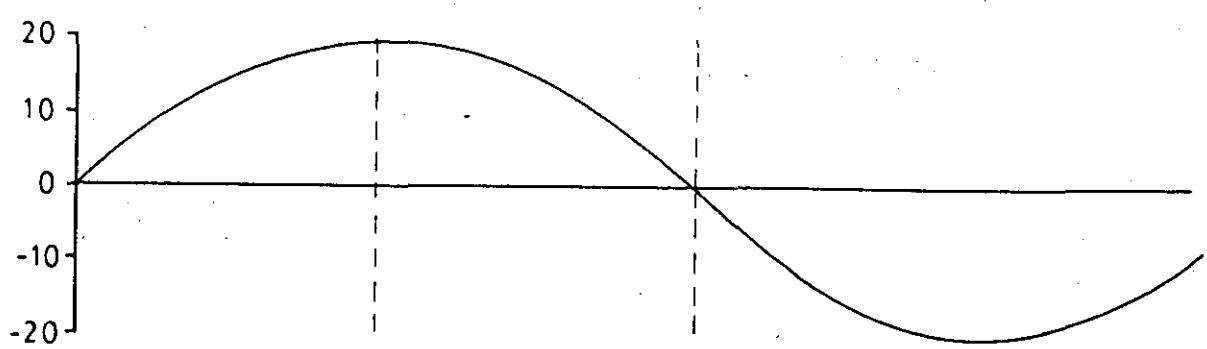
D - AXIS



PHASE VOLTAGE ENVELOPE



ARMATURE CURRENT ENVELOPE



FIELD VOLTAGE (OPEN CIRCUIT)

FIGURE A1.3: Slip test voltage and current envelopes

### 3.4 Direct-axis Magnetising Reactance ( $X_{md}$ )

The magnetising reactance of the d-axis is

$$X_{md} = X_d - X_a$$

giving a value for  $X_{ad}$  of 1.25 pu.

### 3.5 Quadrature axis Magnetising Reactance ( $X_{mq}$ )

The magnetising reactance of the q-axis is

$$X_{mq} = X_q - X_a$$

giving a value for  $X_{mq}$  of 0.73 pu.

### 3.6 Direct-axis Transient Reactance ( $X'_d$ )

The d-axis transient reactance was determined from the transient current waveform following a sudden 3-phase short-circuit applied to the armature operating on open-circuit and at rated speed. The d-axis transient reactance is the ratio of the open-circuit armature voltage to the current obtained by extrapolation of the envelope of the alternating component of the transient current wave to the instant of the application of the short-circuit, neglecting the rapid variation of current during the first few cycles. The d-axis transient reactance is

$$X'_d = \frac{E}{I'}$$

$$= \frac{57.7V}{8A} = 7.15\Omega \text{ /phase (0.44 pu)}$$

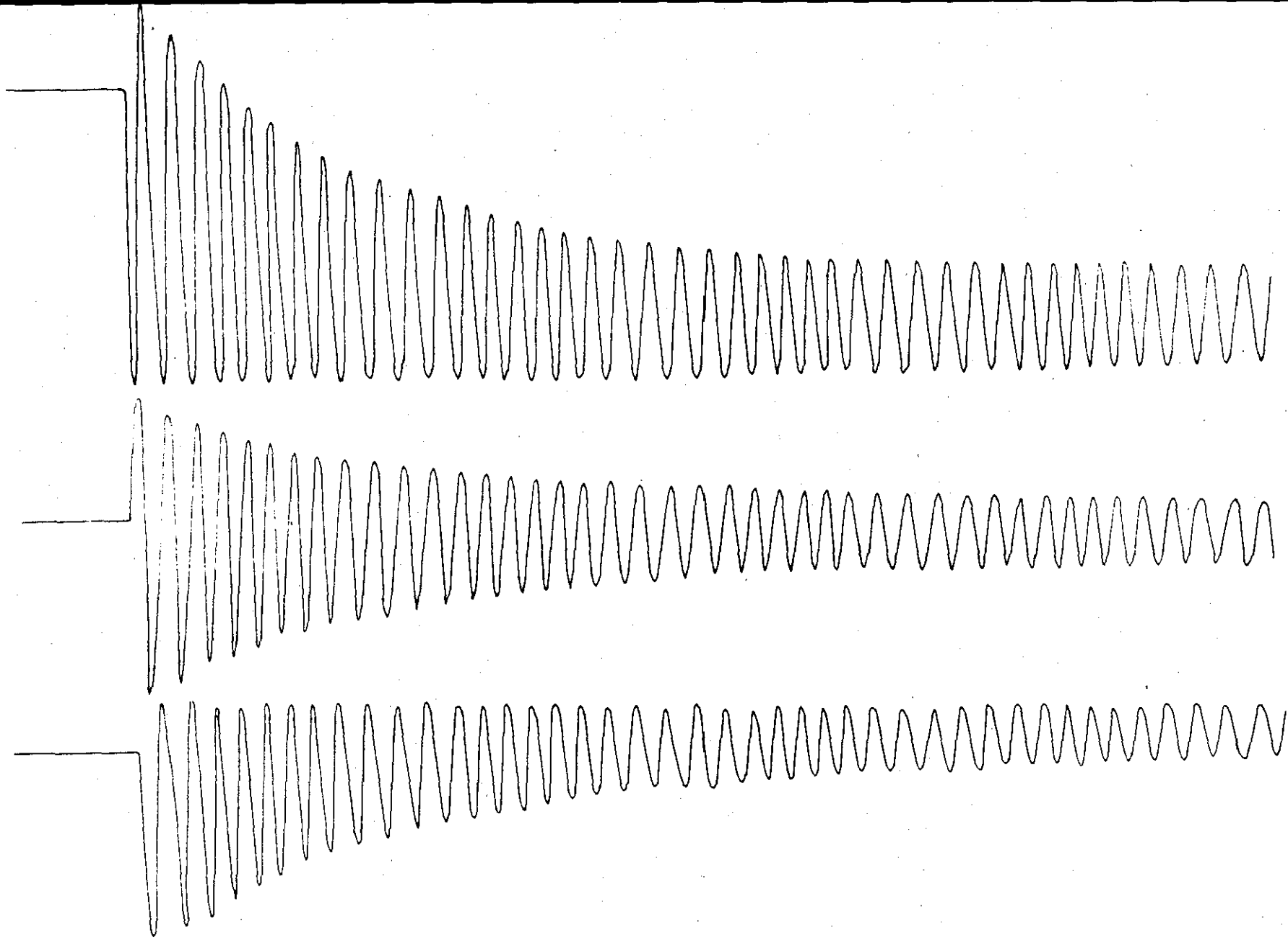


FIGURE A1.4: Oscillogram of 3-phase fault currents on unloaded generator

### 3.7 Direct-axis Subtransient Reactance ( $X_d''$ )

This parameter was measured by connecting two phases of the experimental machine in series and applying a single-phase voltage across them. With the rotor position adjusted until maximum deflection is indicated on an ammeter in series with the short-circuited field winding, the d-axis subtransient reactance is

$$\begin{aligned} X_d'' &= \frac{V}{2 I_{\max}} \\ &= \frac{19V}{2 \cdot 3.1A} = 3.09 \Omega / \text{phase} \quad (0.182 \text{ pu}) \end{aligned}$$

### 3.8 Quadrature-axis Subtransient Reactance ( $X_q''$ )

This was obtained in a similar manner to  $X_d''$ , except that the rotor position was adjusted until minimum deflection was indicated on the ammeter in the field circuit. Under these conditions the q-axis subtransient reactance is

$$\begin{aligned} X_q'' &= \frac{V}{2 I_{\min}} \\ &= \frac{60V}{2 \cdot 2.5A} = 11.9 \Omega / \text{phase} \quad (0.62 \text{ pu}) \end{aligned}$$

### 3.9 Negative-sequence Reactance ( $X_2$ )

To obtain this parameter the field winding was short-circuited and the rotor driven at synchronous speed. Balanced 3-phase voltages were applied to the armature so that a constant amplitude rotating armature mmf was produced in the direction opposed to the rotor rotation. The negative-sequence reactance is then

$$\begin{aligned}
 X_2 &= \frac{V}{\sqrt{3} I} \\
 &= \frac{50A}{\sqrt{3} 4A} = 7.20 \Omega/\text{phase} \text{ (0.44 pu)}
 \end{aligned}$$

### 3.10 Zero-sequence Reactance ( $X_0$ )

This test was performed with the three armature windings connected in series, the field winding short-circuited and the rotor driven at synchronous speed with a single-phase voltage applied to the series-connected armature windings. The zero-sequence reactance is

$$\begin{aligned}
 X_0 &= \frac{V}{3.I} \\
 &= \frac{13.5V}{3.3A} = 1.50 \Omega/\text{phase} \text{ (0.09 pu)}
 \end{aligned}$$

### 4. TIME CONSTANTS ( $T'_{d0}$ , $T_d$ , $T''_d$ )

The d-axis open-circuit transient time constant  $T'_{d0}$  is measured by a conventional load rejection test<sup>46</sup>. The d-axis time constant  $T_d$  and the d-axis subtransient time constant  $T''_d$  are determined from the oscillogram of the short-circuit armature current recorded after the application of a symmetrical short-circuit at the terminals. The d-axis time constants are

$$\begin{aligned}
 T'_{d0} &= 0.9 \text{ sec} \\
 T_d &= 0.28 \text{ sec} \\
 T''_d &= 0.07 \text{ sec}
 \end{aligned}$$

## 5. SUMMARY OF EXPERIMENTAL MACHINE PARAMETERS

$$X_d = 1.30 \text{ pu}$$

$$X_{ad} = 1.25 \text{ pu}$$

$$X_q = 0.78 \text{ pu}$$

$$X_{aq} = 0.73 \text{ pu}$$

$$X_d' = 0.44 \text{ pu}$$

$$X_d'' = 0.184 \text{ pu}$$

$$X_q'' = 0.632 \text{ pu}$$

$$X_o = 0.09 \text{ pu}$$

$$R = 0.005 \text{ pu}$$

$$R_f = 0.259 \text{ pu}$$

$$T_{do}' = 0.9 \text{ sec}$$

$$T_d' = 0.28 \text{ sec}$$

$$T_d'' = 0.07 \text{ sec}$$

APPENDIX IICALCULATION OF PHASE PARAMETERS FROM D-Q PARAMETERS

In order to employ a coupled-circuit approach in the accurate prediction of the performance of a synchronous machine, it is necessary to know the relevant parameters of the machine model. Although phase model parameters may be measured by ballistic techniques<sup>47,56</sup>, the measurement of d-q model parameters is far quicker and the results obtained may subsequently be used to determine the phase model parameters. This was the approach followed to establish the parameters for the experimental machine.

The assumptions made in deriving transformations between d-q and phase model parameters are

- a) The second-harmonic component of the self-inductance of an armature phase is 0.8 times that of the phase/phase mutual inductance in the phase coordinate reference frame. Although application of Park's transformation to the phase coordinate reference frame yields no time-varying coefficients in the d-q reference frame when the two inductances are assumed to have the same magnitudes, it has been shown<sup>57</sup> both theoretically and experimentally, that this assumption is in fact far from valid.
- b) The quadrature-axis short circuit sub-transient time constant  $T_q''$  is equal to the direct-axis short circuit sub-transient time constant  $T_d''$ <sup>58</sup>.
- c) The d-axis damper/d-axis armature turns ratio is unity. The actual ratio is not however critical, since although the actual damper parameters may be incorrect, their referred values, mmf contribution and power dissipation will all be correct<sup>56</sup>.

- d) The q-axis damper/q-axis armature turns ratio is also unity. The arguments of (c) again apply here.

### 1. PARAMETER RELATIONSHIPS

The relationships given below may be found in any standard text book<sup>16,59</sup>. Reactances are in per-unit and time constants in second. A bar above its symbol denotes a per-unit value.

$$1. \bar{X}_d = \bar{X}_{md} + \bar{X}_a$$

$$2. \bar{X}'_d = \bar{X}_d \frac{T'_d}{T_{do}} = \bar{X}_a + \frac{\bar{X}_{md} \cdot \bar{X}_f}{\bar{X}_{md} + \bar{X}_f}$$

$$3. \bar{X}''_d = \bar{X}_d \frac{T'_d T''_d}{T_{do} T''_{do}} = \bar{X}_a + \frac{\bar{X}_{md} \bar{X}_f \bar{X}_{kd}}{\bar{X}_{md} \bar{X}_f + \bar{X}_{md} \bar{X}_{kd} + \bar{X}_f \bar{X}_{kd}}$$

$$4. \bar{X}_q = \bar{X}_{al} + \bar{X}_{mq}$$

$$5. \bar{X}''_q = \bar{X}_q \frac{T''_q}{T''_{qo}} = \bar{X}_a + \frac{\bar{X}_{ma} \bar{X}_{kq}}{\bar{X}_{mq} + \bar{X}_{kq}}$$

$$6. \bar{X}_2 = \frac{1}{2} (\bar{X}''_d + \bar{X}''_q)$$

$$7. T'_{do} = \frac{1}{\omega_0 R_f} (\bar{X}_f + \bar{X}_{md})$$

$$8. T'_d = \frac{1}{\omega_0 R_f} \left( \bar{X}_f + \frac{\bar{X}_{md} \bar{X}_a}{\bar{X}_{md} + \bar{X}_a} \right)$$

$$9. T''_{do} = \frac{1}{\omega_o R_{kd}} \left( \bar{X}_{kd} + \frac{\bar{X}_{md} \bar{X}_f}{\bar{X}_{md} + \bar{X}_f} \right)$$

$$10. T''_d = \frac{1}{\omega_o R_{kd}} \left( \bar{X}_{kd} + \frac{\bar{X}_{md} \bar{X}_a \bar{X}_f}{\bar{X}_{md} \bar{X}_a + \bar{X}_{md} \bar{X}_f + \bar{X}_a \bar{X}_f} \right)$$

$$11. T''_{qo} = \frac{1}{\omega_o R_{kq}} (\bar{X}_{kq} + \bar{X}_{mq})$$

$$12. T''_q = \frac{1}{\omega_o R_{kq}} \left( \bar{X}_{kq} + \frac{\bar{X}_{mq} \bar{X}_a}{\bar{X}_{mq} + \bar{X}_a} \right)$$

$$13. T_d = \frac{\bar{X}_{kd}}{\omega_o R_{kd}}$$

$$14. \bar{L}_d = \frac{\bar{X}_d}{\omega_o} = \bar{L}_o + \bar{M}_o + \frac{3}{2} \bar{L}_2$$

$$15. \bar{L}_q = \frac{\bar{X}_q}{\omega_o} = \bar{L}_{A0} + \bar{M}_o - \frac{3}{2} \bar{L}_2$$

$$16. \bar{L}_{md} = \frac{\bar{X}_{md}}{\omega_o} = \bar{M}_f$$

$$17. \bar{L}_z = \frac{\bar{X}_z}{\omega_o} = \bar{L}_{A0} - 2\bar{M}_o$$

$$18. \bar{L}_{ff} = \bar{L}_{md} + \bar{L}_f$$

$$19. \bar{L}_{kqd} = \bar{L}_{md} + \bar{L}_{kd}$$

$$20. \bar{L}_{kkq} = \bar{L}_{mq} + \bar{L}_{kq}$$

## 2. CONVERSION EQUATIONS

The conversion equations developed below are all derived from the basic relationships defined in the previous section.

### 2.1 D-axis Armature/Field Turns Ratio

The per unit field self-reactance, as defined by Rankin<sup>60,61</sup> is

$$X_{ff} = \frac{3}{2} \left( \frac{N_d}{N_f} \right)^2 \frac{X_{44}}{Z}$$

where  $\frac{N_d}{N_f}$  is the d-axis armature/field turns ratio and  $Z$  is the base impedance given by the ratio of rated phase voltage to rated phase currents.

Therefore

$$\frac{N_d}{N_f} = \sqrt{\frac{2}{3} \frac{X_{ff}}{X_{44}} Z}$$

From relationships 1 and 2 of Appendix II

$$X_f = \frac{\bar{X}_{md}^2}{X_d - X'_d}$$

and from relationship 7

$$\bar{X}_{44} = T_{do} \omega_o R_{44}$$

where  $\omega_o$  is the rated angular supply frequency.

Hence

$$\frac{N_d}{N_f} = \sqrt{\frac{2}{3} \frac{Z \bar{X}_{md}^2}{T_{do} \omega_o R_{44} (X_d - X'_d)}}$$

## 2.2 Phase Parameters (accessible windings)

From relationships 14 and 15

$$L_2 = Z \bar{L}_2 = \frac{Z}{3\omega_0} (\bar{X}_d - \bar{X}_q)$$

From assumption a

$$M_2 = 1.25 L_2$$

From relationships 14 and 17

$$M_0 = \frac{Z}{3\omega_0} (\bar{X}_d - \bar{X}_2) - \frac{1}{2} L_2$$

From relationship 17

$$L_{\Lambda 0} = \frac{Z}{\omega_0} \bar{X}_2 + 2M_0$$

From relationship 7

$$L_{44} = T_{d0}' R_f$$

$$\bar{X}_{md} = \frac{3}{2} \left( \frac{N_d}{N_f} \right) \frac{\omega_0}{Z} M_f$$

Therefore

$$M_f = \frac{2}{3} \left( \frac{N_f}{N_d} \right) \frac{Z}{\omega_0} \bar{X}_{md}$$

$$R_{11} = Z \bar{R}$$

### 2.3 D-axis Damper Winding Parameters

From relationship 3

$$\bar{X}_{kd} = \frac{\bar{X}_{md} \bar{X}_f (\bar{X}_d'' - \bar{X}_a)}{\bar{X}_{md} \bar{X}_f - \bar{X}_{ff} (\bar{X}_d - \bar{X}_a)}$$

$$\bar{X}_{kkd} = \bar{X}_{kd} + \bar{X}_{md}$$

$$\bar{X}_{kkd} = \frac{3}{2} \left( \frac{N_1}{N_5} \right)^2 \frac{\omega_0 L_{55}}{z}$$

Therefore

$$L_{55} = \frac{2}{3} \left( \frac{N_5}{N_1} \right)^2 \frac{z \bar{X}_{kkd}}{\omega_0}$$

Assuming that all the mutual reactances on the d-axis are equal

$$\bar{X}_{md} = \frac{3}{2} \left( \frac{N_1}{N_5} \right) \frac{\omega_0 M_d}{z}$$

Hence

$$M_d = \frac{2}{3} \left( \frac{N_5}{N_1} \right) \frac{z \bar{X}_{md}}{\omega_0}$$

From relationship 3

$$T_{do}'' = \frac{T_d' T_d''}{T_{do}'} \cdot \frac{X_d}{X_d''}$$

From relationship 9

$$R_{kd} = \frac{1}{\omega_o T_{do}} \left( X_{kd} + \frac{X_{md} X_f}{X_{md} + X_f} \right)$$

Therefore

$$R_{44} = \frac{2}{3} \left( \frac{N_5}{N_1} \right)^2 R_{kd} \cdot Z$$

$$M_{45} = \left( \frac{N_5}{N_1} \right) M_{14}$$

#### 2.4 Q-axis Damper Winding Parameters

From relationship 5

$$\bar{X}_{kq} = \frac{(\bar{X}_q'' - \bar{X}_a) \bar{X}_{mq}}{\bar{X}_{mq} + \bar{X}_a - \bar{X}_q''}$$

$$\bar{X}_{kkq} = \bar{X}_{kq} + \bar{X}_{mq}$$

$$\bar{X}_{kkq} = \frac{3}{2} \left( \frac{N_1}{N_6} \right)^2 \frac{\omega_o L_{66}}{Z}$$

Hence

$$L_{66} = \frac{2}{3} \left( \frac{N_6}{N_1} \right)^2 \frac{Z \bar{X}_{kkq}}{\omega_o}$$

$$\bar{X}_{mq} = \frac{3}{2} \left( \frac{N_1}{N_6} \right) \frac{\omega_o M_q}{Z}$$

Therefore

$$M_q = \frac{2}{3} \left( \frac{N_6}{N_1} \right) \frac{Z \bar{X}_{mq}}{\omega_o}$$

$$T_q'' = T_d''$$

From relationship 5

$$T_{q0}'' = \frac{X_q}{X_q''} T_q''$$

$$T_{q0}'' = \frac{L_{66}}{R_{66}}$$

Hence

$$R_{66} = \frac{L_{66}}{T_{q0}''}$$

### 3. PHASE PARAMETERS FOR THE EXPERIMENTAL MACHINE

The measured values of the d-q parameters of the experimental machine are given in Appendix I. Using these d-q parameters and the transformations developed in this Appendix, the phase parameters of the experimental machine are therefore

$$L_{A0} = 0.165 \text{ mH}$$

$$L_2 = 0.055 \text{ mH}$$

$$M_0 = 0.080 \text{ mH}$$

$$M_2 = 0.069 \text{ mH}$$

$$M_f = 0.037 \text{ mH}$$

$$M_d = 0.068 \text{ mH}$$

$$M_q = 0.032 \text{ mH}$$

$$M_{44} = 0.072 \text{ H}$$

$$M_{45} = 1.226 \text{ mH}$$

$$L_{55} = 0.026 \text{ mH}$$

$$L_{66} = 0.116 \text{ mH}$$

$$R_{11} = 0.011 \Omega$$

$$R_{44} = 0.904 \Omega$$

$$R_{55} = 1.672 \text{ m}\Omega$$

$$R_{66} = 0.584 \text{ m}\Omega$$

APPENDIX IIIDETERMINATION OF LOSSES

The various losses in a synchronous generator are:

1. Fixed losses: (a) core-loss, (b) bearing and brush friction loss, (c) windage loss.
2. Field circuit losses: (a) copper-loss in the field winding, (b) brush-resistance loss.
3. Direct load loss: copper-loss in armature windings.
4. Stray load loss: (a) in iron parts, (b) in conductors.

Losses 2(b), 3, and 4(a) when combined are referred to as the short-circuit load loss.

To determine various losses in the laboratory, the experimental machine was used in conjunction with a directly coupled DC shunt motor acting as a prime-mover, with the test described below being performed.

The DC motor armature resistance  $R_m$  was measured as  $0.60\Omega$  using a sub-standard ammeter and voltmeter.

1. LOSSES OF THE DRIVING MOTOR

With the load generator uncoupled, the drive motor was run at the rated speed of the generator, when the power input to the armature is the sum of its armature copper loss, the armature iron loss and the friction and windage loss. If  $V_m$  is the motor armature voltage, when carrying a current  $I_m$ , the power required to supply the windage, friction and iron loss  $P_1$  is then

$$P_1 = V_m I_m - R_m I_m^2$$

This loss was obtained for various values of speeds and its variation with speed is plotted in Figure 6.15.

## 2. WINDAGE, BEARING, FRICTION AND BRUSH-FRICTION LOSSES

With the load generator coupled to the drive motor, and with its field unexcited, the set was run at the synchronous speed of the generator. Under this condition the power input to the motor armature is the total power consumed in the DC machine armature ( $P_1 + I_m^2 R_m$ ) and the generator friction and windage loss. The friction and the windage loss of the generator  $P_2$  is therefore

$$P_2 = V_m I_m - R_m I_m^2 - P_1$$

for the given speed. The friction and the windage loss of generator  $P_2$  is plotted as a function of speed in Figure 6.16.

## 3. OPEN CIRCUIT CORE-LOSS

With the generator coupled to the DC motor and run at the rated speed, its field was excited but the armature was left open circuited. The drive motor armature current  $I_m$  and the motor armature voltage  $V_m$  were recorded as the excitation current of the generator was varied, with the driving motor speed kept constant throughout the test. Under these conditions, the power input to the motor armature  $V_m I_m$  is the sum of the motor armature copper loss  $R I_m^2$ , the DC machine iron, friction and windage loss  $P_1$ , the generator windage and friction loss  $P_2$ , and the generator core losses  $P_c$ . Therefore

$$P_c = V_m I_m - R_m I_m^2 - P_2 - P_1$$

The driving motor armature current  $I_a$ , and the voltage across the motor armature  $V_a$  were recorded as a function of the generator field current and since  $P_1$  and  $P_2$  are known from the results of test 1 and test 2,  $P_c$  may be determined as a function of the generator excitation. The core loss of the generator is plotted in Figure 6.17 as a function of the excitation current.

#### 4. TOTAL LOSSES OF THE GENERATOR

The generator excitation current  $I_f$  was adjusted so that it supplied rated load current at rated voltage and at rated power factor, with the motor-generator set run at synchronous speed. Under these conditions, the generator excitation current  $I_f$ , the voltage of the generator field winding  $V_f$ , the drive motor armature current  $I_m$  and the armature voltage  $V_m$  were all recorded. The generator power output was measured using two wattmeters as  $P_{out}$ . The total losses of the generator are then:

$$P_t = V_m I_m + V_f I_f - R_m I_m^2 - P_1 - P_{out}$$

APPENDIX IVNUMERICAL INTEGRATION METHODS

This appendix studies the errors and instabilities of numerical integration, as well as some integration methods, in relation to the work undertaken in this thesis.

1. ROUND-OFF ERROR

This occurs because it is impossible to perform numerical operations with perfect accuracy. The last digit of a number resulting from a numerical operation is always doubtful, being dependent on the rounding process built into the compiler of the programming language. Estimation of this error is extremely difficult, and is often inadequately treated, although Henrici<sup>62</sup> does consider its statistical behaviour in some simple numerical integration procedures. It suffices to mention here that, for a long integration period, use of a small step length (required to ensure stability, say) increases the number of calculations, and may lead to a significant cumulative round-off error. From a programming viewpoint, this error may be minimised by using double precision arithmetic.

2. TRUNCATION ERROR

This arises because an inexact mathematical process is used to approximate to an actual one, as in truncating an infinite series in a finite number of terms. In numerical integration, the difference equation used to predict the dependence variables may be compared with the Taylor series expansion of the same variables. The order to which the difference equation agrees with the Taylor series expansion is the order of the method, the Lagrangian remainder in the Taylor series neglected by the method being the truncation error of the method. Thus the truncation error of the fourth-order Runge-Kutta

method is proportional to the fifth power of the step length. It is obvious that truncation error may be generally controlled by varying the step length.

### 3. INSTABILITY

The main instabilities are:

1. Inherent instability - this is caused by the ill-conditioning of the differential equations themselves, such that a small change in the initial conditions, or a slight approximation in a digital computation, leads to a large variation in the solution. This instability is independent of the step length and of the method of numerical integration.
2. Partial instability - this arises when the step length is too large, such that the solution given by the difference equation does not tend to the true solution. Consequently, round-off or truncation errors become magnified as the integration proceeds. This instability is intimately related to the original differential equations, the step length and the integration method.
3. Strong instability - this is associated with multi-step integration methods, the difference equations for which may introduce spurious solutions bearing no relation whatsoever to the original differential equations. These spurious solutions are parasitic, and are not removed by a reduction in the step length.

Of these three instabilities, there is little that can be done about 1, although 3 may be avoided by an appropriate selection of the difference equation. Partial instability may clearly be overcome by a suitable choice of the step length.

#### 4. CHOICE OF INTEGRATION METHOD

The set of differential equations to be solved can be expressed as

$$Dy = f(x,y)$$

and a solution is required for given initial conditions over a given period of time. Expansion of the Taylor series about the  $n$ th point (assumed to be known) will, in theory, always produce a solution at the  $(n+1)$ th point

$$y_{n+1} = y_n + h Dy_n + \frac{h^2}{2!} D^2y_n + \frac{h^3}{3!} D^3y_n + \frac{h^4}{4!} D^4y_n + \dots$$

though difficulties in calculating the higher derivatives make this method of little practical value. Most practical numerical integration methods use the Taylor series expansion only as a reference, and can be categorised into three main types

1. One-step methods<sup>63,64,65</sup> (both explicit and implicit)
2. Multi-step methods<sup>66</sup>
3. Iteration methods<sup>67,68,69</sup>

The advantages and disadvantages of each category are summarised in Table A4.1.

The use of iteration methods is complex, and they will not be considered further here. The main difference between one-step and multi-step methods is that the former use information from only the  $n$ th point to calculate the value at the  $(n+1)$ th point, while the latter require data from several points prior to the  $n$ th as well. Use of multi-step methods therefore requires the use also of a one-step method of similar accuracy at any discontinuity in the solution for the first few steps.

TYPE OF METHOD	ADVANTAGES	DISADVANTAGES
One-step methods (explicit and implicit)	<ol style="list-style-type: none"> <li>1. Self-starting</li> <li>2. Changing the step length is easy</li> <li>3. Implicit methods have good stability and hence large step lengths possible</li> <li>4. Explicit methods have high accuracy</li> </ol>	<ol style="list-style-type: none"> <li>1. Slow, as <math>f(x,y)</math> needs to be evaluated several times per step</li> <li>2. Estimate of the per-step truncation error not generally available</li> <li>3. Explicit methods have poor stability</li> </ol>
Multi-step methods	<ol style="list-style-type: none"> <li>1. Relatively fast as <math>f(x,y)</math> evaluated only a few times per step</li> <li>2. Estimate of per-step truncation error usually available</li> <li>3. Generally more stable than explicit one-step methods</li> </ol>	<ol style="list-style-type: none"> <li>1. Not self-starting</li> <li>2. Changing the step length is difficult and requires re-starting the solution</li> </ol>
Iteration Methods	<ol style="list-style-type: none"> <li>1. Good stability, permitting large step length</li> </ol>	<ol style="list-style-type: none"> <li>1. Extremely complex when applied to sets of equation</li> </ol>

TABLE A4.1: Comparison of different types of numerical integration method

#### 4.1 Explicit One-step Numerical Integration Method

The simplest of these is the so-called 'modified Euler method'<sup>63</sup>, in which the Taylor series expansion is truncated after its second derivative. Its accuracy is however poor, and higher-order methods are normally used, an example being the fourth-order Runge-Kutta method<sup>63</sup>

$$y_{n1} = y_n + \frac{h}{6} [K_1 + 2 K_2 + 2 K_3 + K_4]$$

where

$$K_1 = f(x_n, y_n)$$

$$K_2 = f\left(x_n + \frac{h}{2}, y_n + \frac{K_1}{2}\right)$$

$$K_3 = f\left(x_n + \frac{h}{2}, y_n + \frac{K_2}{2}\right)$$

$$K_4 = f(x_n, y_n + K_3)$$

#### 4.2 Implicit One-step Integration Methods

By expressing the dependent variable as a function of its own derivative, an alternative procedure for the solution of the differential equation can be found. Truncating the Taylor series after the second derivative yields the trapezoidal method of numerical integration, expressed as<sup>64,65</sup>

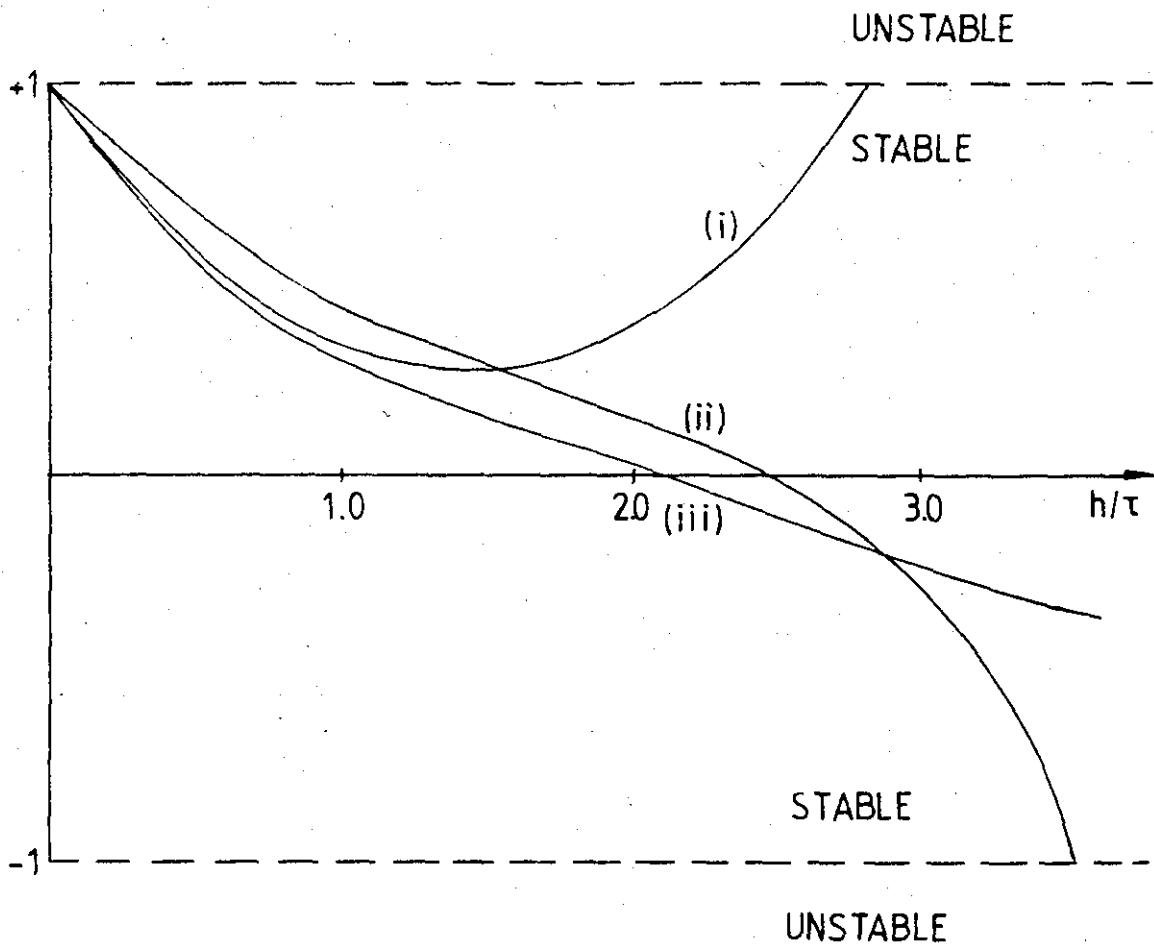
$$y_{n+1} = y_n + \frac{h}{2} [f(x_n, y_n) + f(x_{n+1}, y_{n+1})]$$

Individual features of the Runge-Kutta and trapezoidal methods are summarised in Table A4.2.

Granborg<sup>70</sup> has produced an analysis which derives the optimum step length for a single differential equation, in terms of the system time constant. The results are given in Figure A4.1 and show that, when using the trapezoidal method, a step length several times that for a Runge-Kutta method can be used. The number of steps required for simulation of a given time period can therefore be much reduced, providing that the forcing function is still represented with sufficient accuracy.

RUNGE-KUTTA METHOD	TRAPEZOIDAL METHOD
<ol style="list-style-type: none"> <li>1. Being a 4th order method, it has high accuracy</li> <li>2. From Fig. A4.1 it can be seen that a reasonably large step length can be used</li> <li>3. The method is relatively slow, requiring the evaluation of the function many times per step</li> <li>4. By introducing the modifications due to Merson an estimate of the local truncation error can be found, and used to control the step length</li> </ol>	<ol style="list-style-type: none"> <li>1. It is of low order, and therefore not as accurate as a Runge-Kutta method</li> <li>2. It is evident from Figure A4.1 that a large step length (several times that of a Runge-Kutta method) can be used</li> <li>3. The method is relatively fast</li> <li>4. No estimate of the per-step truncation error is possible</li> </ol>

TABLE A4.2: Comparison of Runge-Kutta and trapezoidal numerical integration methods



- i) 4th order Runge-Kutta
  - ii) Runge-Kutta Merson
  - iii) Trapezoidal
- $h$  = step length  
 $\tau$  = system time constant

FIGURE A4.1: Step length limits for numerical integration procedures

APPENDIX VSOME MATHEMATICAL MANIPULATIONS

The following mathematical manipulations are used in Chapter 4.

$$\begin{aligned} 1. \quad L_{22} + L_{33} &= L_{A0} + L_2 \cos (2\theta - 240^\circ) + L_{A0} + L_2 \cos (2\theta - 120^\circ) \\ &= 2 L_{A0} - L_2 \cos 2\theta \end{aligned}$$

$$\begin{aligned} 2. \quad M_{12} + M_{13} &= -M_0 + M_2 \cos (2\theta - 120^\circ) - M_0 + M_2 \cos (2\theta - 240^\circ) \\ &= -2M_0 - M_2 \cos 2\theta \end{aligned}$$

$$\begin{aligned} 3. \quad M_{24} + M_{34} &= M_f \cos (\theta - 120^\circ) + M_f \cos (\theta - 240^\circ) \\ &= -M_f \cos \theta \end{aligned}$$

$$\begin{aligned} 4. \quad M_{25} + M_{35} &= M_d \cos (\theta - 120^\circ) + M_d \cos (\theta - 240^\circ) \\ &= -M_d \cos \theta \end{aligned}$$

$$\begin{aligned} 5. \quad M_{26} + M_{36} &= M_q \sin (\theta - 120^\circ) + M_q \sin (\theta - 240^\circ) \\ &= -M_q \sin \theta \end{aligned}$$

$$\begin{aligned} 6. \quad L_{22} + L_{33} + 2M_{23} &= L_{A0} + L_2 \cos (2\theta - 240^\circ) + L_{A0} + \\ &\quad L_2 \cos (2\theta - 120^\circ) - 2M_0 + 2M_2 \cos 2\theta \\ &= 2 (L_{A0} - M_0) + (2M_2 - L_2) \cos 2\theta \end{aligned}$$

$$\begin{aligned} 7. \quad L_{11} + L_{22} + L_{33} &= L_{A0} + L_2 \cos 2\theta + L_{A0} + L_2 \cos (2\theta - 120^\circ) \\ &\quad + L_{A0} + L_2 \cos (2\theta - 240^\circ) \\ &= 3L_{A0} \end{aligned}$$

$$\begin{aligned}
 8. \quad L_{11} + M_{12} + M_{13} &= L_{A0} + L_2 \cos 2\theta - M_0 + M_2 \cos (2\theta - 120^\circ) - M_0 \\
 &\quad + M_2 \cos (2\theta - 240^\circ) \\
 &= (L_{A0} - 2M_0) + (L_2 - M_2) \cos 2\theta
 \end{aligned}$$

$$\begin{aligned}
 9. \quad L_{11} + L_{22} + L_{33} + 2M_{12} + 2M_{13} + 2M_{23} &= L_0 + L_2 \cos 2\theta + L_0 \\
 &\quad + L_2 \cos (2\theta - 240^\circ) + L_0 + L_2 \cos (2\theta - 120^\circ) - 2M_0 \\
 &\quad + 2M_2 \cos (2\theta - 120^\circ) - 2M_0 + 2M_2 \cos 2\theta - 2M_0 + 2M_2 \cos (2\theta - 240^\circ) \\
 &= 3(L_0 - 2M_0)
 \end{aligned}$$

$$\begin{aligned}
 10. \quad M_{14} + M_{24} + M_{34} &= M_f \cos \theta + M_f \cos (\theta - 120^\circ) + M_f \cos (\theta - 240^\circ) \\
 &= 0
 \end{aligned}$$

$$\begin{aligned}
 11. \quad M_{15} + M_{25} + M_{35} &= M_d \cos \theta + M_d \cos (\theta - 120^\circ) + M_d \cos (\theta - 240^\circ) \\
 &= 0
 \end{aligned}$$

$$\begin{aligned}
 12. \quad M_{16} + M_{26} + M_{36} &= M_q \cos \theta + M_q \cos (\theta - 120^\circ) + M_q \cos (\theta - 240^\circ) \\
 &= 0
 \end{aligned}$$

$$\begin{aligned}
 13. \quad M_{12} + M_{13} + M_{23} &= -M_0 + M_2 \cos (2\theta - 120^\circ) - M_0 + M_2 \cos 2\theta \\
 &\quad - M_0 + M_2 \cos (2\theta - 240^\circ) \\
 &= -3M_0
 \end{aligned}$$

APPENDIX VISERIES EXPANSION OF SOME MATHEMATICAL EXPRESSIONS

The mathematical expressions necessary for the series expansions used in Chapter IV are given below.

$$1. \frac{1}{x+y+(x-y)\cos 2\theta} = \frac{1}{\sqrt{xy}} \left[ \frac{1}{2} + \sum_{n=1}^{\infty} b^n \cos 2n\theta \right]$$

$$2. \frac{1}{x+y-(x-y)\cos 2\theta} = \frac{1}{\sqrt{xy}} \left[ \frac{1}{2} + \sum_{n=1}^{\infty} (-b)^n \cos 2n\theta \right]$$

$$3. \frac{\sin\theta}{x+y+(x-y)\cos 2\theta} = \frac{1}{y+\sqrt{xy}} \left[ \sin\theta + \sum_{n=1}^{\infty} b^n \sin (2n+1)\theta \right]$$

$$4. \frac{\sin\theta}{x-y-(x-y)\cos 2\theta} = \frac{1}{x+\sqrt{xy}} \left[ \sin\theta + \sum_{n=1}^{\infty} (-b)^n \sin (2n+1)\theta \right]$$

$$5. \frac{\cos\theta}{x+y+(x-y)\cos 2\theta} = \frac{1}{x+\sqrt{xy}} \left[ \cos\theta + \sum_{n=1}^{\infty} b^n \cos (2n+1)\theta \right]$$

$$6. \frac{\cos\theta}{x+y-(x-y)\cos 2\theta} = \frac{1}{y+\sqrt{xy}} \left[ \cos\theta + \sum_{n=1}^{\infty} (-b)^n \cos (2n+1)\theta \right]$$

7. 
$$\frac{\sin \theta \cos \theta}{x + y - (x-y) \cos 2\theta} = \frac{1}{2} \frac{1}{x + \sqrt{xy}} \left( \frac{1}{b} - 1 \right) \sum_{n=1}^{\infty} b^n \sin 2n\theta$$
8. 
$$\frac{\sin \theta \cos \theta}{x + y - (x-y) \cos 2\theta} = \frac{1}{2} \frac{1}{y + \sqrt{xy}} \left( -\frac{1}{b} - 1 \right) \sum_{n=1}^{\infty} (-b)^n \sin 2n\theta$$
9. 
$$\frac{\cos^2 \theta}{x + y + (x-y) \cos 2\theta} = \frac{1}{2} \frac{1}{x + \sqrt{xy}} \left[ 1 + \frac{1+b}{b} \sum_{n=1}^{\infty} b^n \cos 2n\theta \right]$$
10. 
$$\frac{\cos^2 \theta}{x + y - (x-y) \cos 2\theta} = \frac{1}{2} \frac{1}{y + \sqrt{xy}} \left[ 1 - \frac{1-b}{b} \sum_{n=1}^{\infty} (-b)^n \cos 2n\theta \right]$$
11. 
$$\frac{\sin 2\theta}{x + y + (x-y) \cos 2\theta} = \frac{1}{y + \sqrt{xy}} \left( \frac{1}{b} + 1 \right) \sum_{n=1}^{\infty} b^n \sin 2n\theta$$
12. 
$$\frac{\sin 2\theta}{x + y - (x-y) \cos 2\theta} = \frac{1}{x + \sqrt{xy}} \left( -\frac{1}{b} + 1 \right) \sum_{n=1}^{\infty} (-b)^n \sin 2n\theta$$
13. 
$$\frac{\cos 2\theta}{x + y + (x-y) \cos 2\theta} = \frac{1}{2\sqrt{xy}} \left( b + \frac{b^2+1}{b} \right) \sum_{n=1}^{\infty} b^n \cos 2n\theta$$
14. 
$$\frac{\cos 2\theta}{x + y - (x-y) \cos 2\theta} = \frac{1}{2\sqrt{xy}} \left[ -b - \frac{b^2+1}{b} \sum_{n=1}^{\infty} (-b)^n \cos 2n\theta \right]$$
15. 
$$\frac{\cos^3 \theta}{x + y + (x-y) \cos 2\theta} = \frac{1}{2} \frac{1}{x + \sqrt{xy}} \left[ \frac{3+b}{2} \cos \theta + \frac{(b+1)^2}{2b} \sum_{n=1}^{\infty} b^n \cos(2n+1)\theta \right]$$

$$16. \frac{\cos^3 \theta}{x + y - (x-y) \cos 2\theta} = \frac{1}{2} \frac{1}{y + \sqrt{xy}} \left[ \frac{3-b}{2} \cos \theta - \frac{(1-b)^2}{2b} \sum_{n=1}^{\infty} (-b)^n \cos(2n-1)\theta \right]$$

$$17. \frac{\cos 2\theta \cos \theta}{x + y + (x-y) \cos 2\theta} = \frac{1}{2} \frac{1}{x + \sqrt{xy}} \left[ (1+b) \cos \theta + \frac{b^2+1}{2} \sum_{n=1}^{\infty} b^n \cos(2n+1)\theta \right]$$

$$18. \frac{\cos 2\theta \cos \theta}{x + y - (x-y) \cos 2\theta} = \frac{1}{2} \frac{1}{y + \sqrt{xy}} \left[ (1-b) \cos \theta - \frac{b^2+1}{b} \sum_{n=1}^{\infty} (-b)^n \cos(2n+1)\theta \right]$$

APPENDIX VIITRANSFORMATIONS

The transformations used in this thesis are:

1. Park's transformation:

$$f_d = f_a \cos\theta + f_b \cos(\theta - 120^\circ) + f_c \cos(\theta - 240^\circ)$$

$$f_q = f_a \sin\theta + f_b \sin(\theta - 120^\circ) + f_c \sin(\theta - 240^\circ)$$

$$f_o = \frac{1}{3} [f_a + f_b + f_c]$$

2. Modified Park's transformation:

$$f_d = \sqrt{\frac{2}{3}} [f_a \cos\theta + f_b \cos(\theta - 120^\circ) + f_c \cos(\theta - 240^\circ)]$$

$$f_q = \sqrt{\frac{2}{3}} [f_a \sin\theta + f_b \sin(\theta - 120^\circ) + f_c \sin(\theta - 240^\circ)]$$

$$f_o = \frac{1}{3} [f_a + f_b + f_c]$$

3. Clarke's transformation:

$$f_\alpha = \sqrt{\frac{2}{3}} f_a - \frac{1}{\sqrt{6}} f_b - \frac{1}{\sqrt{6}} f_c$$

$$f_\beta = -\frac{1}{\sqrt{2}} f_b + \frac{1}{\sqrt{2}} f_c$$

$$f_o = \frac{1}{3} f_a + \frac{1}{3} f_b + \frac{1}{3} f_c$$

## 4. Modified Clarke's transformation:

$$f_{\alpha} = \sqrt{\frac{2}{3}} f_a - \frac{1}{\sqrt{6}} f_b - \frac{1}{\sqrt{6}} f_c$$

$$f_{\beta} = -\frac{1}{\sqrt{2}} f_b + \frac{1}{\sqrt{2}} f_c$$

$$f_{\gamma} = \frac{1}{\sqrt{3}} f_a + \frac{1}{\sqrt{3}} f_b + \frac{1}{\sqrt{3}} f_c$$

where  $f$  may stand for the current voltages or flux linkage of the generator.

APPENDIX VIII

CALCULATION OF DECREMENT FACTORS FOR  
TERMINAL (1) TO CENTRE POINT FAULT

From equations (5.43) and (5.44),  $i_\alpha$  and  $i_f$  are given by

$$i_\alpha = - \frac{\sqrt{6} E_0}{A'+\sqrt{A'B'}} F_1(t) [\cos\theta + \sum_{n=1}^{\infty} b^n \cos(2n+1)\theta] \\ + \frac{\sqrt{6} E_0 \cos\theta_0}{\sqrt{A'B'}} F_2(t) \left[ \frac{1}{2} + \sum_{n=1}^{\infty} b^n \cos 2n\theta \right] \quad (A8.1)$$

and

$$i_f = I_f(t) + \frac{\sqrt{6}}{2} \frac{M_{af}}{L_f} \frac{E_0}{A'+\sqrt{A'B'}} F_1(t) \left[ 1 + \frac{1+b}{b} \sum_{n=1}^{\infty} b^n \cos 2n\theta \right] \\ - \frac{\sqrt{6}}{2} \frac{M_{af}}{L_f} \frac{E_0 \cos\theta_0}{\sqrt{A'B'}} (1+b) F_2(t) \left[ \cos\theta + \sum_{n=1}^{\infty} b^n \cos(2n+1)\theta \right] \quad (A8.2)$$

respectively. Using the expressions of Appendix VI,  $i_\alpha$  and  $i_f$  can then be summed to give

$$i_\alpha = - \frac{\sqrt{6} E_0 (F_1(t) \cos\theta - F_2(t) \cos\theta_0)}{(A'+B') + (A'-B') \cos 2\theta} \quad (A8.3)$$

and

$$i_f = I_f(t) + \sqrt{6} \frac{M_{af}}{L_f} \frac{E_0 (F_1(t) \cos\theta - F_2(t) \cos\theta_0) \cos\theta}{A'+B' + (A'-B') \cos 2\theta}$$

respectively.

From equation (5.37)

$$(R_f + pL_f) i_f + pM_{af} \cos\theta i_\alpha = 0 \quad (\text{A8.5})$$

When  $i_\alpha$  and  $i_f$  as given by equations (A8.3) and (A8.6), are substituted into equation (A8.5), the result is

$$\begin{aligned} (R_f + pL_f) I_f(t) + \sqrt{6} \frac{M_{af}}{L_f} \frac{E_o (F_1(t) \cos\theta - F_2(t) \cos\theta \cos\theta_o)}{A'+B'+(A'-B')\cos 2\theta} \\ - p \frac{\sqrt{6} E_o M_{af} (F_1(t) \cos^2\theta - F_2(t) \cos\theta \cos\theta_o)}{A'+B'+(A'-B')\cos 2\theta} = 0 \end{aligned} \quad (\text{A8.6})$$

or

$$\begin{aligned} (R_f + pL_f) I_f(t) + \sqrt{6} R_f \frac{M_{af}}{L_f} E_o F_1(t) \frac{\cos^2\theta}{A'+B'+(A'-B')\cos 2\theta} \\ + \sqrt{6} M_{af} E_o p F_1(t) \frac{\cos^2\theta}{A'+B'+(A'-B')\cos 2\theta} \\ - \sqrt{6} M_{af} E_o p F_2(t) \cos\theta_o \frac{\cos\theta}{A'+B'+(A'-B')\cos 2\theta} \\ + \sqrt{6} E_o M_{af} p F_1(t) \frac{\cos^2\theta}{A'+B'+(A'-B')\cos 2\theta} \\ = 0 \end{aligned} \quad (\text{A8.7})$$

Using the series expansions given in Appendix VI

$$\begin{aligned}
& (R_f + pL_f)I_f(t) + \frac{\sqrt{6}}{2} R_f \frac{M_{af}}{L_f} E_0 \frac{F_1(t)}{A'+\sqrt{A'B'}} \left[ 1 + \frac{1+b}{b} \sum_{n=1}^{\infty} b^n \cos 2n\theta \right] \\
& + \frac{\sqrt{6}}{2} M_{af} E_0 \frac{pF_1(t)}{A'+\sqrt{A'B'}} \left[ 1 + \frac{1+b}{b} \sum_{n=1}^{\infty} b^n \cos 2n\theta \right] \\
& - \sqrt{6} R_f \frac{M_{af}}{L_f} E_0 F_2(t) \left[ \cos \theta_0 \frac{1}{A'+\sqrt{A'B'}} \cos \theta \right. \\
& \quad \left. + \sum_{n=1}^{\infty} b^n \cos (2n+1)\theta \right] \\
& - \sqrt{6} M_{af} E_0 \cos \theta_0 \frac{pF_2(t)}{A'+\sqrt{A'B'}} \left[ \cos \theta + \sum_{n=1}^{\infty} b^n \cos (2n+1)\theta \right] \\
& + \frac{\sqrt{6}}{2} M_{af} E_0 \cos \theta_0 \frac{F_1(t)}{A'+\sqrt{A'B'}} \left[ 1 + \frac{1+b}{b} \sum_{n=1}^{\infty} b^n \cos 2n\theta \right] \\
& = 0 \tag{A8.8}
\end{aligned}$$

Neglecting the derivative of the decrement factor, and equating the coefficients of the DC terms

$$(R_p + pL_f) I_f(t) + \frac{\sqrt{6}}{2} R_f \frac{M_{af}}{L_f} E_0 \frac{F_1(t)}{A'+\sqrt{A'B'}} = 0 \tag{A8.9}$$

From (4.91)

$$\sqrt{\frac{3}{2}} E_0 \sin \theta = p M_{af} \cos \theta i_f + \left( r + p \left( A + \frac{L}{2} Y + B \cos 2\theta \right) \right) i_\alpha \quad (\text{A8.10})$$

Substituting  $i_f$  and  $i_\alpha$  into equation (A8.10)

$$\begin{aligned} \sqrt{\frac{3}{2}} E_0 \sin \theta &= p M_{af} \cos \theta I_f(t) + p \sqrt{6} \frac{M_{af}^2}{L_f} \frac{E_0 (F_1(t) \cos \theta - F_2(t) \cos \theta_0) \cos^2 \theta}{(A'+B')+(A'-B') \cos 2\theta} \\ &- r \frac{\sqrt{6} E_0 (F_1(t) \cos \theta - F_2(t) \cos \theta_0)}{A'+B'+(A'-B') \cos 2\theta} \\ &- p \left( A + \frac{L}{2} Y \right) \frac{\sqrt{6} E_0 (F_1(t) \cos \theta - F_2(t) \cos \theta_0)}{A'+B'+(A'-B') \cos 2\theta} \\ &- p \frac{\sqrt{6} B E_0 (F_1(t) \cos \theta - F_2(t) \cos \theta_0) \cos 2\theta}{A'+B'+(A'-B') \cos 2\theta} \quad (\text{A8.11}) \end{aligned}$$

or

$$\begin{aligned} \sqrt{\frac{3}{2}} B_0 \sin \theta &= p M_{af} \cos \theta I_f(t) + p \sqrt{6} \frac{M_{af}^2}{L_f} E_0 F_1(t) \frac{\cos^3 \theta}{A'+B'+(A'-B') \cos 2\theta} \\ &- p \sqrt{6} \frac{M_{af}^2}{L_f} E_0 F_2(t) \cos \theta_0 \frac{\cos^2 \theta}{A'+B'+(A'-B') \cos 2\theta} \end{aligned}$$

$$\begin{aligned}
& -r\sqrt{6} E_0 F_1(t) \frac{\cos\theta}{A'+B'+(A'-B')\cos 2\theta} + r\sqrt{6} E_0 F_2(t) \cos\theta_0 \frac{1}{A'+B'(A'-B')\cos 2\theta} \\
& -p\left(A + \frac{L}{2} Y\right) F_1(t) \frac{\cos\theta}{A'+B'+(A'-B')\cos 2\theta} \\
& + p\left(A + \frac{L}{2} Y\right) \sqrt{6} E_0 F_2(t) \cos\theta_0 \frac{1}{A'+B'A(A'-B')\cos 2\theta} \\
& -p \sqrt{6} B E_0 F_1(t) \frac{\cos\theta \cos 2\theta}{A'+B'+(A'-B')\cos 2\theta} \\
& + p\sqrt{6} B E_0 F_2(t) \cos\theta_0 \frac{\cos 2\theta}{A'+B'+(A'-B')\cos 2\theta} \tag{A8.12}
\end{aligned}$$

Using the series expansions given in Appendix VI

$$\begin{aligned}
\sqrt{\frac{3}{2}} E_0 \sin\theta &= pM_{af} \cos\theta I_f(t) \\
& + p \frac{\sqrt{6}}{2} \frac{M_{af}^2}{L_f} E_0 \frac{F_1(t)}{A'+\sqrt{A'B'}} \left[ \frac{3+b}{2} \cos\theta + \frac{(b+1)^2}{2b} \sum_{n=1}^{\infty} b^n \cos(2n+1)\theta \right] \\
& - p \frac{\sqrt{6}}{2} \frac{M_{af}^2}{L_f} E_0 \frac{F_2(t) \cos\theta_0}{A'+\sqrt{A'B'}} \left[ 1 + \frac{1+b}{b} \sum_{n=1}^{\infty} b^n \cos 2n\theta \right]
\end{aligned}$$

$$\begin{aligned}
& -r \sqrt{6} E_0 \frac{1}{A'+\sqrt{A'B'}} F_1(t) \left[ \cos\theta + \sum_{n=1}^{\infty} b^n \cos(2n+1)\theta \right] \\
& + r \frac{\sqrt{6}}{\sqrt{A'B'}} E_0 F_2(t) \cos\theta_0 \left[ \frac{1}{2} + \sum_{n=1}^{\infty} b^n \cos 2n\theta \right] \\
& - \sqrt{6} p \left( A + \frac{L_Y}{2} \right) E_0 \frac{1}{A'+\sqrt{A'B'}} F_1(t) \left[ \cos\theta + \sum_{n=1}^{\infty} b^n \cos(2n+1)\theta \right] \\
& + p \left( A + \frac{L_Y}{2} \right) \frac{\sqrt{6}}{\sqrt{A'B'}} E_0 F_2(t) \cos\theta_0 \left[ \frac{1}{2} + \sum_{n=1}^{\infty} b^n \cos 2n\theta \right] \\
& - pB \frac{\sqrt{6}}{2} \frac{E_0}{A'+\sqrt{A'B'}} F_1(t) \left[ (1+b) \cos\theta + \frac{b^2+1}{b} \sum_{n=1}^{\infty} b^n \cos(2n+1)\theta \right] \\
& + pB \frac{\sqrt{6}}{2} \frac{1}{\sqrt{A'B'}} E_0 F_2(t) \cos\theta_0 \left[ b + \frac{b^2+1}{b} \sum_{n=1}^{\infty} b^n \cos 2n\theta \right] \quad (A8.13)
\end{aligned}$$

Equating the sine terms on the two sides of the above equation, and neglecting any resistances present in the harmonic terms

$$\begin{aligned}
\sqrt{\frac{3}{2}} E_0 \sin\theta &= -\omega M_{af} \sin\theta I_f(t) \\
& - \omega \frac{\sqrt{6}}{2} \frac{M_{af}^2}{L_f} E_0 \frac{F_1(t)}{A'+\sqrt{A'B'}} \frac{3+b}{2} \sin\theta \\
& + \omega \frac{\sqrt{6}}{2} 2 \left( A + \frac{L_Y}{2} \right) E_0 \frac{1}{A'+\sqrt{A'B'}} F_1(t) \sin\theta \\
& + \omega \frac{\sqrt{6}}{2} B E_0 \frac{1}{A'+\sqrt{A'B'}} F_1(t) (1+b) \sin\theta \quad (A8.14)
\end{aligned}$$

After performing the necessary mathematical manipulation, this equation may be re-written as

$$\sqrt{\frac{3}{2}} E_0 = -\omega M_{af} I_f(t) + \sqrt{\frac{3}{2}} E_0 F_1(t) \quad (\text{A8.15})$$

Equating the coefficients of the DC terms in equation (A8.13)

$$\begin{aligned} -p \frac{\sqrt{6}}{2} \frac{M_{af}^2}{L_f} E_0 \frac{F_2(t) \cos \theta_0}{A' + \sqrt{A'B'}} + r \frac{\sqrt{6}}{\sqrt{A'B'}} E_0 F_2(t) \cos \theta_0 \frac{1}{2} \\ + p \left( A + \frac{L_f}{2} \right) \frac{\sqrt{6}}{\sqrt{A'B'}} E_0 F_2(t) \cos \theta_0 \frac{1}{2} + pB \frac{\sqrt{6}}{2} \frac{1}{\sqrt{A'B'}} B_0 F_2(t) \cos \theta_0 \quad b=0 \end{aligned} \quad (\text{A8.16})$$

which may be re-written as

$$r F_2(t) + p \frac{\sqrt{A'B'}}{\omega} F_2(t) = 0 \quad (\text{A8.17})$$

The required decrement factors may be calculated by solving equations (A8.9) and (A8.15) and (A8.17) simultaneously. Thus, on obtaining the Laplace transform of equation (A8.17)

$$r F_2(s) + \frac{\sqrt{A'B'}}{\omega} (s F_2(s) - 1) = 0 \quad (\text{A8.18})$$

or

$$F_2(s) = \frac{1}{s + \frac{r\omega}{\sqrt{A'B'}}} \quad (\text{A8.19})$$

Taking the inverse Laplace transformation

$$F_2(t) = e^{-t/\tau_a} \quad (\text{A8.20})$$

where

$$\tau_a = \frac{\sqrt{A'B'}}{r\omega} \quad (\text{A8.21})$$

Taking the Laplace transforms of equations (A8.9) and (A8.15) yields respectively

$$-\sqrt{\frac{3}{2}} \frac{E_0}{s} = \omega M_{af} I_f(s) - \sqrt{\frac{3}{2}} E_0 F_1(s) \quad (\text{A8.22})$$

$$(R_f + sL_f) I_f(s) + \sqrt{\frac{3}{2}} R_f \frac{M_{af}}{L_f} E_0 \frac{1}{A' + \sqrt{A'B'}} I_f(s) = 0 \quad (\text{A8.23})$$

which may be solved simultaneously to give

$$I_f(s) = \sqrt{\frac{3}{2}} E_0 \frac{M_{af}}{L_f} \frac{1}{X_d + X_0 + X_2} \left[ \frac{1}{s + \frac{1}{\tau_a}} - \frac{1}{s} \right] \quad (\text{A8.24})$$

and

$$F_1(s) = \frac{X'_d + X_o + X_2}{X_d + X_o + X_2} \left[ \frac{X_d - X'_d}{X_d + X_o + X_2} \frac{1}{s + \frac{1}{\tau_a}} + \frac{1}{s} \right] \quad (\text{A8.25})$$

where

$$X_2 = \sqrt{A'B'} - 0.5 X_o$$

$$\tau'_{do} = \frac{L_f}{R_f} \quad (\text{A8.26})$$

$$\bar{\tau}'_d = \tau'_{do} \frac{X'_d + X_o + X_2}{X_d + X_a + X_2}$$

Taking inverse Laplace transforms of equations (A8.22) and (A8.25)

$$I_f(t) = \sqrt{\frac{3}{2}} E_o \frac{M_{af}}{L_f} \frac{1}{X_d + X_o + X_2} [e^{-t/\tau'_a} - 1]$$

(A8.27)

$$F_1(t) = \frac{X'_d + X_o + X_2}{X_d + X_o + X_2} \left[ \frac{X_d - X'_d}{X_d + X_o + X_2} e^{-t/\tau'_d} + 1 \right]$$

APPENDIX IX

CALCULATION OF DECREMENT FACTORS FOR  
TERMINAL (2)- TO-CENTRE POINT FAULT

From equations (5.69) and (5.70),  $i_\alpha$  and  $i_f$  are

$$\begin{aligned} i_\alpha &= - \frac{\sqrt{6} E_0}{C' + \sqrt{C'D'}} F_1(t) \left[ \cos\theta + \sum_{n=1}^{\infty} b^n \cos(2n+1)\theta \right] \\ &= \frac{\sqrt{6} E_0 \cos\theta_0}{\sqrt{C'D'}} F_2(t) \left[ \frac{1}{2} + \sum_{n=1}^{\infty} b^n \cos 2n\theta \right] \end{aligned} \quad (A9.1)$$

and

$$\begin{aligned} i_f &= I_f(t) + \frac{\sqrt{6} M_{af}}{2 L_f} \frac{E_0}{C' + \sqrt{C'D'}} F_1(t) \left[ 1 + \frac{1+b}{b} \sum_{n=1}^{\infty} b^n \cos 2n\theta \right] \\ &\quad - \frac{\sqrt{6} M_{af}}{2 L_f} \frac{E_0 \cos\theta_0}{\sqrt{C'D'}} (1+b) F_2(t) \left[ \cos\theta + \sum_{n=1}^{\infty} b^n \cos(2n+1)\theta \right] \end{aligned} \quad (A9.2)$$

respectively. Using the expressions of Appendix VI,  $i_\alpha$  and  $i_f$  can be summed to give

$$i_\alpha = - \frac{\sqrt{6} E_0 (F_1(t) \cos\theta - F_2(t) \cos\theta_0)}{C' + D' + (C' - D') \cos 2\theta} \quad (A9.3)$$

and

$$i_f = I_f(t) + \sqrt{6} \frac{M_{af}}{L_f} \frac{E_0 (F_1(t) \cos\theta - F_2(t) \cos\theta_0) \cos\theta}{C' + D' + (C' - D') \cos 2\theta} \quad (A9.4)$$

respectively.

From equation (5.64)

$$(R_f + pL_f)i_f + pM_{af} \cos\theta i_\alpha = 0 \quad (A9.5)$$

If the values of  $i_\alpha$  and  $i_f$  obtained from equations (A9.3) and (A9.6) are substituted into equation (A9.5)

$$(R_f + pL_f)[I_f(t) + \sqrt{6} \frac{M_{af}}{L_f} \frac{E_o(F_1(t) \cos^2\theta - F_2(t)\cos\theta \cos\theta_o)}{C' + D' + (C' - D')\cos 2\theta}]$$

$$- p \frac{\sqrt{6} E_o M_{af} (F_1(t) \cos^2\theta - F_2(t)\cos\theta \cos\theta_o)}{C' + D' + (C' - D')\cos 2\theta} = 0$$

or

$$(R_f + pL_f)I_f(t) + \sqrt{6} R_f \frac{M_{af}}{L_f} E_o F_1(t) \frac{\cos^2\theta}{C' + D' + (C' - D') \cos 2\theta}$$

$$+ \sqrt{6} M_{af} E_o p F_1(t) \frac{\cos^2\theta}{C' + D' + (C' - D') \cos 2\theta}$$

$$+ \sqrt{6} M_{af} E_o p F_2(t) \cos\theta_o \frac{\cos\theta}{C' + D' + (C' - D') \cos 2\theta}$$

$$+ \sqrt{6} E_o M_{af} p F_1(t) \frac{\cos^2\theta}{C' + D' + (C' - D') \cos 2\theta}$$

$$= 0$$

Using the series expansions given in Appendix VI:

$$\begin{aligned}
 (R_f + pL_f)I_f(t) &+ \frac{\sqrt{6}}{2} R_f \frac{M_{af}}{L_f} E_o \frac{F_1(t)}{C' + \sqrt{C'D'}} \left[ 1 + \frac{1+b}{b} \sum_{n=1}^{\infty} b^n \cos 2n\theta \right] \\
 &+ \frac{\sqrt{6}}{2} M_{af} E_o \frac{pF_1(t)}{C' + \sqrt{C'D'}} \left[ 1 + \frac{1+b}{b} \sum_{n=1}^{\infty} b^n \cos 2n\theta \right] \\
 &- \sqrt{6} R_f \frac{M_{af}}{L_f} E_o F_2(t) \cos \theta_o \frac{1}{C' + \sqrt{C'D'}} \left[ \cos \theta + \sum_{n=1}^{\infty} b^n \cos (2n+1)\theta \right] \\
 &- \sqrt{6} M_{af} E_o \cos \theta_o \frac{pF_2(t)}{C' + \sqrt{C'D'}} \left[ \cos \theta + \sum_{n=1}^{\infty} b^n \cos (2n+1)\theta \right] \\
 &+ \frac{\sqrt{6}}{2} M_{af} E_o \cos \theta_o \frac{F_1(t)}{C' + \sqrt{C'D'}} \left[ 1 + \frac{1+b}{b} \sum_{n=1}^{\infty} b^n \cos 2n\theta \right] \\
 &= 0
 \end{aligned} \tag{A9.8}$$

Neglecting the derivative of the decrement factor and equating the coefficients of the DC terms

$$(R_f + pL_f) I_f(t) + \frac{\sqrt{6}}{2} R_f \frac{M_{af}}{L_f} E_o \frac{F_1(t)}{C' + \sqrt{C'D'}} = 0 \tag{A9.9}$$

From (4.136)

$$\sqrt{\frac{3}{2}} E_0 \sin\theta = pM_{af} \cos\theta i_f + [3R + p(A + 2L_\gamma + B \cos 2\theta)] i_\alpha \quad (A9.10)$$

Substituting equations (A9.3) and (A9.4) into equation (A9.10)

$$\begin{aligned} \sqrt{\frac{3}{2}} E_0 \sin\theta &= pM_{af} \cos\theta I_f(t) + p\sqrt{6} \frac{M_{af}^2 E_0 (F_1(t)\cos\theta - F_2(t)\cos\theta_0)\cos^2\theta}{C' + D' + (C' - D')\cos 2\theta} \\ &- 3R \frac{\sqrt{6} E_0 (F_1(t)\cos\theta - F_2(t)\cos\theta_0)}{C' + D' + (C' - D')\cos 2\theta} \\ &- p(A + 2L_\gamma) \frac{\sqrt{6} E_0 (F_1(t)\cos\theta - F_2(t)\cos\theta_0)}{C' + D' + (C' - D')\cos 2\theta} \\ &- p \frac{\sqrt{6} E_0 (F_1(t)\cos\theta - F_2(t)\cos\theta_0)\cos 2\theta}{C' + D' + (C' - D')\cos 2\theta} \quad (A9.11) \end{aligned}$$

or

$$\begin{aligned} \sqrt{\frac{3}{2}} E_0 \sin\theta &= pM_{af} \cos\theta I_f(t) + p\sqrt{6} \frac{M_{af}^2}{L_f} E_0 F_1(t) \frac{\cos^3\theta}{C' + D' + (C' - D')\cos 2\theta} \\ &- p\sqrt{6} \frac{M_{af}^2}{L_f} E_0 F_2(t) \cos\theta_0 \frac{\cos^2\theta}{C' + D' + (C' - D')\cos 2\theta} \\ &- 3R \sqrt{6} E_0 F_1(t) \frac{\cos\theta}{C' + D' + (C' - D')\cos 2\theta} \\ &+ 3R\sqrt{6} E_0 F_2(t) \cos\theta_0 \frac{1}{C' + D' + (C' - D')\cos 2\theta} \end{aligned}$$

$$\begin{aligned}
 & -p(A+2L_\gamma)F_1(t) \frac{\cos\theta}{C'+D'+(C'-D')\cos 2\theta} + p(A+2L_\gamma)\sqrt{6} E_0 \cos\theta_0 \frac{1}{C'+D'+(C'-D')\cos 2\theta} \\
 & -p\sqrt{6} B E_0 F_1(t) \frac{\cos\theta \cos 2\theta}{C'+D'+(C'-D')\cos 2\theta} + p\sqrt{6} B E_0 F_2(t) \cos\theta_0 \frac{\cos 2\theta}{C'+D'+(C'-D')\cos 2\theta}
 \end{aligned}
 \tag{A9.12}$$

Using the series expansions given in Appendix VI

$$\begin{aligned}
 \sqrt{\frac{3}{2}} E_0 \sin\theta &= p M_{af} \cos\theta I_f(t) \\
 &+ p \frac{\sqrt{6}}{2} \frac{M_{af}^2}{L_f} E_0 \frac{F_1(t)}{C'+\sqrt{C'D'}} \left[ \frac{3+b}{2} \cos\theta + \frac{(b+1)^2}{2b} \sum_{n=1}^{\infty} b^n \cos(2n+1)\theta \right] \\
 &- p \frac{\sqrt{6}}{2} \frac{M_{af}^2}{L_f} E_0 \frac{F_2(t) \cos\theta_0}{C'+\sqrt{C'D'}} \left[ 1 + \frac{1+b}{b} \sum_{n=1}^{\infty} b^n \cos 2n\theta \right] \\
 &- 3R\sqrt{6} R_0 \frac{1}{C'+\sqrt{C'D'}} F_1(t) \left[ \cos\theta + \sum_{n=1}^{\infty} b^n \cos(2n+1)\theta \right] \\
 &+ 3R \frac{\sqrt{6}}{\sqrt{C'D'}} E_0 F_2(t) \cos\theta_0 \left[ \frac{1}{2} + \sum_{n=1}^{\infty} b^n \cos 2n\theta \right] \\
 &- \sqrt{6} p(A+2L_\gamma) E_0 \frac{1}{C'+\sqrt{C'D'}} F_1(t) \left[ \cos\theta + \sum_{n=1}^{\infty} b^n \cos(2n+1)\theta \right] \\
 &+ p(A+2L_\gamma) \frac{\sqrt{6}}{\sqrt{C'D'}} E_0 F_2(t) \cos\theta_0 \left[ \frac{1}{2} + \sum_{n=1}^{\infty} b^n \cos 2n\theta \right]
 \end{aligned}$$

$$\begin{aligned}
 & - p B \frac{\sqrt{6}}{2} \frac{E_0}{C'+\sqrt{C'D'}} F_1(t) [(1+b)\cos\theta + \frac{b^2+1}{b} \sum_{n=1}^{\infty} b^n \cos(2n+1)\theta] \\
 & + pB \frac{\sqrt{6}}{2} \frac{1}{\sqrt{C'D'}} E_0 F_2(t) \cos\theta_0 [b + \frac{b^2+1}{b} \sum_{n=1}^{\infty} b^n \cos 2n\theta] \quad (A9.13)
 \end{aligned}$$

Equating the sin terms on the two sides of equation (A9.13), and neglecting any resistances present in the harmonic terms,

$$\begin{aligned}
 \sqrt{\frac{3}{2}} E_0 \sin\theta &= - \omega M_{af} \sin\theta I_f(t) \\
 & - \omega \frac{\sqrt{6}}{2} \frac{M_{af}^2}{L_f} E_0 \frac{F_1(t)}{C'+\sqrt{C'D'}} \frac{3+b}{2} \sin\theta \\
 & + \omega \frac{\sqrt{6}}{2} 2(A+2L_\gamma) E_0 \frac{1}{C'+\sqrt{C'D'}} F_1(t) \sin\theta \\
 & + \omega \frac{\sqrt{6}}{2} B E_0 \frac{1}{C'+\sqrt{C'D'}} F_1(t) (1+b) \sin\theta \quad (A9.14)
 \end{aligned}$$

Equation (A9.14) may be re-written as

$$\sqrt{\frac{3}{2}} E_0 = - \omega M_{af} I_f(t) + \sqrt{\frac{3}{2}} E_0 F_1(t) \quad (A9.15)$$

Equating the coefficients of the DC terms in equation (A9.13)

$$\begin{aligned}
 & -p \frac{\sqrt{6}}{2} \frac{M_{af}^2}{L_f} E_0 \frac{F_2(t) \cos \theta_0}{C + \sqrt{C'D'}} + 3R \frac{\sqrt{6}}{\sqrt{C'D'}} E_0 F_2(t) \cos \theta_0 \frac{1}{2} \\
 & + p(A+2L_\gamma) \frac{\sqrt{6}}{\sqrt{C'D'}} E_0 F_2(t) \cos \theta_0 \frac{1}{2} + pB \frac{\sqrt{6}}{2} \frac{1}{\sqrt{C'D'}} E_0 F_2(t) \cos \theta_0 \quad b=0
 \end{aligned}
 \tag{A9.16}$$

After considerable mathematical manipulation, equation (A9.16) may be re-written as

$$3R F_2(t) + p \frac{\sqrt{C'D'}}{\omega} F_2(t) = 0 \tag{A9.17}$$

The required decrement factors can be calculated by solving equations (A9.9) and (A9.15) and (A9.17) simultaneously. Thus, taking Laplace transforms of equation (A9.17)

$$3R F_2(s) + \frac{\sqrt{C'D'}}{\omega} (s F_2(s) - 1) = 0 \tag{A9.18}$$

or

$$F_2(s) = \frac{1}{s + \frac{3R\omega}{\sqrt{C'D'}}} \tag{A9.19}$$

Taking the inverse Laplace transformation of  $F_2(s)$

$$F_2(t) = e^{-t/\tau_b} \quad (A9.20)$$

where

$$\tau_b = \frac{\sqrt{C'D'}}{3R\omega} \quad (A9.21)$$

Taking Laplace transform of equations (A9.9) and (A9.15) yields

$$-\sqrt{\frac{3}{2}} \frac{E_0}{s} = \omega M_{af} I_f(s) - \sqrt{\frac{3}{2}} E_0 F_1(s) \quad (A9.12)$$

$$(R_f + sL_f) I_f(s) + \sqrt{\frac{3}{2}} R_f \frac{M_{af}}{L_f} E_0 \frac{1}{C' + \sqrt{C'D'}} F_1(s) = 0 \quad (A9.23)$$

which may be solved simultaneously to give

$$I_f(s) = \sqrt{\frac{3}{2}} E_0 \frac{M_{af}}{L_f} \frac{1}{X_d + 4X_o + X_2} \left[ \frac{1}{s + \frac{1}{\tau_d}} - \frac{1}{s} \right] \quad (A9.24)$$

and

$$F_1(s) = \frac{X'_d + 4X_o + X_2}{X_d + 4X_o + X_2} \left[ \frac{X_d - X'_d}{X_d + 4X_o + X_2} \frac{1}{s + \frac{1}{\tau_d}} + \frac{1}{s} \right] \quad (A9.25)$$

where

$$X_2 = \sqrt{C'D'} - 2X_0 \quad (\text{A9.26})$$

$$\tau_{do} = \frac{L_f}{R_f} \quad (\text{A9.27})$$

$$\tau'_d = \tau'_{do} \frac{X'_d + 4X_0 + X_2}{X_d + 4X_0 + X_2} \quad (\text{A9.28})$$

Taking inverse Laplace transforms of equations (A9.24) and (A9.25)

$$I_f(t) = \sqrt{\frac{3}{2}} E_0 \frac{M_{af}}{L_f} \frac{1}{X_d + 4X_0 + X_2} [e^{-t/\tau'_d} - 1] \quad (\text{A9.29})$$

$$F_1(t) = \frac{X'_d + 4X_0 + X_2}{X_d + 4X_0 + X_2} \frac{X_d - X'_d}{X_d + 4X_0 + X_2} [e^{-t/\tau'_d} + 1] \quad (\text{A9.30})$$

APPENDIX XCALCULATION OF DECREMENT FACTORS FOR  
DOUBLE LINE-TO-CENTRE POINT FAULT

From equations (5.98) and (5.99),  $i_\alpha$  and  $i_f$  are given by

$$i_\alpha = \frac{\sqrt{6} E_0}{G' + \sqrt{G'H'}} F_1(t) [\cos \theta + \sum_{n=1}^{\infty} b^n \cos (2n+1)\theta] \\ + \frac{\sqrt{6} E_0 \cos \theta_0}{\sqrt{G'H'}} F_2(t) \left[ \frac{1}{2} + \sum_{n=1}^{\infty} b^n \cos 2n\theta \right] \quad (\text{A10.1})$$

and

$$i_f = I_f(t) + \frac{\sqrt{6}}{2} \frac{M_{af}}{L_f} \frac{E_0}{G' + \sqrt{G'H'}} F_1(t) \left[ 1 + \frac{1+b}{b} \sum_{n=1}^{\infty} b^n \cos 2n\theta \right] \\ - \frac{\sqrt{6}}{2} \frac{M_{af}}{L_f} \frac{E_0 \cos \theta_0}{\sqrt{G'H'}} (1+b) F_2(t) \left[ \cos \theta + \sum_{n=1}^{\infty} b^n \cos (2n+1)\theta \right] \quad (\text{A10.2})$$

respectively. Using the expressions in Appendix VI,  $i_\alpha$  and  $i_f$  may be summed to give

$$i_\alpha = \frac{\sqrt{6} E_0 (F_1(t) \cos \theta - F_2(t) \cos \theta_0)}{(G' + H') + (G' - H') \cos 2\theta} \quad (\text{A10.3})$$

and

$$i_f = I_f(t) + \sqrt{6} \frac{M_{af}}{L_f} \frac{E_0 (F_1(t) \cos \theta - F_2(t) \cos \theta_0) \cos \theta}{G' + H' + (G' - H') \cos 2\theta} \quad (\text{A10.4})$$

respectively.

From equation (5.92)

$$(R_f + pL_f) i_f + p M_{af} \cos \theta i_\alpha = 0 \quad (\text{A10.5})$$

If the values of  $i_\alpha$  and  $i_f$  obtained from equations (A10.3) and (A10.4) are substituted into equation (A10.5), the result is

$$(R_f + pL_f) [I_f(t) + \sqrt{6} \frac{M_{af}}{L_f} \frac{E_o (F_1(t) \cos^2 \theta - F_2(t) \cos \theta \cos \theta_o)}{(G' + H') + (G' - H') \cos 2\theta}] - p \frac{\sqrt{6} E_o M_{af} (F_1(t) \cos^2 \theta - F_2(t) \cos \theta \cos \theta_o)}{(G' + H') + (G' - H') \cos 2\theta} = 0 \quad (\text{A10.6})$$

or

$$\begin{aligned} (R_f + pL_f) I_f(t) + \sqrt{6} R_f \frac{M_{af}}{L_f} E_o F_1(t) \frac{\cos^2 \theta}{(G' + H') + (G' - H') \cos 2\theta} \\ + \sqrt{6} M_{af} E_o p F_1(t) \frac{\cos^2 \theta}{(G' + H') + (G' - H') \cos 2\theta} \\ - \sqrt{6} R_f \frac{M_{af}}{L_f} E_o F_2(t) \cos \theta_o \frac{\cos \theta}{(G' + H') + (G' - H') \cos 2\theta} \\ - \sqrt{6} M_{af} E_o p F_2(t) \cos \theta_o \frac{\cos \theta}{(G' + H') + (G' - H') \cos 2\theta} \\ + \sqrt{6} E_o M_{af} p F_1(t) \frac{\cos^2 \theta}{(G' + H') + (G' - H') \cos 2\theta} \end{aligned} \quad (\text{A10.7})$$

Using the series expansions for the mathematical expressions given in Appendix VI

$$\begin{aligned}
 (R_f + pL_f) I_f(t) &+ \frac{\sqrt{6}}{2} R_f \frac{M_{af}}{L_f} E_o \frac{F_1(t)}{G' + \sqrt{G'H'}} \left[ 1 + \frac{1+b}{b} \sum_{n=1}^{\infty} b^n \cos 2n\theta \right] \\
 &+ \frac{\sqrt{6}}{2} M_{af} E_o \frac{pF_1(t)}{G' + \sqrt{G'H'}} \left[ 1 + \frac{1+b}{b} \sum_{n=1}^{\infty} b^n \cos 2n\theta \right] \\
 &- \sqrt{6} R_f \frac{M_{af}}{L_f} E_o F_2(t) \cos \theta_o \frac{1}{G' + \sqrt{G'H'}} \left[ \cos \theta + \sum_{n=1}^{\infty} b^n \cos 2n\theta \right] \\
 &- \sqrt{6} M_{af} E_o \cos \theta_o \frac{pF_2(t)}{G' + \sqrt{G'H'}} \left[ \cos \theta + \sum_{n=1}^{\infty} b^n \cos (2n+1)\theta \right] \\
 &+ \frac{\sqrt{6}}{2} M_{af} E_o \cos \theta_o \frac{F_1(t)}{G' + \sqrt{G'H'}} \left[ 1 + \frac{1+b}{b} \sum_{n=1}^{\infty} b^n \cos 2n\theta \right]
 \end{aligned} \tag{A10.8}$$

Equating the coefficients of the DC terms and neglecting the derivative of the decrement factor

$$(R_f + pL_f) I_f(t) + \frac{\sqrt{6}}{2} R_f \frac{M_{af}}{L_f} E_o \frac{F_1(t)}{G' + \sqrt{G'H'}} = 0 \tag{A10.9}$$

From (5.91)

$$\sqrt{\frac{3}{2}} E_o \sin \theta = pM_{af} \cos \theta i_f + (R + p(A+B \cos 2\theta)) i_\alpha \tag{A10.10}$$

Substituting equations (A10.3) and (A.104) into equation (A10.10)

$$\begin{aligned}
 \sqrt{\frac{3}{2}} E_0 \sin\theta &= p M_{af} \cos\theta I_f(t) + p\sqrt{6} \frac{M_{af}^2 E_0 (F_1(t)\cos\theta - F_2(t)\cos\theta_0)\cos^2\theta}{L_f (G'+H')+(G'-H')\cos 2\theta} \\
 &- R \frac{\sqrt{6} E_0 (F_1(t)\cos\theta - F_2(t)\cos\theta_0)}{(G'+H')+(G'-H')\cos 2\theta} \\
 &- pA \frac{\sqrt{6} E_0 (F_1(t)\cos\theta - F_2(t)\cos\theta_0)}{(G'+H')+(G'-H')\cos 2\theta} \\
 &- p \frac{\sqrt{6} B E_0 (F_1(t)\cos\theta - F_2(t)\cos\theta_0)\cos 2\theta}{(G'+H')+(G'-H')\cos 2\theta} \quad (A10.11)
 \end{aligned}$$

or

$$\begin{aligned}
 \sqrt{\frac{3}{2}} E_0 \sin\theta &= p M_{af} \cos\theta I_f(t) + p\sqrt{6} \frac{M_{af}^2 E_0 F_1(t) \cos^3\theta}{L_f (G'+H')+(G'-H')\cos 2\theta} \\
 &- p\sqrt{6} \frac{M_{af}^2 E_0 F_2(t) \cos\theta_0 \cos^2\theta}{L_f (G'+H')+(G'-H')\cos 2\theta} \\
 &- R\sqrt{6} E_0 F_1(t) \frac{\cos\theta}{(G'+H')+(G'-H')\cos 2\theta} \\
 &+ R\sqrt{6} E_0 F_2(t)\cos\theta \frac{1}{(G'+H')+(G'-H')\cos 2\theta}
 \end{aligned}$$

$$\begin{aligned}
 & -pA F_1(t) \frac{\cos\theta}{G'+H'+(G'-H')\cos 2\theta} + pA\sqrt{6} E_0 F_2(t) \cos\theta_0 \frac{1}{G'+H'+(G'-H')\cos 2\theta} \\
 & -p\sqrt{6} B E_0 F_1(t) \frac{\cos\theta \cos 2\theta}{G'+H'+(G'-H')\cos 2\theta} \\
 & + p\sqrt{6} B E_0 F_2(t) \cos\theta_0 \frac{\cos 2\theta}{(G'+H')+(G'-H')\cos 2\theta} \quad (A10.12)
 \end{aligned}$$

Using the expressions given in Appendix VI.

$$\sqrt{\frac{3}{2}} E_0 \sin\theta = p M_{af} \cos\theta I_f(t)$$

$$+ p \frac{\sqrt{6}}{2} \frac{M_{af}^2}{L_f} E_0 \frac{F_1(t)}{G'+\sqrt{G'H'}} \left[ \frac{3+b}{2} \cos\theta + \frac{(b+1)^2}{2b} \sum_{n=1}^{\infty} b^n \cos(2n+1)\theta \right]$$

$$-p \frac{\sqrt{6}}{2} \frac{M_{af}^2}{L_f} E_0 \frac{F_2(t)\cos\theta_0}{G'+\sqrt{G'H'}} \left[ 1 + \frac{1+b}{b} \sum_{n=1}^{\infty} b^n \cos 2n\theta \right]$$

$$-R\sqrt{6} E_0 \frac{1}{G'+\sqrt{G'H'}} F_1(t) \left[ \cos\theta + \sum_{n=1}^{\infty} b^n \cos(2n+1)\theta \right]$$

$$+ R \frac{\sqrt{6}}{\sqrt{G'H'}} E_0 F_2(t) \cos\theta_0 \left[ \frac{1}{2} + \sum_{n=1}^{\infty} b^n \cos 2n\theta \right]$$

$$-\sqrt{6} p A E_0 \frac{1}{G'+\sqrt{G'H'}} F_1(t) \left[ \cos\theta + \sum_{n=1}^{\infty} b^n \cos(2n+1)\theta \right]$$

$$\begin{aligned}
& + pA \frac{\sqrt{6}}{\sqrt{G^2 + H^2}} E_0 F_2(t) \cos\theta_0 \left[ \frac{1}{2} + \sum_{n=1}^{\infty} b^n \cos 2n\theta \right] \\
& - pB \frac{\sqrt{6}}{2} \frac{E_0}{G^2 + \sqrt{G^2 + H^2}} F_1(t) \left[ (1+b) \cos\theta + \frac{b^2+1}{b} \sum_{n=1}^{\infty} b^n \cos(2n+1)\theta \right] \\
& + pB \frac{\sqrt{6}}{2} \frac{1}{\sqrt{G^2 + H^2}} E_0 F_2(t) \cos\theta_0 \left[ b + \frac{b^2+1}{b} \sum_{n=1}^{\infty} b^n \cos 2n\theta \right] \quad (A10.13)
\end{aligned}$$

Equating the  $\sin\theta$  terms the on the two sides of equation (A10.13), and neglecting any small resistances in the harmonic terms, gives

$$\begin{aligned}
\sqrt{\frac{3}{2}} E_0 \sin\theta & = -\omega M_{af} \sin\theta I_f(t) \\
& - \omega \frac{\sqrt{6}}{2} \frac{M_{af}^2}{L_f} E_0 \frac{F_1(t)}{G^2 + \sqrt{G^2 + H^2}} \frac{3+b}{2} \sin\theta \\
& + \omega \frac{\sqrt{6}}{2} 2 A E_0 \frac{1}{G^2 + \sqrt{G^2 + H^2}} F_1(t) \sin\theta \\
& + \omega \frac{\sqrt{6}}{2} B E_0 \frac{1}{G^2 + \sqrt{G^2 + H^2}} F_1(t) (1+b) \sin\theta \quad (A10.14)
\end{aligned}$$

After considerable mathematical manipulation, equation (A10.14) may be re-written as

$$\sqrt{\frac{3}{2}} E_0 = -\omega M_{af} I_f(t) + \frac{\sqrt{6}}{2} E_0 F_1(t) \quad (\text{A10.15})$$

Equating the coefficients of the DC terms in equation (A10.13)

$$\begin{aligned} -p \frac{\sqrt{6}}{2} \frac{M_{af}^2}{L_f} E_0 \frac{F_2(t) \cos \theta_0}{G' + \sqrt{G'H'}} + R \frac{\sqrt{6}}{\sqrt{G'H'}} E_0 F_2(t) \cos \theta_0 \frac{1}{2} \\ + pA \frac{\sqrt{6}}{\sqrt{G'H'}} E_0 F_2(t) \cos \theta_0 \frac{1}{2} + pB \frac{\sqrt{6}}{2} \frac{1}{\sqrt{G'H'}} E_0 F_2(t) \cos \theta_0 b=0 \end{aligned} \quad (\text{A10.16})$$

After considerable mathematical manipulation, equation (A10.1) may be re-written as

$$RF_2(t) + p \frac{\sqrt{G'H'}}{\omega} F_2(t) = 0 \quad (\text{A10.17})$$

The required decrement factors may be calculated by solving simultaneously equations (A9.9) and (A10.15) and (A.10.17).

The Laplace transform of equation (A10.17) is

$$RF_2(s) + \frac{\sqrt{G'H'}}{\omega} (s F_2(s) - 1) = 0 \quad (\text{A10.18})$$

or

$$F_2(s) = \frac{1}{s + \frac{R\omega}{\sqrt{G'H'}}} \quad (\text{A10.19})$$

or, on taking the inverse Laplace transformation of  $F_2(s)$

$$F_2(t) = e^{-t/\tau_c} \quad (\text{A10.20})$$

where

$$\tau_c = \frac{\sqrt{G'H'}}{R\omega} \quad (\text{A10.21})$$

Taking Laplace transform of equations (A10.9) and (A10.15) yields

$$-\frac{\sqrt{6}}{2} \frac{E_0}{s} = \omega M_{af} I_f(s) - \frac{\sqrt{6}}{2} E_0 F_1(s) \quad (\text{A10.22})$$

$$(R_f + sL_f) I_f(s) + \frac{\sqrt{6}}{2} R_f \frac{M_{af}}{L_f} E_0 \frac{1}{G' + \sqrt{G'H'}} F_1(s) = 0 \quad (\text{A10.23})$$

which may be solved simultaneously to give

$$I_f(s) = \frac{\sqrt{6}}{2} E_0 \frac{M_{af}}{L_f} \frac{1}{X_d + X_2} \left[ \frac{1}{s + \frac{1}{\tau_d}} - \frac{1}{s} \right] \quad (\text{A10.24})$$

and

$$F_1(s) = \frac{X_d' + X_2}{X_d + X_2} \left[ \frac{X_d - X_d'}{X_d + X_2} \frac{1}{s + \frac{1}{\tau_d}} - \frac{1}{s} \right] \quad (\text{A10.25})$$

where

$$X_2 = \sqrt{G'H'}$$

$$\tau'_{do} = \frac{L_f}{R_f} \quad (A10.26)$$

$$\tau'_d = \tau'_{do} \frac{X'_d + X_2}{X_d + X_2}$$

The inverse Laplace transforms of equation (A10.24) and (A10.25) are

$$I_f(t) = \frac{\sqrt{6}}{2} E_o \frac{M_{af}}{L_f} \frac{1}{X_d + X_2} [e^{-t/\tau'_d} - 1]$$

and

$$F_1(t) = \frac{X'_d + X_2}{X_d + X_2} \left[ \frac{X_d - X'_d}{X_d + X_2} e^{-t/\tau'_d} + 1 \right] \quad (A10.27)$$

respectively.

## APPENDIX XI

CALCULATION OF DECREMENT FACTORS FOR  
LINE-TO-LINE FAULT OF EDISON-DELTA CONNECTION

From equations (5.125) and (5.126),  $i_\alpha$  and  $i_f$  are given by

$$i_\alpha = - \frac{\sqrt{6} E_0}{M' + \sqrt{M'N'}} F_1(t) \left[ \cos\theta + \sum_{n=1}^{\infty} b^n \cos(2n+1)\theta \right] \\ + \frac{\sqrt{6} E_0 \cos\theta_0}{\sqrt{M'N'}} F_2(t) \left[ \frac{1}{2} + \sum_{n=1}^{\infty} b^n \cos 2n\theta \right] \quad (\text{A11.1})$$

and

$$i_f = I_f(t) + \frac{\sqrt{6}}{2} \frac{M_{af}}{L_f} \frac{E_0}{M' + \sqrt{M'N'}} F_1(t) \left[ 1 + \frac{1+b}{b} \sum_{n=1}^{\infty} b^n \cos 2n\theta \right] \\ - \frac{\sqrt{6}}{2} \frac{M_{af}}{L_f} \frac{E_0 \cos\theta_0}{\sqrt{M'N'}} (1+b) F_2(t) \left[ \cos\theta + \sum_{n=1}^{\infty} b^n \cos(2n+1)\theta \right] \quad (\text{A11.2})$$

respectively. Using the expressions of Appendix VI,  $i_\alpha$  and  $i_f$  may be summed to give

$$i_\alpha = - \frac{\sqrt{6} E_0 (F_1(t)\cos\theta - F_2(t)\cos\theta_0)}{(M'+N') + (M'-N')\cos 2\theta} \quad (\text{A11.3})$$

and

$$i_f = I_f(t) + \sqrt{6} \frac{M_{af}}{L_f} \frac{E_0 (F_1(t)\cos\theta - F_2(t)\cos\theta_0)\cos\theta}{M' + N' + (M'-N')\cos 2\theta} \quad (\text{A11.4})$$

respectively.

From equation (5.119)

$$(R_f + pL_f)i_f + pM_{af} \cos\theta i_\alpha = 0 \quad (\text{A11.5})$$

If the values of  $i_\alpha$  and  $i_f$  from equations (A11.3) and (A11.4) are substituted into equation (A11.5), the result is

$$\begin{aligned} (R_f + pL_f)[I_f(t) + \sqrt{6} \frac{M_{af}}{L_f} \frac{E_0(F_1(t)\cos^2\theta - F_2(t)\cos\theta \cos\theta_0)}{(M'+N') + (N'-N')\cos 2\theta}] \\ - p \frac{\sqrt{6} E_0 M_{af} (F_1(t)\cos^2\theta - F_1(t)\cos\theta \cos\theta_0)}{(M'+N') + (M'-N')\cos 2\theta}] = 0 \quad (\text{A11.6}) \end{aligned}$$

or

$$\begin{aligned} (R_f + pL_f)I_f(t) + \sqrt{6} R_f \frac{M_{af}}{L_f} E_0 F_1(t) \frac{\cos^2\theta}{(M'+N') + (M'-N')\cos 2\theta} \\ + \sqrt{6} M_{af} E_0 p F_1(t) \frac{\cos^2\theta}{(M'+N') + (M'-N')\cos 2\theta} \\ - \sqrt{6} R_f \frac{M_{af}}{L_f} E_0 F_2(t) \cos\theta_0 \frac{\cos\theta}{(M'+N') + (M'-N')\cos 2\theta} \\ - \sqrt{6} M_{af} E_0 p F_2(t) \cos\theta_0 \frac{\cos\theta}{(M'+N') + (M'-N')\cos 2\theta} \\ + \sqrt{6} E_0 M_{af} p F_1(t) \frac{\cos^2\theta}{(M'+N') + (M'-N')\cos 2\theta} \quad (\text{A11.7}) \end{aligned}$$

Using the expressions given in Appendix VI

$$\begin{aligned}
 (R_f + pL_f)I_f(t) &+ \frac{\sqrt{6}}{2} R_f \frac{M_{af}}{L_f} E_0 \frac{F_1(t)}{M' + \sqrt{M'N'}} \left[ 1 + \frac{1+b}{b} \sum_{n=1}^{\infty} b^n \cos 2n\theta \right] \\
 &+ \frac{\sqrt{6}}{2} M_{af} E_0 \frac{pF_1(t)}{M' + \sqrt{M'N'}} \left[ 1 + \frac{1+b}{b} \sum_{n=1}^{\infty} b^n \cos 2n\theta \right] \\
 &- \sqrt{6} R_f \frac{M_{af}}{L_f} E_0 F_2(t) \cos \theta_0 \frac{1}{M' + \sqrt{M'N'}} \left[ \cos \theta + \sum_{n=1}^{\infty} b^n \cos 2n\theta \right] \\
 &- \sqrt{6} M_{af} E_0 \cos \theta_0 \frac{p F_2(t)}{M' + \sqrt{M'N'}} \left[ \cos \theta + \sum_{n=1}^{\infty} b^n \cos (2n+1)\theta \right] \\
 &+ \frac{\sqrt{6}}{2} M_{af} E_0 \cos \theta_0 \frac{F_1(t)}{M' + \sqrt{M'N'}} \left[ 1 + \frac{1+b}{b} \sum_{n=1}^{\infty} b^n \cos 2n\theta \right]
 \end{aligned} \tag{A11.8}$$

Equating the coefficients of the DC terms in equation (A11.8) and neglecting the derivative of the decrement factor

$$(R_f + pL_f)I_f(t) + \frac{\sqrt{6}}{2} R_f \frac{M_{af}}{L_f} E_0 \frac{F_1(t)}{M' + \sqrt{M'N'}} = 0 \tag{A11.9}$$

From equation (5.118)

$$\sqrt{\frac{3}{2}} E_0 \sin \theta = p M_{af} \cos \theta i_f + (R + p(A + B \cos 2\theta)) i_\alpha \tag{A11.10}$$

Substituting  $i_\alpha$  and  $i_f$  from equations (A11.3) and (A11.4) into equation (A11.10)

$$\begin{aligned} \sqrt{\frac{3}{2}} E_0 \sin\theta &= p M_{af} \cos\theta I_f(t) + p\sqrt{6} \frac{M_{af}^2}{L_f} E_0 \frac{(F_1(t)\cos\theta - F_2(t)\cos\theta_0)\cos\theta}{(M'+N')+(M'-N')\cos 2\theta} \\ &- R \frac{\sqrt{6} E_0 (F_1(t)\cos\theta - F_2(t)\cos\theta_0)}{(M'+N')+(M'-N')\cos 2\theta} \\ &- pA \frac{\sqrt{6} E_0 (F_1(t)\cos\theta - F_2(t)\cos\theta_0)}{(M'+N')+(M'-N')\cos 2\theta} \\ &- p \frac{\sqrt{6} B E_0 (F_1(t)\cos\theta - F_2(t)\cos\theta_0)\cos 2\theta}{(M'+N')+(M'-N')\cos 2\theta} \end{aligned}$$

or

(A11.11)

$$\begin{aligned} \sqrt{\frac{3}{2}} E_0 \sin\theta &= p M_{af} \cos\theta I_f(t) + p\sqrt{6} \frac{M_{af}^2}{L_f} E_0 F_1(t) \frac{\cos^3\theta}{(M'+N')+(M'-N')\cos 2\theta} \\ &- p\sqrt{6} \frac{M_{af}^2}{L_f} E_0 F_2(t) \cos\theta_0 \frac{\cos^2\theta}{(M'+N')+(M'-N')\cos 2\theta} \\ &- R\sqrt{6} E_0 F_1(t) \frac{\cos\theta}{M'+N'+(M'-N')\cos 2\theta} \\ &+ R\sqrt{6} E_0 F_2(t) \cos\theta_0 \frac{1}{M'+N'+(M'-N')\cos 2\theta} \end{aligned}$$

$$\begin{aligned}
& - pA F_1(t) \frac{\cos\theta}{M'+N'+(M'-N')\cos 2\theta} + pA\sqrt{6} E_0 F_2(t) \cos\theta_0 \frac{1}{M'+N'+(M'-N')\cos 2\theta} \\
& - p\sqrt{6} B E_0 F_1(t) \frac{\cos\theta \cos 2\theta}{M'+N'+(M'-N')\cos 2\theta} + p\sqrt{6} B E_0 F_2(t) \frac{\cos 2\theta}{M'+N'+(M'-N')\cos 2\theta}
\end{aligned}
\tag{A11.12}$$

Using the expressions of Appendix VI

$$\sqrt{\frac{3}{2}} E_0 \sin\theta = p M_{af} \cos\theta I_f(t)$$

$$+ p \frac{\sqrt{6}}{2} \frac{M_{af}^2}{L_f} E_0 \frac{F_1(t)}{M'+\sqrt{M'N'}} \left[ \frac{3+b}{2} \cos\theta + \frac{(b+1)^2}{2b} \sum_{n=1}^{\infty} b^n \cos(2n+1)\theta \right]$$

$$- p \frac{\sqrt{6}}{2} \frac{M_{af}^2}{L_f} E_0 \frac{F_2(t)\cos\theta_0}{M'+\sqrt{M'N'}} \left[ 1 + \frac{1+b}{b} \sum_{n=1}^{\infty} b^n \cos 2n\theta \right]$$

$$- R\sqrt{6} E_0 \frac{1}{M'+\sqrt{M'N'}} F_1(t) \left[ \cos\theta + \sum_{n=1}^{\infty} b^n \cos(2n+1)\theta \right]$$

$$+ R \frac{\sqrt{6}}{\sqrt{M'N'}} E_0 F_2(t) \cos\theta_0 \left[ \frac{1}{2} + \sum_{n=1}^{\infty} b^n \cos 2n\theta \right]$$

$$- \sqrt{6} pA E_0 \frac{1}{M'+\sqrt{M'N'}} F_1(t) \left[ \cos\theta + \sum_{n=1}^{\infty} b^n \cos(2n+1)\theta \right]$$

$$\begin{aligned}
& + pA \frac{\sqrt{6}}{\sqrt{M^2+N^2}} E_0 F_2(t) \cos\theta_0 \left[ \frac{1}{2} + \sum_{n=1}^{\infty} b^n \cos 2n\theta \right] \\
& - pB \frac{\sqrt{6}}{2} \frac{E_0}{M^2+\sqrt{M^2N^2}} F_1(t) \left[ (1+b)\cos\theta + \frac{b^2+1}{b} \sum_{n=1}^{\infty} b^n \cos(2n+1)\theta \right] \\
& + pB \frac{\sqrt{6}}{2} \frac{1}{\sqrt{M^2N^2}} E_0 F_2(t) \cos\theta_0 \left[ b + \frac{b^2+1}{b} \sum_{n=1}^{\infty} b^n \cos 2n\theta \right]
\end{aligned}
\tag{A11.13}$$

Equating the coefficients of the  $\sin\theta$  terms on the two sides of equation (A11.13), and neglecting any small resistances in the harmonic terms, gives

$$\begin{aligned}
\sqrt{\frac{3}{2}} E_0 \sin\theta &= -\omega M_{af} \sin\theta I_f(t) \\
& -\omega \frac{\sqrt{6}}{2} \frac{M_{af}^2}{L_f} \frac{F_1(t)}{M^2+\sqrt{M^2N^2}} \frac{3+b}{2} \sin\theta \\
& +\omega \frac{\sqrt{6}}{2} 2A E_0 \frac{1}{M^2+\sqrt{M^2N^2}} F_1(t) \sin\theta \\
& +\omega \frac{\sqrt{6}}{2} B E_0 \frac{1}{M^2+\sqrt{M^2N^2}} F_1(t) (1+b) \sin\theta
\end{aligned}
\tag{A11.14}$$

After considerable mathematical manipulation equation (A11.14) may be re-written as

$$\sqrt{\frac{3}{2}} E_0 = -\omega M_{af} I_f(t) + \frac{\sqrt{6}}{2} E_0 F_1(t) \quad (\text{A11.15})$$

Equating the coefficients of the DC terms in equation (A11.13)

$$\begin{aligned} -p \frac{\sqrt{6}}{2} \frac{M_{af}^2}{L_f} E_0 \frac{F_2(t) \cos \theta_0}{M^2 + \sqrt{M^2 N^2}} + R \frac{\sqrt{6}}{\sqrt{M^2 N^2}} E_0 F_2(t) \cos \theta_0 \frac{1}{2} \\ + pA \frac{\sqrt{6}}{\sqrt{M^2 N^2}} E_0 F_2(t) \cos \theta_0 \frac{1}{2} + pB \frac{\sqrt{6}}{2} \frac{1}{\sqrt{M^2 N^2}} E_0 F_2(t) \cos \theta_0 \frac{1}{2} = 0 \end{aligned} \quad (\text{A11.16})$$

After considerable mathematical manipulation, equation (A11.16) may be re-written as

$$R F_2(t) + p \frac{\sqrt{M^2 N^2}}{\omega} F_2(t) = 0 \quad (\text{A11.17})$$

The required decrement factors may be obtained by solving simultaneously equations (A11.9) and (A11.15) and (A11.17). Taking Laplace transforms of equation (A11.17)

$$R F_2(s) + \frac{\sqrt{M^2 N^2}}{\omega} (s F_2(s) - 1) = 0 \quad (\text{A11.18})$$

or

$$F_2(s) = \frac{R\omega}{s + \frac{R\omega}{\sqrt{M^2 N^2}}} \quad (\text{A11.19})$$

The inverse Laplace transform of  $F_2(s)$  is

$$F_2(t) = e^{-t/\tau_c} \quad (\text{A11.20})$$

where

$$\tau_c = \frac{\sqrt{M'N'}}{R\omega} \quad (\text{A11.21})$$

The Laplace transforms of equations (A11.9) and (A11.15) are

$$-\frac{\sqrt{6}}{2} \frac{E_0}{s} = \omega M_{af} I_f(s) - \frac{\sqrt{6}}{2} E_0 F_1(s) \quad (\text{A11.22})$$

and

$$(R_f + pL_f) I_f(s) + \frac{\sqrt{6}}{2} R_f \frac{M_{af}}{L_f} E_0 \frac{1}{M' + \sqrt{M'N'}} F_1(s) = 0 \quad (\text{A11.23})$$

respectively, which may be solved simultaneously to give

$$I_f(s) = \frac{\sqrt{6}}{2} E_0 \frac{M_{af}}{L_f} \frac{1}{X_a + X_2} \left[ \frac{1}{s + \frac{1}{\tau_d}} - \frac{1}{s} \right] \quad (\text{A11.24})$$

and

$$F_1(s) = \frac{X_d' + X_2}{X_d + X_2} \left[ \frac{X_d - X_d'}{X_d + X_2} \frac{1}{s + \frac{1}{\tau_d}} + \frac{1}{s} \right] \quad (\text{A11.25})$$

where

$$X_2 = \sqrt{M'N'}$$

$$\tau'_{do} = \frac{L_f}{R_f} \quad (\text{A11.26})$$

$$\tau'_d = \tau'_{do} \frac{X'_d + X_2}{X_d + X_2}$$

The inverse Laplace transform of equations (A11.24) and (A11.25) are

$$I_f(t) = \frac{\sqrt{6}}{2} E_o \frac{M_{af}}{L_f} \frac{1}{X_d + X_2} [e^{-t/\tau'_d} - 1]$$

and

$$F_1(t) = \frac{X'_d + X_2}{X_d + X_2} \left[ \frac{X_d - X'_d}{X_d + X_2} e^{-t/\tau'_d} + 1 \right] \quad (\text{A11.27})$$

respectively.

## REFERENCES

REFERENCES

1. GRIFFIN, J.  
"Standby generator re-connections", International Power Generation, 1979, Vol. 2, No. 2, pp 17-25.
2. FORTESCUE, C L.  
"Method of symmetrical coordinates applied to the solution of polyphase networks", AIEE Trans., 1918, Vol. 37, Part II, pp 1027-1140.
3. WAGNER, L F. and EVANS, R D.  
"Symmetrical components", McGraw-Hill Book Co Inc., New York, 1933.
4. ANDERSON, P M.  
"Analysis of faulted power systems", The Iowa State University Press, Ames, Iowa, 1973.
5. LYON, W V.  
"Application of the method of symmetrical components", McGraw-Hill Book Co Inc., New York, 1937.
6. CALABRESE, G O.  
"Symmetrical components applied to electric power networks", Ronald Press, New York, 1959.
7. BLONDEL, A E.  
"Synchronous machines and converters", McGraw-Hill Book Co Inc., New York, 1913.
8. DOHERTY, R E and NICKLE, C A.  
"Synchronous machines, an extension of Blondel's two-reaction theory I", AIEE Trans., 1926, Vol. 45, pp 912-926.

9. DOHERTY, R E and NICKLE, C A.  
"Synchronous machines, an extension of Blondel's two-reaction theory II", AIEE Trans., 1926, Vol. 45, pp 927-947.
10. DOHERTY, R E and NICKLE, C A.  
"Synchronous machines III, torque-angle characteristics under transient conditions", AIEE Trans., 1927, Vol. 46, pp 1-18.
11. DOHERTY, R E and NICKLE, C A.  
"Synchronous machines IV, single-phase short circuits", AIEE Trans., 1927, Vol. 47, pp 457-492.
12. DOHERTY, R E and NICKLE, C A.  
"Synchronous machines V, 3-phase short-circuits", AIEE Trans., 1930, Vol. 49, pp 700-714.
13. PARK, R H.  
"Definition of an ideal synchronous machine and formula for the flux linkages", G.E. Review, 1928, Vol. 31, pp 332-334.
14. PARK, R H.  
"Two-reaction theory of synchronous machines - Part I", AIEE Trans., 1929, Vol. 48, pp 716-730.
15. PARK, R H.  
"Two-reaction theory of synchronous machines - Part II", AIEE Trans., 1933, Vol. 52, pp 352-355.
16. ADKINS, B. and HARLEY, R G.  
"The general theory of alternating current machines", Chapman and Hall, 1975.
17. CHING, V K and ADKINS, B.  
"Transient theory of synchronous generator under unbalanced conditions", Proc. IEE, 1956, Vol. 11, Part IV, pp 166-182.

18. SUBRAMANIAM, P and MALIK, O P.  
"Digital simulation of a synchronous generator in direct-phase quantities", Proc. IEE, 1971, Vol. 118, pp 1309-1318.
19. SMITH, I R and SNIDER, L A.  
"Prediction of transient performance of isolated saturated synchronous generator", Proc. IEE, 1972, Vol. 119, pp 1309-1318.
20. CONCORDIA, C.  
"Synchronous machines", John Wiley and Sons Inc., New York, 1951.
21. SARMA, M S.  
"Synchronous machines: their theory, stability, and excitation systems", Gordon and Breach Science Publishers, New York, 1979.
22. ELGERD, O I.  
"Electric energy systems theory: an introduction", McGraw-Hill Book Company, New York, 1971.
23. MAJMUDAR, H.  
"Electromechanical energy converters", Allyn and Bacon, New York, 1965.
24. LYON, W V.  
"Transient analysis of alternating current machinery", John Wiley, New York, 1954.
25. KRAUSE, P C.  
"Analysis of electric machinery", McGraw-Hill Book Co. Inc., New York, 1986.
26. MORGAN, A T.  
"General theory of electrical machines", Heyden and Son, London, 1979.

27. KOVACS, P K.  
"Transient phenomena in electric machines", Elsevier Book Co. Inc., New York, 1984.
28. GIBBS, W J.  
"Electric machine analysis using matrices", Sir Isaac Pitman and Sons Ltd., London, 1962.
29. BEWLEY, L Y.  
"Tensor analysis of electric circuits and machines", The Ronald Press Company, New York, 1961.
30. LEWIS, W A.  
"A basic analysis of synchronous machines. Part I", AIEE Trans., 1958, Vol 77, pp 436-453.
31. LEWIS, W A.  
"The principles of synchronous machines", Illinois Institute of Technology, 1959.
32. HWANG, H H.  
"Unbalanced operation of AC machines", IEEE Trans., PAS-84, 1965, pp 1054-1066.
33. HWANG, H H.  
"Mathematical analysis of double line-to-ground short circuit of an alternator", IEEE Trans., PAS-86, 1967, pp 1254-1257.
34. HWANG, H H.  
"Transient analysis of unbalanced short circuits of synchronous machines", IEEE Trans., PAS-88, 1969, pp 67-72.
35. HWANG, H H.  
"Unbalanced operations of three-phase machines with damper circuits", IEEE Trans., 1969, PAS-88, pp 1585-1593.

36. HWANG, H H.  
"Transient analysis of simultaneous unbalanced short circuits of synchronous machines", IEEE Trans., 1971, PAS-90 pp 1815-1821.
37. HANCOCK, N N.  
"Matrix analysis of electrical machinery", 2nd ed. Pergamon Press, 1974.
38. SMITH, R T.  
"Analysis of electrical machines", Pergamon Press, London, 1982.
39. DUESTERHOEFT, W C, SCHULZ, M W, and CLARKE, E.  
"Determination of instantaneous currents and voltages by means of alpha, beta and zero components", AIEE Trans. 1951, Vol. 70, pp 1248-1255.
40. CLARKE, E.  
"Circuit analysis of AC power system", Vol. I, Wiley, New York, 1943.
41. CLARKE, E.  
"Circuit analysis of AC per system", Vol. II, Wiley, New York, 1950.
42. YAKUBOVICH, V A and STARZHINSKII, V M.  
"Linear differential equations with periodic coefficients", Vol. I, Krieger, New York, 1975.
43. YAKUBOVICH, V A and STARZHINSKII, V M.  
"Linear differential equations with periodic coefficients", Vol. II, Krieger, New York, 1975.
44. IEEE Working Group on Power System Harmonics  
"Power system harmonics: an overview". IEEE Trans. 1983, PAS-102, pp 2455-2459.

45. GONEN, T.  
"Electric power distribution systems engineering", McGraw-Hill Book Co. Inc., New York, 1985.
46. "Test Procedure for Synchronous Machines". IEEE Publ. 115, 1965.
47. SNIDER, L A, and SMITH, I R.  
"Measurement of inductance coefficients of saturated synchronous machines", Proc IEE, 1972, Vol. 119, No 5, pp 592-602.
48. DUNFIELD, J C, and BARTON, T H.  
"Effect of mmf and permeance harmonics in electrical machines, with special reference to synchronous machines", Proc. IEE, 1972, Vol 119, No 9, pp 1309-1318.
49. DANDENO, P L, and PORAY, A T.  
"Development of detailed turbogenerator equivalent circuits from standstill frequency response measurements", IEEE, 1981, PAS-100, pp 1646-1655.
50. DANDENO, P L; KUNDUR, P; PORAY, A T and ZEIN EI-DIN, H M.  
"Adaptation and validation of turbogenerator model parameters through on-line frequency response measurements", IEEE, 1981, PAS-100, pp 1656-1664.
51. DANDENO, P L; KUNDUR, P; PORAY, A T and COULTES, M E.  
"Validation of turbogenerator stability models by comparisons with the power system tests", IEEE, 1981, PAS-100, pp 1637-1645.
52. SOLLECITO, W E. and SWANN, D A.  
"Computer evaluation of high temperature aircraft AC electrical system design", AIEE Trans., 1960, Vol 78, pp 434-444.
53. MOORE, R C.  
"Minimizing harmonics in standby generators", Allis-Chalmers Engineering Review, 1971, Vol 36, pp 21-26.

54. ROGERS, G J. and SMITH, J R.  
"Synchronous machine model including eddy currents", IEE Proc. Vol 120, No 4, 1973, pp 461-468.
55. ROBERTSON, B L.  
"Tests on armature resistance of synchronous machines", AIEE, Trans., 1935, Vol. 54, pp 705-709.
56. JONES, C V.  
"The unified theory of electrical machines", Butterworths, 1967.
57. CARTER, G W; LEACH, W I. and SUDWORTH, J.  
"The inductance coefficients of a salient-pole alternator in relation to the two-axis theory", Proc. IEE, Vol 108, 1961, pp 263-270.
58. KIMBARK, E W.  
"Power system stability: synchronous machines", Dover Publications, New York, 1968.
59. FITZGERALD, A E; KINGSLEY, C and UMANS, D S.  
"Electric machinery", 4th Ed., McGraw-Hill, New York, 1983.
60. RANKIN, A W.  
"Per-unit impedance of synchronous machines", Trans. AIEE, 1945, Vol. 64, pp 569-572.
61. RANKIN, A W.  
"Per-unit impedance of synchronous machines - Part II", Trans. AIEE, 1945, Vol. 64, pp 839-841.
62. HENRICI, P.  
"Discrete variable methods in ordinary differential equations", John Wiley and Sons Inc., New York, 1962.

63. GERALD, C F.  
"Applied numerical analysis", Addison-Wesley Publishing Company,  
New York, 1978.
64. CHUA, L O. and LIN, PM.  
"Computer aided analysis of electronic circuits: algorithms and  
computational techniques", Prentice-Hall, New York, 1975.
65. ADBY, P R.  
"Applied circuit theory: matrix and computer methods", John Wiley  
and Sons Ltd., New York, 1980.
66. HUMPAGE, W D. and STOTT, B.  
"Predictor-corrector methods of numerical integration in digital  
computer analysis of power system transient stability", Proc. IEE,  
1965, Vol. 112, pp 1557-1562.
67. WILF, H S.  
"An open formula for the numerical integration of first order  
differential equations, Part I", Mathematical tables and other aids  
to the computation, 1957, Vol. 11, pp 201-203
68. WILF, H S.  
"An open formula for the numerical integration of first order  
differential equations, Part II", Mathematical tables and other  
aids to the computation, 1958, Vol. 12, pp 55-58.
69. FOWLER, M E.  
"A new numerical method for simulation", Simulation, 1965, Vol. 4,  
pp 321-330.
70. GRANBORG, B S H.  
"Computational stability in system analysis", Proc. 7th Allerton  
Conference on Circuit and System Theory, IEEE, 1969, pp 216-224.

